**UNIVERSITY OF SASSARI**

**PH.D. SCHOOL IN NATURAL SCIENCES END ITS RESOURCES**

**VIA MURONI 25, I-07100 SASSARI, ITALY**

*Dissertation for the Degree of Doctor of Philosophy in Science and Technology of the Minerals and Rocks of Industrial Interest presented at Sassari University in 2015*

XXVIII cycle

# TECTONICS UNITS OF CENTRAL SARDINIA:

# STRUCTURAL EVOLUTION AND RELATED ORES

PH.D. CANDIDATE: ***Dr. Mattia Alessio Meloni***

DIRECTOR OF THE SCHOOL: ***Prof. Marco Curini-Galletti***

SUPERVISOR: ***Prof. Giacomo Oggiano***

## Acknowledgments

*I wish to special thanks for my supervisor, Prof. Giacomo Oggiano, for the continuous support of my Ph.D study and related research, for his patience, motivation, immense knowledge and huge opportunities of scientific growth. His guidance helped me in all the time of research and writing of this thesis. I could not have imagined having a better supervisor and mentor for my Ph.D study.*

*Many thanks to Prof. Alfredo Loi and Dr. Antonio Funedda, for their attention in my study and for being always available to help me through discussions and important notions of scientific thinking.*

*All my gratitude goes to: Dr. Leonardo Casini, Dr. Stefano Cuccuru, Dr. Guido Cerri, Dr. Paola Mameli, Dr. Antonio Puccini, Dr. Valeria Testone, Dr. Antonio Brundu, Dr. Vittorio Longo, for their scientific support, understanding and the interest shown about this research.*

*I would like to express my gratitude to Prof. Laura Gaggero who gave me access to the laboratory and research facilities. Without his precious support it would not be possible to conduct this research.*

*I must also acknowledge Nicola Campomenosi for the Technical support and to the laboratory analysis.*

*Many thanks to Prof. Ulf Linnemann and all the members of the Department of Geochronology of Dresden, for their attention in my study.*

*Very Special thanks to Antonella Floris for the continuous support gave me.*

# CONTENTS

# ABSTRACT

Many studies consider the Variscides of Sardinia as the result of the Lower Carboniferous amalgamation between the north Gondwana margin and the ribbon of Gondwana-detached terranes. The orogenic wedge in Sardinia is best preserved in the Nappe zone, where a huge stack of tectonic units, is well exposed from NW to SE. Though this zone was satisfactory outlined under stratigraphic and structural point of view, several questions still remain open for the lack of basic modern geological maps and for the lack of geochronological data on the sequences of some tectonic units (Barbagia Units) where the metamorphism erases any fossil record. Bridging this gap made necessary undertaking the detailed mapping of the nappe zone in the southern slope of the Gennargentu using new tools, such as gamma ray portable spectrometry, able to discrimate undistinguishable units on geochemical base. In this way a new vast area was mapped. The study and dating of detrital zircons was performed on some metamorphic units. In this way a maximum age to the Barbagia Units was assigned and the formations of the Meana Sardo unit were discriminated. The provenance of the clastic component was located in the cratonic areas facing the Galatian Terrenes. These results allowed defining the structural frame and evolution of this sector of chain. Moreover he new knowledge on the structural, stratigraphic and geochronological scenario allowed a new hypothesis on the genesis of the ore deposits.

# FIRST PART (INTRODUCTION AND METHODS)

# 1. INTRODUCTION

## 1.1. AIM OF THE RESEARCH

This research targets are:

- reconstruction of the structural model of the Variscan basement of central Sardinia by mean of detailed geological and structural mapping and refining the chrono-stratigraphy of the different units by mean of gamma ray survey and detrital zircon geochronology;
- reconstruct the tectonic evolution, distinguishing late-collisional deformation phases from those post-collisional;
- to improve the knowledge of the different tectonic units in terms of provenance and maximum age by studying the detrital zircons ;
- investigate the evolution of post-collisional tectonic and magmatism and their relations with the main mineralizations.

## 1.2. GEOLOGICAL BACKGROUND

The Sardinia segment of the of the Variscan chain is one of the best exposed across all the South Variscan Branch (**Fig.1**). In fact the reconstruction of the Variscan Southern branch (VSB) from Bohemia to the South through the Alps (Guillot et al., 2008), the Maures massif (Bellot, 2005), Corsica and Sardinia (Rossi et al 2009), is more uncertain because a large part was parcelled out by Stephanian dextral transpressive faulting (Edel et al. 2014; Bard, 1997) and/or partly missing due the Tethyan oceanisation, the alpine collision and the opening of the western Mediterranean back-arc basins. Restoring the Corsica-Sardinia micro-continent on its original position, before the Miocene rotation, strong fittings can be found between Maures and NW-Sardinia. They are documented by similar prograde, collision-related, tectono-metamorphic features and similar post-collisional evolution in the Variscan basement as well as by strong analogies in Mesozoic covers, including a Mid-Cretaceous bauxite-bearing stratigraphic gap (Mameli et al., 2007).

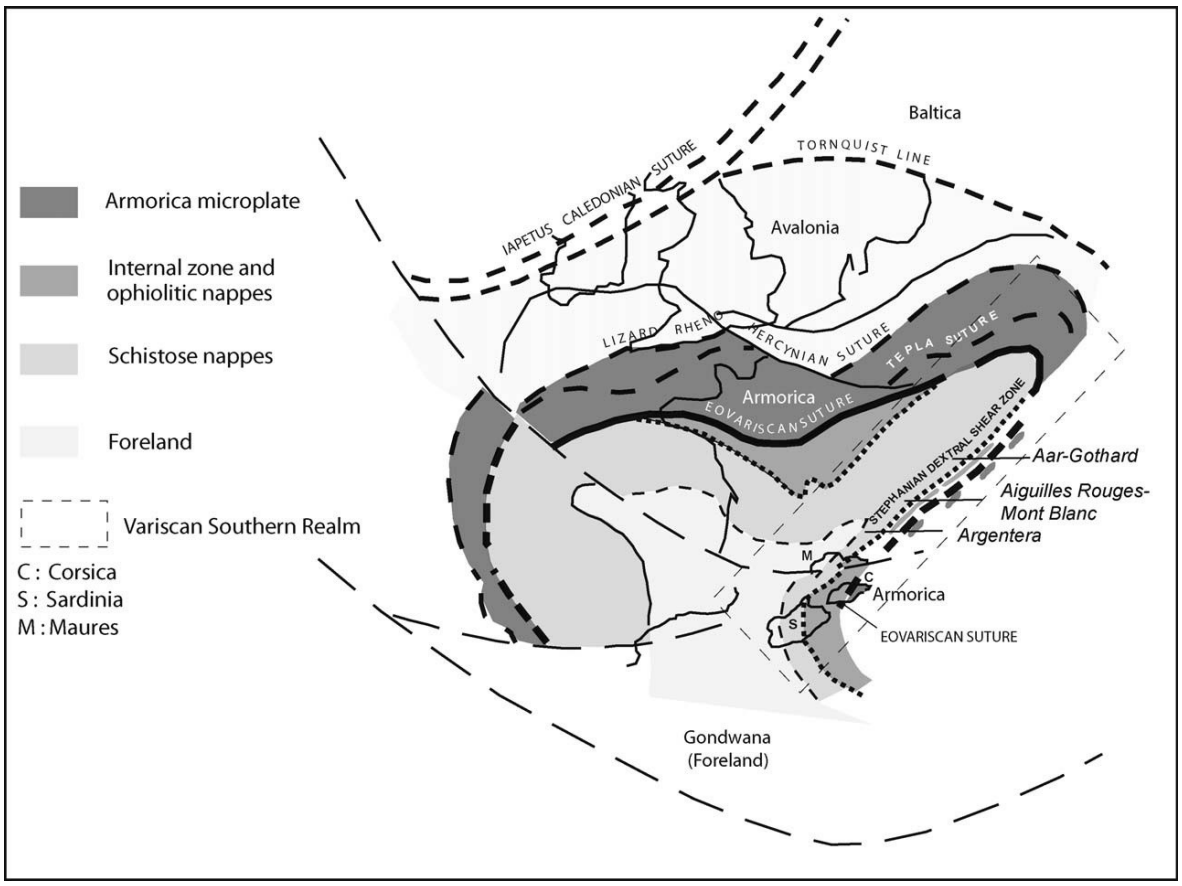


*Figure 1) The southern Variscan realm in western Europe (Rossi et al., 2009).*

Classically the segment of the Variscan Chain in Sardinia is subdivided into three large domains of differing tectonic-metamorphic evolution; from the south to the north they are as follows (**Fig.2**):

1) The external zone of the chain, corresponding to Sulcis-Iglesiente, recognized by an anchi-metamorphic fold and Thrust belt;

2) The Nappe Zone, corresponding mainly to the basement exposed on the Island, consists of a nappe stack within the Greenschist facies;

3) An axial zone, corresponding to Gallura, to Asinara Island and to most of Corsica, formed of high to medium grade metamorphic rocks.

The direction of motion of the tectonic units during the collisional events is initially NW-SE (Carmignani 1978 a, b) then changing from W to E (Conti et al. 2001; Carosi e Oggiano, 2002). The metamorphism is prograde and the metamorphic grade increases from south to north (Franceschelli et al. 1989b) where, an hypothetical suture zone with relict eclogites (Cappelli et al. 1992) separates the units constructed at the expose of the northern Gondwana margin from those which would have incorporated elements of peri-Gondwanan terranes (Armorica terranes Assemblage; Franke, 2000; Galatian Terranes; Von Raumer, 2008).

The succession of the external zone has a broad stratigraphic range from the Vendian to the Lower Carboniferous. This is formed by terrigenous and carbonate sedimentary sequence of Ediacaran-Tremadoc age uncomformably overlain by a discordant (Sardic-Phase of Stille, 1939) continental deposit (Puddinga auctorum) of Mid-Ordovician age (Martini et al 1992). The successive epicontinental succession ranges from the Upper Ordovician up to the Devonian (Carmignani et al. 2001 and references therein) .

The Palaeozoic succession of the nappe zone differs significantly from the external zone; some differences may also be found among the diverse tectonic units of the nappe zone proceeding from the internal to the external nappes and in particular:

a) The subareal Mid- Ordovician calcalkaline volcanites (Di Pisa et al., 1992; Giacomini et al. 2006; Oggiano et al. 2010; Gaggero et al. 2012) are missing in the external zone and the alkaline-transitionals (Gaggero et al 2012) that, instead, are characteristic of nappe zone, are scarcely represented (Beccaluva et al. 1981).

b) The occurrence of huge syntectonic continental deposits assigned to a vast system of alluvial system including fan delta (Martini et al. 1992), the occurrence of glaciomarine diamictite (Loi e Dabard 1997) in the foreland that are absent in the nappe zone.

As for the differences among the tectonic units of the nappe building, the internal nappes differ from the external nappe for the decrease or absence of calcalkaline volcanites of Middle Ordovician and the absence of carbonate successions of Devonian age, which probably were replaced by terrigenous deposits (**Fig.3**). Conversely the internal nappes exhibit an increase in the volume of alkaline metabasites at the Ordovician-Silurian transition, coinciding with a regression, possibly

related to the Hirnantian glaciation (Oggiano & Mameli 2006). A high grade metamorphic complex overrides the nappe zone, which at the base has induced an inverse metamorphism zonation (Carmignani et al 1994). These features together with the presence of eclogite boudins allow comparing the high grade Complex with the inner crystalline nappe of the Massif Central (Burg et al.1984), hence this Complex is probably rooted inside the a south-Variscan suture. The metamorphic evolution of this complex may be attributed to an eclogite phase followed by a granulitic phase and a definitive re-equilibration in the amphibolite facies (Ghezzo et al 1979; Franceschelli et al. 2005 ; Cortesogno et al 2004).

Corsica constitutes the hinterland of the chain where a non-metamorphic Paleozoic succession rests upon a Pan-African basement (Rossi et al. 1995), which is not comparable with the succession in Sardinia (Barca et al. 1996). The late-collisional evolution of the chain is documented by retrograde dextral mega shear zones (Elter et al 1990); subsequent to the emplacement of the Magnesio-Potassic intrusive complex, which is found only in Corsica (Cocherie et al.,1994; Rossi et al., 2006). The importance of these transcurrent mega shears for the re-organization of the south European Variscides should not be under-estimated as they may have caused the juxtaposition of units belonging to diverse palaeogeographic domains (Bard, 1997) also in Sardinia.

The post-collisional evolution is documented by HT/LP metamorphism (Cortesogno et al.,1998), exhumation of the core complex (Casini e Oggiano, 2008), emplacement of the Corsica–Sardinia Batholith (C-S Batholith) (Bralia e Ghezzo, 1981; Rossi e Cocherie, 1991), volcanic activity and formation of Carboniferous-Permian intra-cratonic basins (Cassinis et al. 2003; Buzzi et al. 2008). The chain, thus demolished, was incorporated within stable Europe from which it would break away during the Burdigalian between 20 and 17 Ma from the present (Vigliotti and Langheneim 1995; Gattacecca et al. 2004; Oudet et al. 2010).

Although the collisional and post-collisional scenario of Variscan Sardinia has been almost defined, some questions still need to be resolved regarding the reconstruction of the pre-collisional and late post-collisional geodynamic events of the Variscan cycle. In particular, it still remains to be understood whether the basement of the Sardinia-Corsica block was formed from a sector of Gondwana with a Palaeozoic history constrained within a substantially homogenous palaeogeographic domain or whether it comprises combined crustal sectors with independent

Paleozoic histories. Some authors considered the Variscan basement of Sardinia substantially homogeneous on the base of similar radiometric ages in the volcanic rocks of different tectonic units separated by first order tectonic contact (Giacomini et al. 2006).

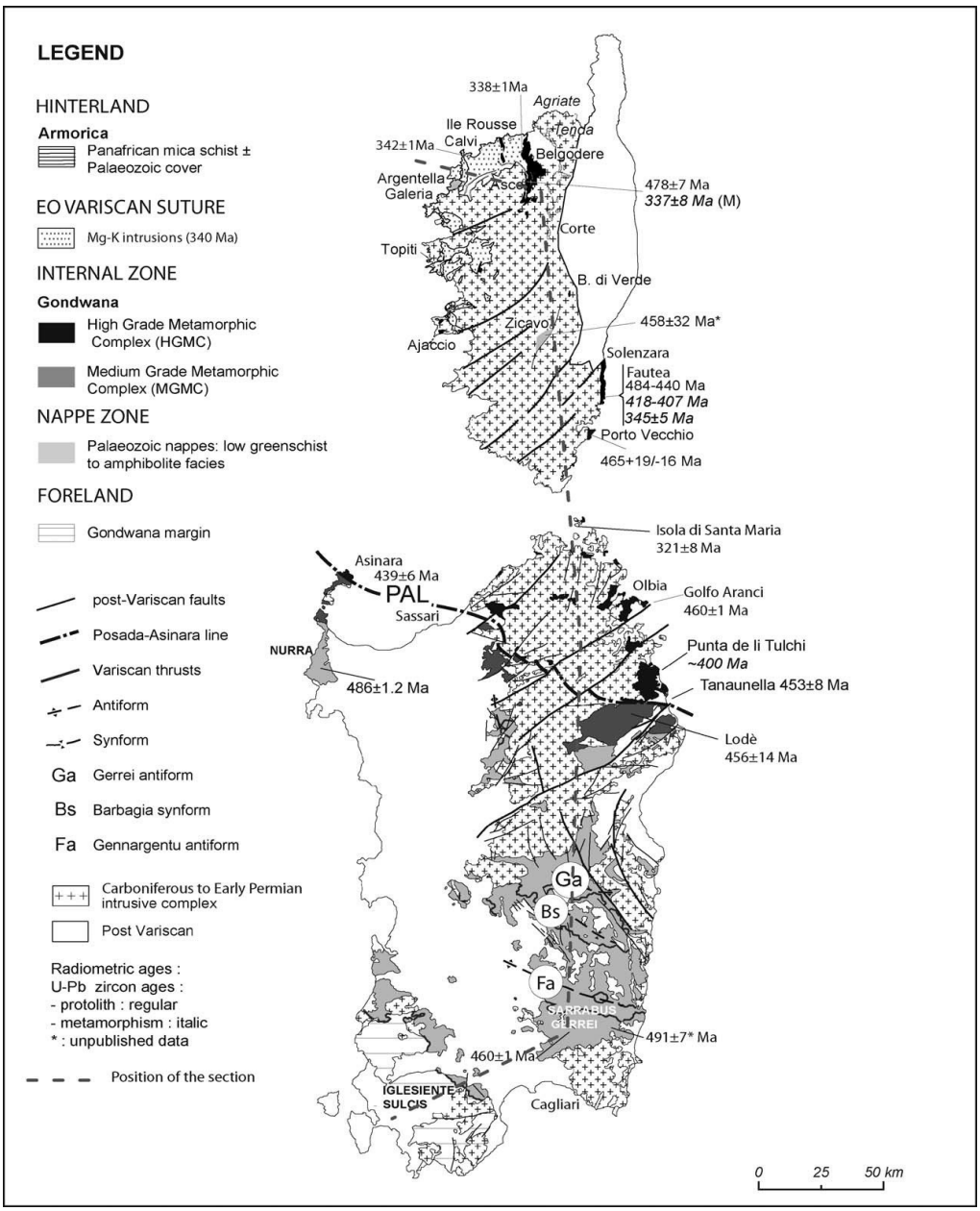


*Figure 2) Location of the main Variscan zones in Sardinia and Corsica (Rossi et al., 2009).*

This line of argument seems rather weak considering that the dispersion of the Variscan terranes from the north Gondwana margin is post-Ordovician. The absence of Ordovician arc volcanism in

some tectonic units of the inner nappe zone and in the external zone of Sardinia and in Corsica, the absence of Sardic Discordance in Corsica and in the internal nappes of Sardinia, the meaningful sedimentological differences between the low grade successions of Corsica and Sardinia and also between the different tectonic units of Sardinia (Carmignani et al. 2001) and finally, but not of lesser importance, the presence of metabasites with MORB affinities and Devonian eclogitic imprint (Cortesogno et al 2004) in the High Grade Metamorphic Complex, suggest that the Variscan chain of the Sardinia-Corsica block was derived from the assemblage of crustal sectors of diverse provenance after the closure of an oceanic seaway. Consequently the mechanisms, which lead to the juxtaposition of such diverse domains, the direction of tectonic motion of the nappes and the dextral mega-transcurrent movements, which require precise dating, should be taken into consideration to resolve the puzzle derived from the collisions among different peri-Gondwana terranes.

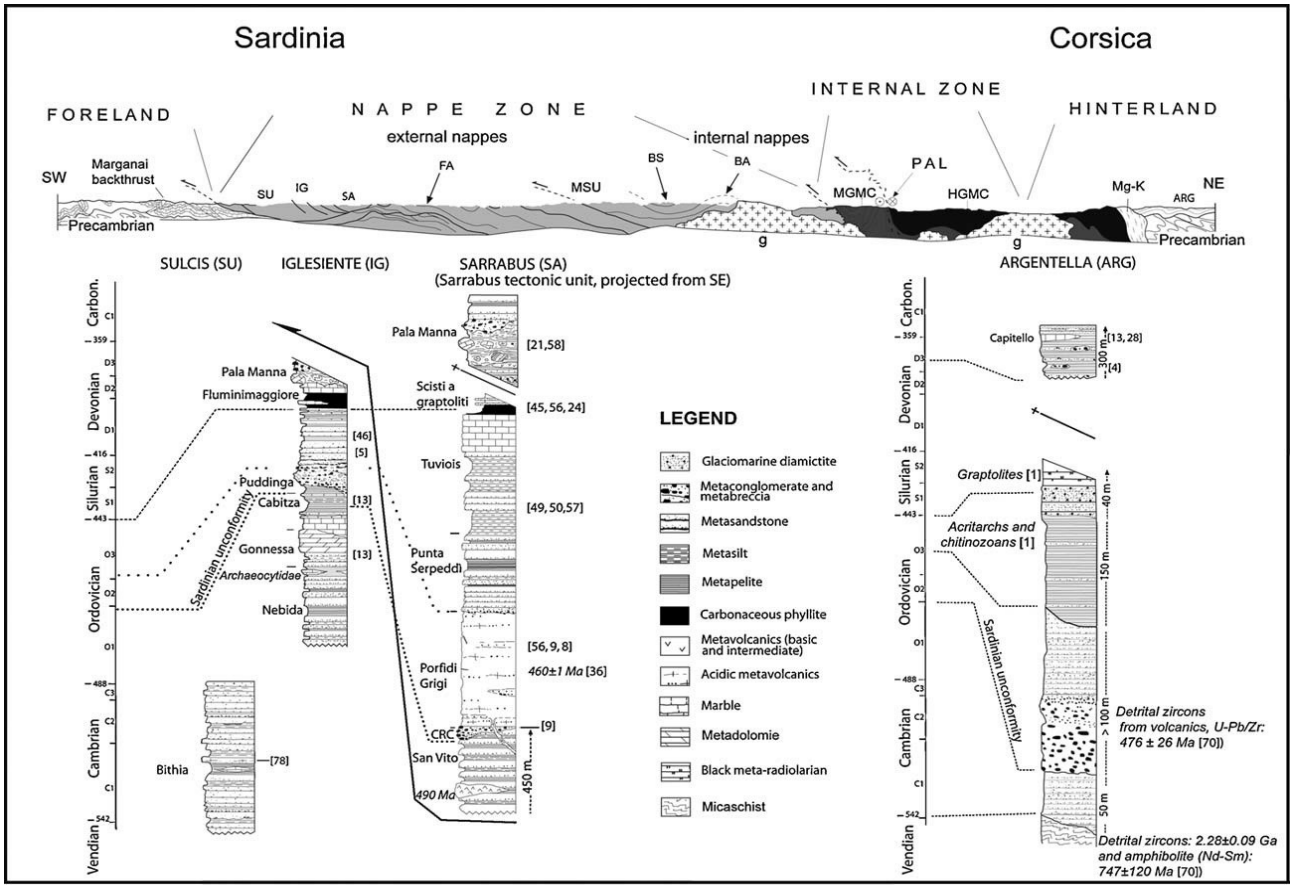


*Figure 3) Schematic section through the Variscan southern realm along the Corsica–Sardinia (Rossi et al., 2009).*

Considering the great temporal and spatial diffusion, within the diverse tectonic units, of volcanic products, often associated with undated terrigenous metasediments, dating the former and establish the provenance and the maximum age for the latter in a still poorly known sector of the nappe building ( i.e. the Barbagia region in Central Sardinia) along with detailed geological and structural mapping is an essential goal for:

a) reconstruct the kinematics of the syn and post-collisional (transpressive) shear zones in an attempt to highlight new tectonic units with motion top to the west and new late Variscan dextral transcurrent movements which seem to have dislocated the chain by several hundred kilometers;

b) verify possible differences, within tectonic units with differing motion, in terms detrital zircon provenances by investigating particular sedimentary levels within the nappes with low grade metamorphism.

### 1.2.1. Structural outlines

The Sardinia segment of the Variscan chain is divided into the four aforementioned tectono-metamorphic zones from NE to SW. The structural frame of the Variscides transect is best exposed in South Sardinia where the superposition of the nappes stack and the complex polyphasal deformation (Carmignani et al., 1994c) from shortening to post-collision extension (Conti et al., 1999; Casini and Oggiano 2008) are well decipherable. The shortening event (D1) can be divided into three main synmetamorphic deformation phases: firstly south-verging overturned folds and top-to-south thrusts with the emplacement of several tectonic units one over each other; afterward a late nappe emplacement occurred with a top to the west tectonic transport that generated the stronger deformation in the External zone (Conti et al., 2001) (**Fig.4**); a third phases occurred with another change of the shortening direction (again north-south) that folded all the nappe pile, resulting in large upright antiforms and synforms with an axial extension up to 50km and that are one of the more evident regional structural in the Sardinian basement. The extensional event (D2) is characterized by recumbent folds that deformed the nppe stack, and by low-angle normal faults that re activated older thrust in a brittle-ductile condition; the extension probably started when the tangential shortening ceased and the whole nappe pile suffered an isostatic balancing. The D2 phase ended with the emplacement of late-orogenic granitoids and the development of Late Carboniferous

Lower Permian basins that are common features in the South European Variscides related generally to an intraplate strike slip tectonics.

### 1.2.2. Nappe Zone

In Sardinia, the a Cambrian to Early Carboniferous succession is involved in the Nappe Zone that extend from Sarrabus in the southeast (External nappes) to Nurra in the northwest (Internal nappes) with deformation and metamorphic grade increasing northward from lower greenschist to amphibolite facies. The Sardinian Nappe zone consists of several tectonic units characterized by slightly different lithostratigraphic successions, mainly in the Ordovician volcanic successions, equilibrated under greenschist facies, imbricated and emplaced with a general top to south-west transport.

The External nappe are characterized by a well recognizable and datable lithostratigraphic succession, whereas in the Internal nappe the recognition of a detailed lithostratigraphic succession is prevented by the lacking of bio-stratigraphic marker and by a more penterative, polyphasic deformation.

The **Internal Nappe Zone** comprises low to medium-grade sequences of metasandstones, quartzites, phyllites, marbles, and a limited amount of middle Ordovician metavolcanic rocks, which lack completely in the nappe of northwest Sardinia (Gaggero et al. 2012) and the minor amount or absence of Devonian carbonate rocks. The inner nappes are affected by Barrovian metamorphic conditions reaching the upper green (Bt+/-Gr). In Barbagia, Goceano, and southern Nurra, the metamorphic conditions are limited to low grade (Carmignani et al. 1979; Carmignani et al., 1994b). The structural evolution of the Internal nappe is characterized by the occurrence of at least two widespread folding events with associated penetrative axial planar cleavage.

In the **External Nappe Zone**, the tectonic units are exposed from Goceano in the north to Sarrabus-Gerrei, where the best section of the nappe stack is exposed along the Flumendosa Valley which crosscut the huge Flumendosa antiform (Carmignani et al., 1982). Several tectonic units were recognized in this area from the lower to the upper they are: M. Grighini Unit.; Riu Gruppa Unit.; Gerrei Unit.; Meana Sardo Unit.; Sarrabus Unit. In the Arburese areas the nappe front overrides directly the foreland.

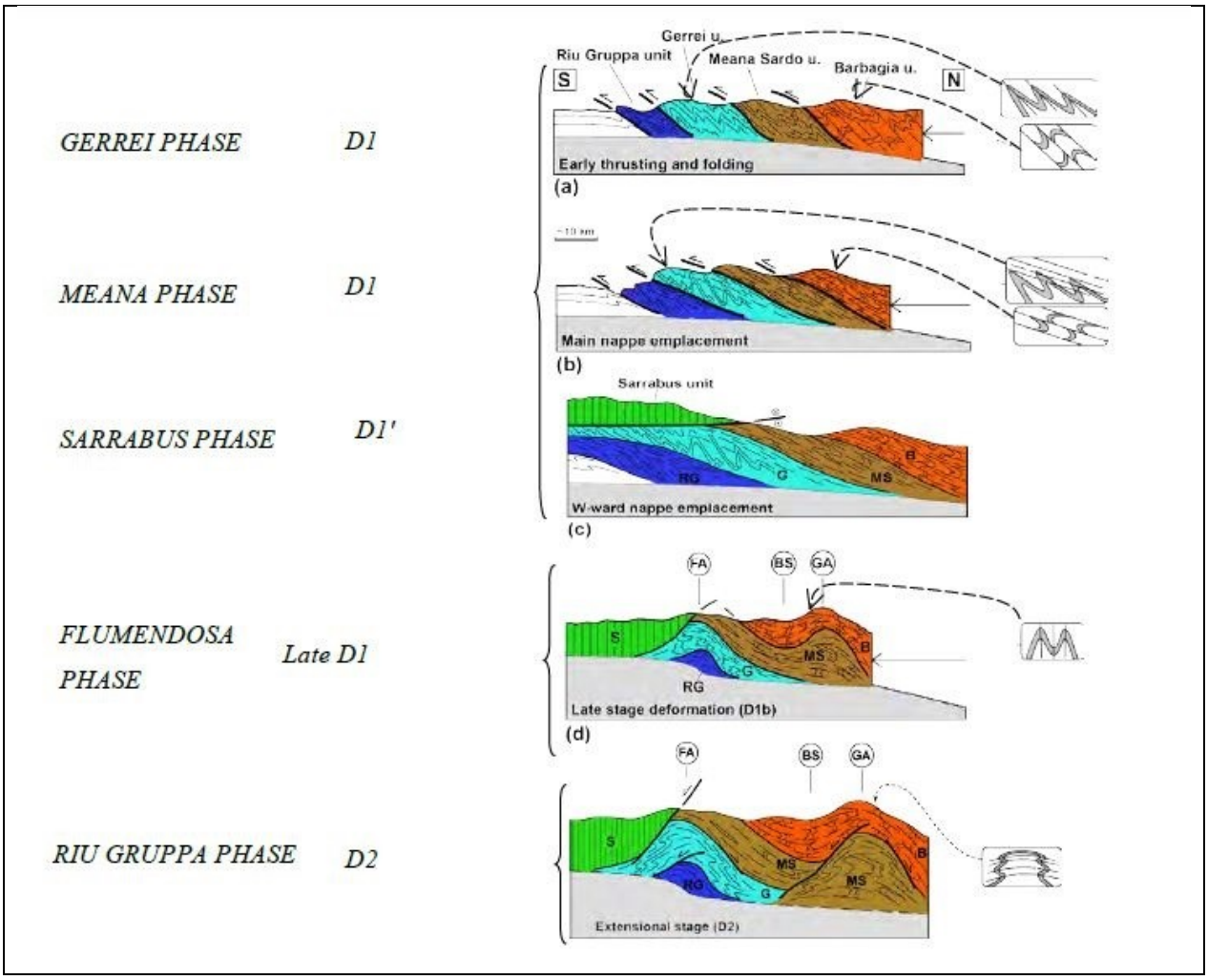


*Fiure 4) Reconstruction of the tectonic evolution of the External nappe in Sardinia (after Conti et al., 2001 modified).*

## 1.3. THE STUDY AREA

The study area is located in the central Sardinia (Italy); it covers an area of about 400 square kilometers around the Gennargentu massif. It's composed by two main zones: the Laconi area and the Gadoni area. The Laconi area stretches between 8856′00″/39855′00″ (NW corner) and 9803′00″/39850′00″ (SE corner). The Gadoni area has the following coordinates as limits 39°56'20"/9°04'59" (NW corner) and 39°51'47"/9°13'16" (SE corner); (**Fig.5**).

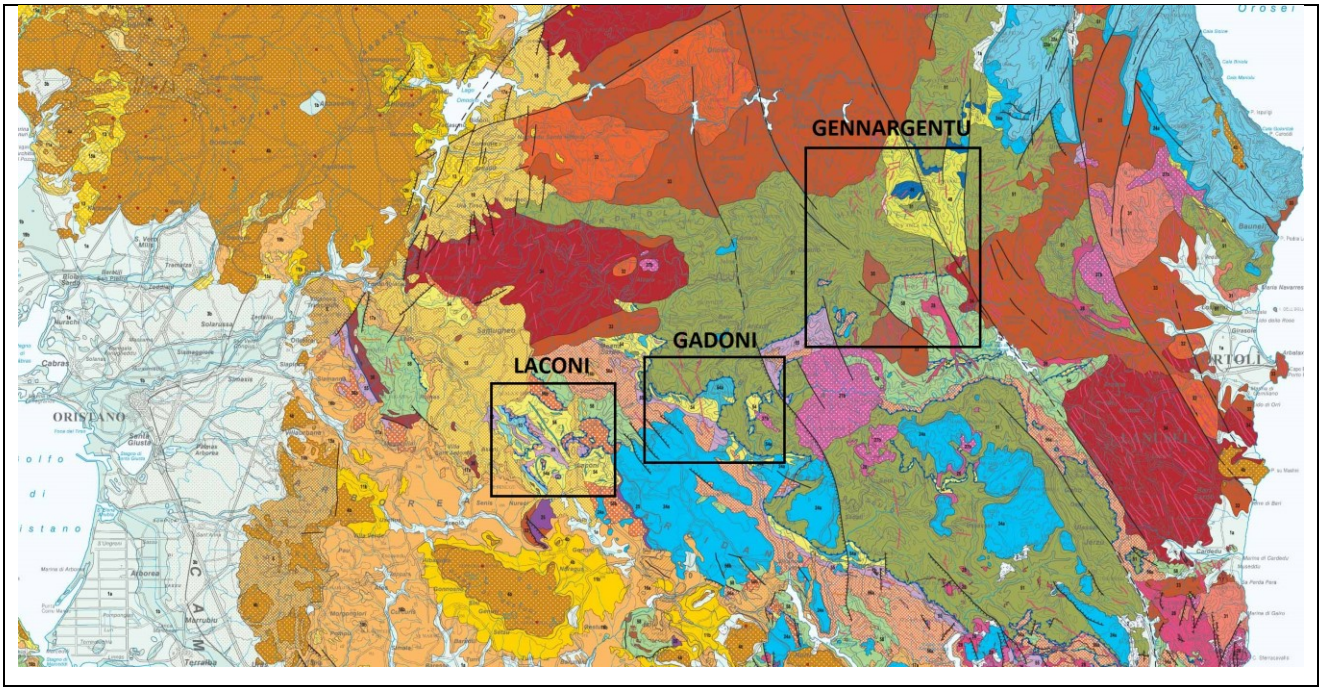


*Figure 5) Geographical location of the study area in the geological sketch map of the Sardinia 1:250.000 (Carmignani et al., 2008).*

The whole area is located in the Nappe Zone in central Sardinia. The central Sardinia is one of the key sites for the geology of the Nappe Zone (Carmignani et al., 1994; Carmignani, Carmignani et al., 2001, and references therein). The first studies date back to the early 19$^{th}$ century, when a thriving mining activity developed, in particular in the Gadoni mining (Dessau G., 1937). Other contributions to the study were given between 1960 and 1980 (Ogniben, G. & De Pieri, R. 1967; Bosellini A. & Ogniben G. 1968) and (Dessau et al., 1982 (**Fig.6**); Carmignani, Minzoni et al. 1982 (**Fig.7**). The above reported sequences of maps show the state of art of the geological knowledge of the area; apart the recent 1: 250,000 (Carmignani et al. 2008), which is a broad scale synthesis of the geologic acquirements, only two geologic works with modern structural interpretation are available, in any case referable at the eighties of the last century. These works, though relatively up to date for that time are based on a poor stratigraphical detail due to lack of fossil record and are based on an outdated structural model, particularly the paper of Carmignani et al. 1982, which considered a huge sequence inclosing Precambrian rocks and did not takes in account the extensional tectonic phase.

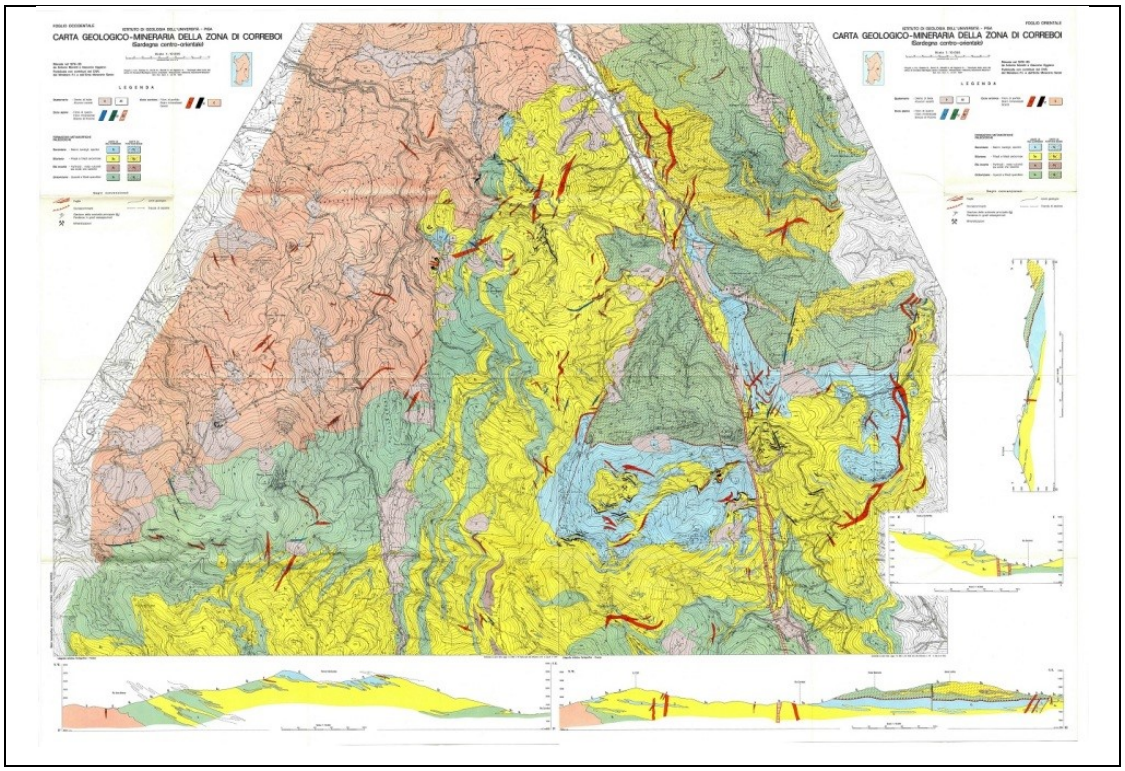


*Figure 6) Geological map of the Correboi area, Central Sardinia; (Dessau G., et al., 1982).*

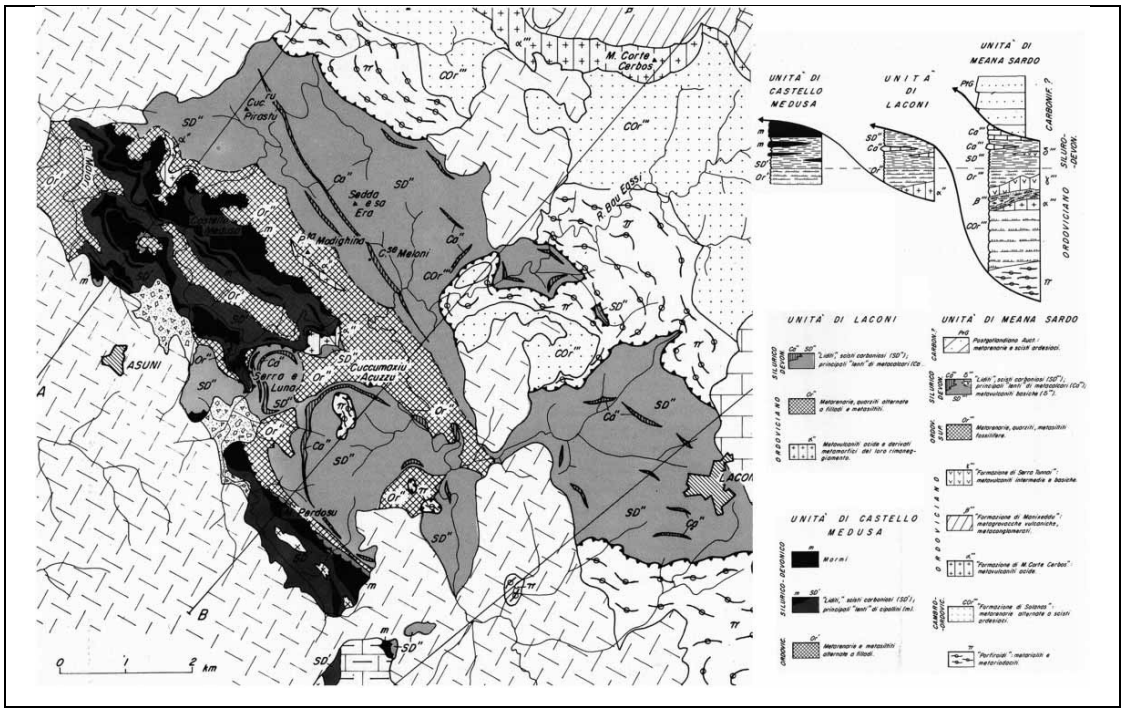


*Figure 7) Geological sketch map of the Laconi-Asuni area by Carmignani, Minzoni et al. (1982).*

## 1.4. PROBLEMS STATEMENT

The study area is characterized by polyphasic deformation, regional and contact metamorphism, which mask almost completely the primary lithological characters of the formations, making problematical any correlations among the different units of this sector of chain. Even more difficult are correlations with the well dated units of the foreland and the external nappe zone. The lack of certain stratigraphic attribution, besides, does not allow good structural reconstruction within this portion of orogenic wedge. In central Sardinia lithostratigraphic correlations have good reliability only between the lower tectonic unit (i.e. the Meana Sardo Unit; Carmignani et al., 1982) and the Gerrei and Sarrabus units, thanks to a few fossil records. The successions of the nappes that form the structure of the Gennargentu area were only tentatively attributed to the Middle Cambrian-Devonian interval, even though the only lithological affinity with other domains is restricted to the Silurian-Devonian black phyllites and metalimestones which retain few remnants of conodonts. The other, dominant, metapelitic and meta-arenaceous terms were dated only on the base of their position with respect to the Siluro-Devonian rocks. In this way the metamorphic clastic succession above the Silurian–Devonian deposit (Postgotlandiano auct.) were considered of lower carboniferous age, and only after the improvement of the knowledge of the Variscan tectonic in Sardinia were considered allochthonous terrains of possibly Cambrian age and tentatively correlated with the San Vito Formation (Dessau et al.1982) As a whole the central part of the Sardinia Variscan segment was poorly known in all its aspect including the widespread s ore bodies of the Gadoni area, which were considered synsedimentary stratabounds deposits linked to the Silurian metasediments. For this reason the first step in deepening the knowledge of this Variscan sector implies a good geological mapping as no mapping as recent as the seventies enriched in heavy minerals deposited in a nearshore environment existed apart single areas of mining interest. Through geological mapping and structural analyses supported by different analytical tools, including detrital zircon dating, this work aim to face the following open questions:

- Is the Postgotlandiano auct., a Cambro-Ordovician succession corresponding to the San Vito formation? Is its tectonic and sedimentary provenance comparable to that of the San Vito Fm;

- If so, are the huge quartzite attributed to this unit referable to lower Ordovician and comparable to the Armorican Quartzite, with which could have shared the feeding area?
- What can account the different deformational pattern of this unit with respect that of the lower units?
- Are the mineralizations of sedimentary nature or is their occurrence tied to late variscan intrusions?

## REFERENCES

Barca S., Gnoli M., Olivieri R. & Serpagli E. (1986) – New stratigraphic data and evidence of Lower and Upper Devonian based on Conodonts in Sarrabus area. Riv. It. Paleont. Strat.: 92, 299-320, Milano.

Barca, S., Carmignani, L., Oggiano, G., Pertusati, P. C., & Salvatori, I. (1996). Carta geologica della Sardegna, Servizio Geologico Nazionale. Litografia Artistica Cartografica, Firenze.

Beccaluva L., Leone F., Maccioni L. & Macciotta G. (1981) -Petrology and tectonic setting of the paleozoic basic rocks from Iglesiente-Sulcis (Sardinia-Italy). N. Jb. Miner. Abh.: 140,184-201, Stuttgart.

J.P. Bellot, The Palaeozoic evolution of the Maures Massif (France) and its potential correlation with other areas of the Variscan belt: a review. J. Virtual Explorer 19 (2005) (Paper 4).

J.P. Bard, Démembrement antémésozoïque de la chaîne varisque d'Europe occidentale et d'Afrique du Nord : rôle essentiel des grands décrochements transpressifs dextres accompagnant la rotation–translation horaire de l'Afrique durant le Stéphanien, C. R. Acad. Sci. Paris, Ser. IIa 324 (1997) 693–704.

Bosellini A. & Ogniben G. (1968) - Ricoprimenti ercinici nella Sardegna centrale. Ann. Univ. Ferrara: 1, 1-15, Ferrara.

Bralia A., Ghezzo C., Guasparri G. & Sabatini G. (1981) - Aspetti genetici del batolite sardo-corso. Rend. Soc. It. Min. Petr.: 38, 701-764, Milano.

Burg J.P., Leyreloup A., Marchand J. & Matte P. (1984) - Inverted metamorphic zonation and large-scale thrusting in the Variscan belt: an example in the French Massif Central. In: Hutton D.H.W. & Sanderson D.J. (Eds.), Variscan tectonics of the North-Atlantic region. Geological Society of London Special Publications, 14, 47-61, London.

Buzzi L., Gaggero L. & Oggiano G. 2008. The Santa Giusta ignimbrite (NW Sardinia): a clue for the magmatic, structural and sedimentary evolution of a Variscan segment between Early Permian and Triassic. Ital. J. Geosci., 127(3), 683–695.

Carosi, R., & Oggiano, G. (2002). Transpressional deformation in northwestern Sardinia (Italy): insights on the tectonic evolution of the Variscan belt. Comptes Rendus Geoscience, 334(4), 287-294.

A. Cocherie, Ph. Rossi, A.M. Fouillac, Ph. Vidal, Crust and mantle contributions to granite genesis. An example from the Variscan batholith of Corsica studied by trace element and Nd– Sr–O isotope systematics, Chem. Geol. (Isot. Geoscience section) 115 (1994) 173–211.

Conti, P., Carmignani, L., & Oggiano, G. (1999). From thickening to extension in the Variscan belt—kinematic evidence from Sardinia (Italy). Terra Nova,11(2-3), 93-99.

Conti, P., Carmignani, L., & Funedda, A., 2001. Change of nappe transport direction during the Variscan collisional evolution of central-southern Sardinia Italy. Tectonophysics , 332, 255-273

Capelli, B., Carmignani, L., Castorina, F., Di Pisa A., Oggiano G, Petrini R., 1992. A Hercynian suture zone in Sardinia: geological and geochemical evidence. Geodin Acta , 51, 101-118.

Carmignani L., Cocozza T., Minzoni N. & Pertusati P.C. (1978a) - Falde di ricoprimento erciniche nella Sardegna a Nord-Est del Campidano. Mem. Soc. Geol. It.: 19, 501-510, Roma.

Carmignani L., Cortecci G., Dessau G., Duchi G., Oggiano G., Pertusati P. & Saitta M. (1978b) - The antimony and tungsten deposit of Villasalto in South-Eastern Sardinia and its relationship with Hercynian tectonics. Schweiz. mineral. petrogr. Mitt.: 58, 163-188, Zürich.

Carmignani L., Cocozza T., Ghezzo C., Pertusati P.C. & Ricci C.A. (1982b) - Guida alla Geologia del Paleozoico Sardo, Guide Geologiche Regionali, Società Geologica Italiana,pp. 215, Cagliari.

Carmignani, L., Minzoni, N., Pertusati, P. C., & Gattiglio, M. (1982). Lineamenti geologici principali del Sarcidano-Barbagia di Belvı`. In L. Carmignani, T. Cocozza, C. Ghezzo, P. C. Pertusati & C. A. Ricci (Eds.), Guida alla Geologia del Paleozoico Sardo (pp. 119–125). Guide Geologiche Regionali. Societa` Geologica Italiana.

Carmignani, L., Oggiano, G. & Pertusati, P.C., 1994a. Geological outlines of the Hercynian basement of Sardinia. Petrology, Geology and ore deposits of the palaeozoic basement of Sardinia. Guide book to the field excursion Carmignani, L., Carosi, R., Di Pisa, A., Gattiglio, M., Musumeci, G., Oggiano, G. & Pertusati, P.C. 1994. The Hercynian chain in Sardinia (Italy). Geodin. Acta, 7, 31–47.

Carmignani L., Carosi R., Di Pisa A., Gattiglio M., Musumeci G., Oggiano G. & Pertusati P.C. (1994b) – The Hercynian chain in Sardinia (Italy). Geodinamica Acta: 7, 31-47, Paris.

Carmignani L., Decandia F.A., Fantozzi P.L., Lazzarotto A., Liotta D. & Meccheri M. (1994c) - Tertiary extensional tectonics in Tuscany (Northern Apennines, Italy). Tectonophysics: 238, 295-315, Amsterdam.

Carmignani, L., Decandia, F. A., Disperati, L., Fantozzi, P., Lazzarotto, A., Liotta, D., 1995. Relationships between the Tertiary structural evolution of the Sardinia-Corsica-Provençal Domain and the Northern Apennines. Terra Nova , 7, 128–137.

Carmignani, L., Oggiano, G., Barca, S., Conti, P., Salvadori, I., Eltrudis, A., Funedda, A. & Pasci, S., 2001. Geologia della Sardegna. Note illustrative della Carta Geologica in scala 1:200.000. Servizio Geologico d'Italia: Roma .

Carmignani, L., Oggiano, G., Funedda, A., Conti, P., Pasci, S., & Barca, S. (2008). Geological map of Sardinia, scale 1: 250000. Litografia Artistica Cartografica, Firenze.

Carosi, R., & Oggiano, G., 2002. Transpressional deformation in NW Sardinia Italy: insights on the tectonic evolution of the Variscan belt. Comptè Rendus Geoscience , 334, 273-278.

Cortesogno, L., Cassinis, G., Dallagiovanna, G., Gaggero, L., Oggiano, G., Ronchi, A., ... & Vanossi, M. (1998). The Variscan post-collisional volcanism in late Carboniferous–Permian sequences of Ligurian Alps, southern Alps and Sardinia (Italy): A synthesis. Lithos, 45(1), 305-328.

Cortesogno, L., Gaggero, L., Oggiano, G., & Paquette, J. L. (2004). Different tectono-thermal evolutionary paths in eclogitic rocks from the axial zone of the Variscan chain in Sardinia (Italy) compared with the Ligurian Alps. Ofioliti, 29(2), 125-144.

Casini, L., & Oggiano, G., 2008. Late orogenic collapse and thermal doming in the northern Gondwana margin incorporated in the Variscan Chain: A case study from the Ozieri Metamorphic Complex, northern Sardinia, Italy. Gondwana Research , 13, 396-406.

Cassinis, G., Durand, M., & Ronchi, A. (2003). Permian-Triassic continental sequences of Northwest Sardinia and South Provence: stratigraphic correlations and palaeogeographical implications. Bollettino della Società Geologica Italiana, 2, 119-129.

Dessau, G. (1937): Studi sulla miniera di Fontana Raminosa (Sardegna). Per. Miner., 8, 177-215.

Dessau G., Duchi G., Moretti A. & Oggiano G. (1982) – Geologia della zona del Valico di Correboi (Sardegna centro-orientale). Rilevamento, tettonica e giacimenti minerari. Boll. Soc. Geol. It.: 101, 497-522, Roma.

Di Pisa, A., Gattiglio M. & Oggiano, G., 1992. Pre-Hercynian magmatic activity in the nappe zone (internal and external) of Sardinia: evidence of two within plate basaltic cycles. In: Carmignani, L., Sassi, F.P. (Eds.), Contribution to the Geology of Italy With Special Regards to the Palaeozoic basement. A volume dedicated to Tommaso Cocozza. IGCP Project N. 276. Newsletter, vol. 5. Siena, pp. 33–44.

J.B. Edel, R. Montigny, R. Thuizat, Late Paleozoic rotations of Corsica and Sardinia: new evidence from paleomagnetic and K– Ar studies, Tectonophysics 79 (1981) 201–223.

Elter F.M., Musumeci G. & Pertusati P.C. (1990) - Late Hercynian shear zones in Sardinia. Tectonophysics: 176, 387-404, Amsterdam.

Franceschelli M., Memmi I., Pannuti F. & Ricci C.A. (1989b) - Diachronous metamorphic equilibria in the hercynian basement of northern Sardinia. In: Daly J.S., Cliff R.A. & Yardley B.W.D. (Eds.), Evolution of Metamorphic Belts, Geological Society of London Special Publications: 43, 371- 375.

Franceschelli, M., M., G. P., Dinandi, A., & Loi, M., 2005. Layered amphibolite sequence in NE Sardinia, Italy: Remnant of a pre-Variscan mafic silicic layered intrusion? Contributions to Mineralogy and Petrology , 149, 164-180.

Franke, W., 2000. The mid-European segment of the Variscides: tectono-stratigraphic units, terrane boundaries and plate tectonic evolution. J. Geol. Soc. London, Special Publications, 179, 35–61.

Gaggero, L., Oggiano, G., Funedda, A. & Buzzi, L., 2012. Rifting and arc-related early Paleozoic volcanism along the North Gondwana margin: geochemical and geological evidence from Sardinia (Italy). The Journal of Geology.

Gattacceca, J., & Rochette, P., 2004. Toward a robust relative paleointensity estimate in meteorites. Earth and Planetary Science Letters , 227, 377-393.

Ghezzo C., Memmi I. & Ricci C.A. (1979) - Un evento granulitico nella Sardegna nord-orientale. Mem. Soc. Geol. It.: 20, 23-38, Roma.

Giacomini, F., Bomparola, R., Grezzo, C., & Guldbransen, H., 2006. The geodynamic evolution of the Southern European Variscides: constraints from the U/Pb geochronology and geochemistry of the lower Paleozoic magmatic-sedimentary sequences of Sardinia Italy. Contrib Mineral Petrol , 152, 19–42.

S. Guillot, S. di Paola, R.P. Ménot, P. Ledru, M.I. Spalla, G. Gosso, S. Schwartz, Two Variscan suture zones in the External Crystalline Massifs of Western Alps and the importance of the dextral ECMs shear zone for Palaeozoic reconstruction, 2008 (submitted to Intern. J. Earth Sci.).

Loi, A., & Dabard, M. P. (1997). Zircon typology and geochemistry in the palaeogeographic reconstruction of the Late Ordovician of Sardinia (Italy).Sedimentary Geology, 112(3), 263-279.

Loriga, C. B., & Cassinis, G. (2003). 8 The Permo-Triassic boundary in the Southern Alps (Italy) and in adjacent Periadriatic regions. Permo-Triassic Events in the Eastern Tethys: Stratigraphy Classification and Relations with the Western Tethys, 2, 78.

P. Mameli, G. Mongelli, G. Oggiano, E. Dinelli, Geological, geochemical and mineralogical features of some bauxite deposits from Nurra (Western Sardinia, Italy): insights on conditions of formation and parental affinity, Inter. J. Earth Sci. 96 (2007) 877–902.

Martini, I., Oggiano, G. & Mazzei, R., 1992. Siliciclastic–carbonate sequences of Miocenegrabens of northern Sardinia, western Mediterranean Sea. Sed. Geol. 76, 63–78.

Matte, P., 2001. The Variscan collage and orogeny 480-290 Ma and the tectonic definition of the Armorica microplate: A review. Terra Nova , 13, 122-128.

G. Oggiano, P. Mameli, Diamictite and oolitic ironstones, a metasedimentary association at the Ordovician–Silurian transition in the North Gondwana margin: new evidence from the inner nappe of Sardinia Variscides (Italy), Gondwana Res. 9/4 (2006) 500–511.

Oggiano G., Gaggero L., Funedda A., Buzzi L. & Tiepolo M. 2010. Multiple early Paleozoic volcanic events at the northern Gondwana margin: U–Pb age evidence from the Southern Variscan branch (Sardinia, Italy). Gondwana Research 17, 44–58.

Ogniben, G. & De Pieri, R. (1967): I minerali di alterazione di Su Fruscu (Giacimento di Funtana Raminosa, Sardegna). Per. Miner., 36, 659-82.

Oudet, J., Münch, P., Borgomano, J., Quillevere, F., Melinte-Dobrinescu, M. C., Demory, F., ... & Cornee, J. J. (2010). Land and sea study of the northeastern golfe du Lion rifted margin: the Oligocene–Miocene of southern Provence (Nerthe area, SE France). Bulletin de la Société Géologique de France, 181(6), 591-607.

Pertusati, P. C., Sarria, E., Cherchi, G. P., Carmignani, L., Barca, S., Benedetti, M., ... & Pintus, C. (2002). Note Illustrative della Carta Geologica d 'Italia alla scala 1: 50.000, Foglio 541 Jerzu.

P. Rossi, A. Cocherie, Genesis of a Variscan batholith: field, mineralogical and geochemical evidence from the Corsica–Sardinia batholith, in: The European Geotraverse, Part 7, Tectonophysics195 (1991) 319–346.

Ph. Rossi, M. Durand-Delga, Cocherie A, Identification en Corse d'un socle panafricain (cadomien), conséquences sur la paléogéographie de l'orogène varisque sud-européen, C. R. Acad. Sci. Paris, Ser. IIa 321 (1995) 983–992.

Ph. Rossi, A. Cocherie, C. Fanning, E. Deloule, Variscan to eo-Alpine events recorded in European lower-crust zircons sampled from the French Massif Central and Corsica, France, Lithos 87 (2006) 235–260.

Rossi, P., Oggiano, G., & Cocherie, A. (2009). A restored section of the "southern Variscan realm" across the Corsica–Sardinia microcontinent. Comptes Rendus Geoscience, 341(2), 224-238.

Stampfli, G.M., von Raumer, J.F. & Borel, G.D., 2002, Paleozoic evolution of pre-Variscan terranes: From Gondwana to the Variscan collision. In: Martínez Catalán, J.R., Hatcher Jr., R.D., Arenas, R., Díaz García, F. (Eds.), Variscan-Appalachian dynamics: The building of the late Paleozoic basement: Boulder, Colorado. Geological Society of America Special Paper 364, pp. 263–280.

Stille H. (1939) - Bemerkungen betreffend die "Sardische" Faultung und den Ausdruck "Ophiolitisch". Z. dt. geol. Ges.: 91, 771-773, Stuttgart.

Vigliotti L. & Langenheim V.E. (1995) - When did Sardinia stop rotating? New paleomagnetic results. Terra Nova: 7, 424-435, Oxford.

Von Raumer, J., Stampfli, G., & Bussy, F., 2003. Gondwana-derived microcontinents — the constituents of the Variscan and Alpine collisional orogens. Tectonophysics , 365, 7–22.

Von Raumer, J., & Stampfli, G., 2008. The birth of the Rheic Ocean-Early Palaeozoic subsidence patterns and subsequent tectonic plate scenarios. Tectonophysics , 461, 9-20.

# 2. METHODS

This part will describe the approaches chosen and the methodologies used to conduct the research and how the procedures have been performed. The topics discussed are Bibliographic investigation of published work; geological and structural survey; sampling; natural radioactivity (portable gamma-rayspectrometry); whole rock geochemistry; isotopic analysis of detrital and magmatic zircons; cathodo-luminescence imaging and field observation**.**

## 2.1. GEOLOGICAL AND STRUCTURAL SURVEY AND SAMPLING

The geological survey was performed on CTR topographic base at 1: 10.000, trying to highlight the geometric relationships between geological bodies, analyzing the planar and linear scale meso and microscopic. It covers an area of about 400 square kilometers around the Gennargentu massif and Barbagia-Sarcidano areas. It's composed by three main zones: the Laconi-Asuni area (100 square kilometers), the Gadoni area (100 square kilometers), and the Gennargentu area (250 square kilometers). Field activity occurred in three years of the Phd Course. They were collected approximately 180 samples for petrographic analysis, structural analysis and microanalysis in thin section. Moreover were collected 7 samples for the geochronological analysis. From these samples they were extracted the zircons for typological study and geochronological study. They were collected the samples for the geochemistry analysis and spectrometric analysis.

## 2.2. PORTABLE GAMMA-RAY SPECTROMETRY

As some formations have a characteristic gamma-ray signal. Gamma-ray measures give us additional information that fill the deficiency of stratigraphic and lithologic markers in this area. Even if many natural elements have radioactive isotopes, only potassium, uranium and thorium decay series, have radioisotopes that produce gamma rays of sufficient energy and intensity to be measured by instruments. Average crustal abundances of these elements quoted in the literature are in the range 2-2.5% K, 2-3 ppm U and 8-12 ppm Th (Erdi-Krausz et al., 2003).

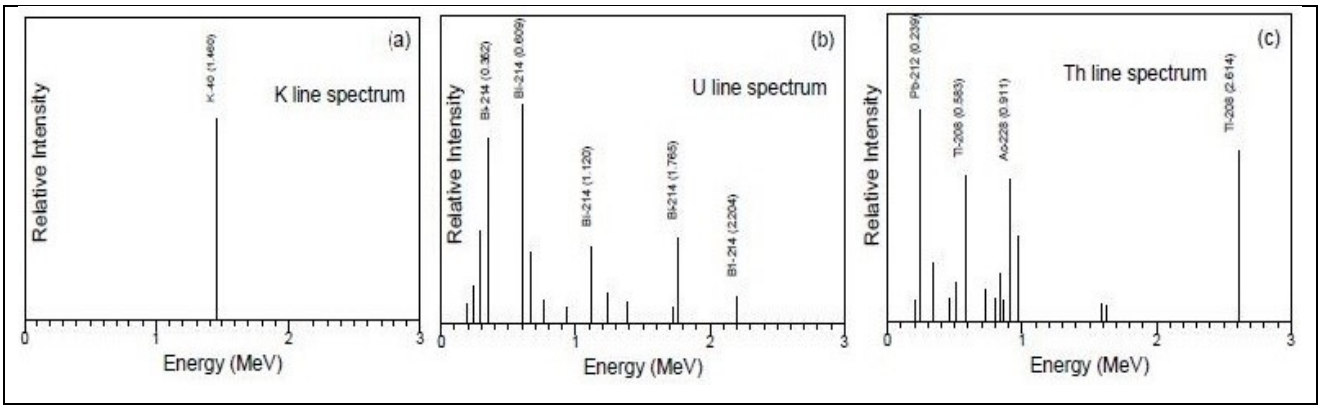


*Figure 8) Typical examples of potassium,m uranium (b) and thorium (c) spectra recorded by a NaI(Tl) detector with long integration times.*

Modern gamma ray spectrometers typically record 256 (or 512) channels of information in the energy range 0-3.0 MeV. The K energy window monitors the 1.46 MeV gamma rays emitted by 40K. The U and Th energy windows monitor gamma ray emissions of decay products in the U and Th decay series (**Fig.8 & 9**).

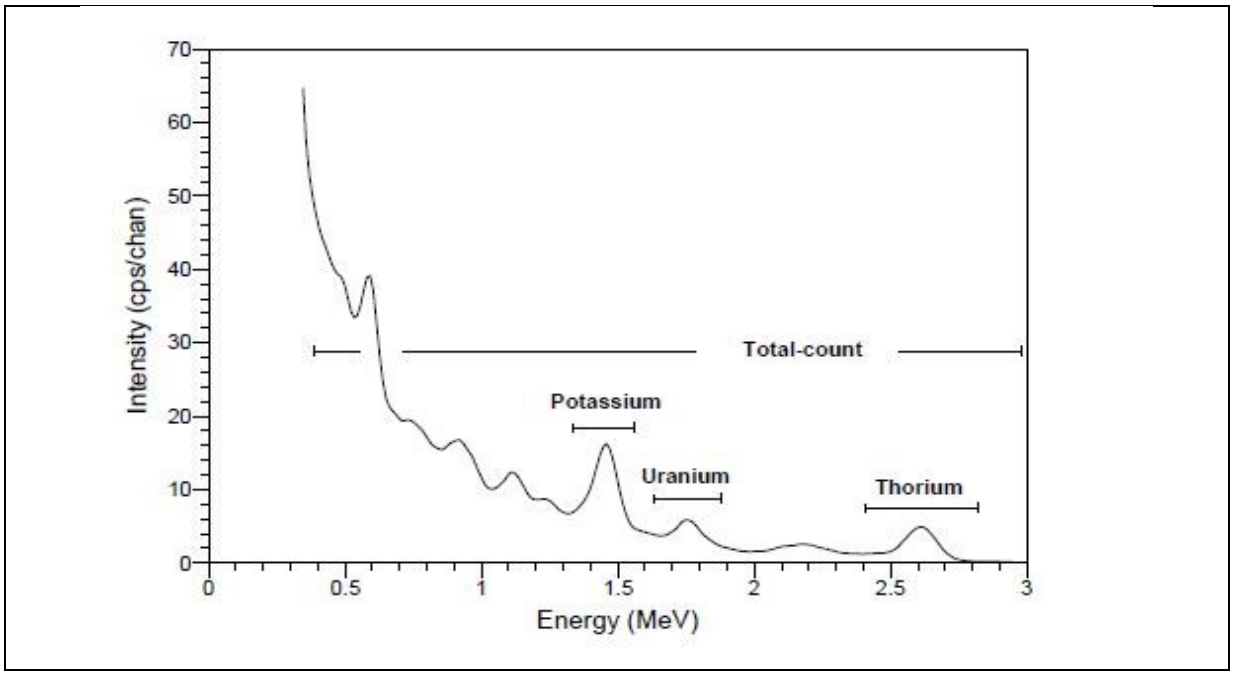


*Figure 9) Typical airborne gamma ray spectrum showing the positions of the conventional energy windows*

## 2.2.1. THE RS-230 SUPER SPEC PORTABLE SPECTROMETER

Field gamma-ray spectrometry was performed using a RS-230 Super Spec portable spectrometer (Radiation Solutions, Inc., Canada) (**Fig.10**), characterized by a 103 ccm bismuth-germanate (BGO) scintillation detector, whose sensitivity reaches approximately 80% of the commonly used 350 ccm NaI(Tl) crystals. Approximately 90% of the photons entering the scintillation detectors come from a dish-shaped volume of rock located in front of the detector, with a diameter and depth ranging from 50 to 90 cm and 15 to 35 cm, respectively, depending on the absorption coefficients of the material (Šimíček et al., 2012). The counts per minutes (cpm) in the selected windows are converted to concentrations in K (%), U (ppm) and Th (ppm). Potassium (K) is present in K-feldspars, micas and illitic clays. Thorium (Th) is concentrated in heavy minerals, such as monazite and zircon (Dabard et al., 2015; Pistis et al., 2015), or in the fine-grained fraction, in association with selected clay minerals (Herron & Matteson 1993) and as authigenic phosphates (Hurst 1990; Hurst & Midlowski 1994). Uranium (U) also occurs within the heavy minerals but can, additionally, be concentrated in anoxic sediments (Anderson et al. 1989; Lovley et al. 1991). In the study area we performed about 400 measures, with a counting time of 120 seconds each. These measures were distributed along the formations in order to identify their specific signal.

*Figure 10) The RS-230 Super Spec portable spectrometer (Radiation Solutions, Inc., Canada).*

## 2.3. GEOCHEMISTRY

The samples for the determination of major element oxides were sent to Actlabs laboratory (Canada) and results are reported in (**Table 1,2 & 3**) in the annexes section.

### 2.3.1. Instrumental Neutron Activation Analysis (INNA)

Neutron activation analysis is a useful method for the simultaneous determination of a large number (about 25-40) of major, minor and trace elements in small geological sample, without necessarily destroying the sample. The method allows the higly selective determination of elements (especially rare earth elements Sc, Cr, Co, Rb, Hf, Ta, W, Th, U and other elements of the platinum group) in the ppm and ppb concentration range with or without chemical treatment.

### 2.3.2. Inductively Coupled Plasma-Mass Spectometry (ICP-MS)

Inductively Coupled Plasma-Mass Spectrometry (or ICP-MS) is an analytical technique used for elemental determinations and was commercially introduced in 1983. ICP-MS has many advantages over other elemental analysis techniques such as atomic absorption and optical emission spectrometry and they are linked to a superior detection capability, particularly for the rare-earth elements (REEs), Ta, Nb, Hf, Th and U (typically less than 0,05 ng/ml), and ability to obtain isotopic information (Jarvis 1990; Hall et al. 1990). An ICP-MS combines a high-temperature ICP (Inductively Coupled Plasma) source with a mass spectrometer.

### 2..3.3. Scanning Electron Microscopy and EDS Analysis

The scanning electron microscope (SEM) consists of an electron gun and a number of electromagnetic lenses, all within an evacuated column where a electrons beam is accelerated by a high voltage and then focused by two condenser lenses onto the thin specimen. Finally, the objective focused the beam onto the sample surface and the beam is moved or scanned across an area. At any instant, signals being generated by the beam can be collected by appropriate detectors and one of them used to control the intensity on a cathode ray tube. Latter is scanned synchronously with the incident beam so that an image of the area as it is scanned is build up on the cathode ray tube. Thus, the scanning electron microscope permits the observation and characterization of heterogeneous organic and inorganic materials on a nanometer (nm) to micrometer (μm) scale and it

provides information about the surface structure of the specimen. The popularity of the SEM, in fact, stems from its capability of obtaining three-dimensional-like images of the surfaces of a very wide range of materials (Goldstein et al. 2003).

## 2.4. ZIRCONS GEOCHEMISTRY

Zircon (ZrSiO4) is a common accessory mineral in nature, occurring in a wide variety of sedimentary, igneous, and metamorphic rocks. Known to incorporate an assortment of minor and trace elements, zircon has the ability to retain substantial chemical and isotopic information, leading to its use in a wide range of geochemical investigations, including studies on the evolution of Earth's crust and mantle (Hanchar et al. 1994; Hanchar et al. 1994, Bowring 1995; Vervoort et al. 1996) as well as age dating (Gibson and Ireland 1995; Bowring et al. 1998; Solar et al. 1998).

The physical and chemical durability of zircon is a major factor in it being the mineral by which many of Earth's oldest known rocks have been dated. (Bowring et al. 1989; Maas et al. 1992; Buick et al. 1995; Bowring and Williams 1999; Wilde et al. 2001)

Analyses of zircon commonly report trace amounts (or more) of P, Y, Hf, U, Th, and REE (Sawka 1988; Bea, 1996; O'Hara et al. 2001). These elements are importantgeochemically as process indicators or parent isotopes for age determination. The importance of zircon in crustal evolution studies is underscored by its predominant use in U-Th-Pb geochronology and investigations of the temporal evolution of both the crust and lithospheric mantle.

### 2.4.1. U-Pb Geochronology of Zircon

The potential of zircon as geochronometria has been recognized by Holmes (1911), among others, well before isotopes of Pb could be measured, and long before the identification of the 235U as the second radioactive isotope of uranium. It is now known that there are three distinct series of radioactive decay involving the parent isotope 238U, 235U and 232Th, which respectively produce the daughter isotopes 206Pb, 207Pb and 208Pb. The whole process of decay can be mathematically described by a single equation of decay that relates atoms remaining parent isotope (eg .: 238U) and the number of atoms of the isotope daughter (for example, 206Pb *) with time:

$$206Pb^* / 238U = e^{\lambda 238t} - 1$$

where e is the exponential function, t is time, and λ is the decay constant for this specific pattern of decay, that is, λ238 = 1.55125e-10. 206Pb * refers to radiogenic 206Pb accumulated in the crystal as a result of the decay of 238U. In the case of 238U, it takes about 4,468,000 years to transform half of 238U initially present in the crystal in 206Pb. This is the half-life, characteristic of the specific pattern of decay. Similar expressions can be formulated for 207Pb * produced by the decay of 235U and 232Th to 208Pb * product, with λ235 = 9.8485e-10 and λ232 = 4.9475e-11.

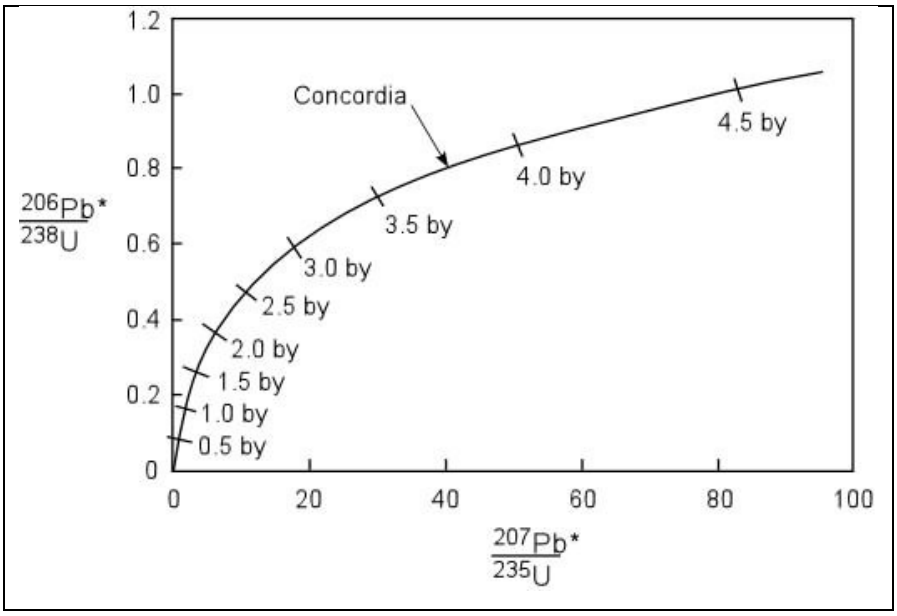


*Figure 11) The U-Pb Concordia Pb206/U238 and Pb207/U235.*

The usual approach in geochronological studies based on zirconium is to consider the system U-Pb alone, thanks to the absence of fractionation phenomena natural 235U from 238U. Moreover, the current ratio 235U / 238U is well known (1 / 137.88), it is not necessary to analyze very low concentrations of 235U. Instead of solving systems of 235U and 238U decay separately, you can draw the diagram 206Pb * / 238U vs. 207Pb * / 235U in which the isotopic ratios grow over time since their formation (ie the age of zircon or its microdomain). This is the basis of the diagram concord (Wetherill, 1956). The concordia curve (**Fig.11**) itself is the locus of points where the relationships 207Pb * / 235U and 206Pb * / 238U, increase in concordance from the origin.

## 2.4.2. Cathodoluminescence Imaging

A **cathodoluminescence (CL) microscope** combines methods from electron and regular (light optical) microscopes. It is designed to study the luminescence characteristics of polished thin sections of solids irradiated by an electron beam. Using a cathodoluminescence microscope, structures within crystals or fabrics can be made visible which cannot be seen in normal light conditions (Gotze, 2002). Thus, for example, valuable information on the growth of minerals can be obtained. In this research the technique of cathodoluminescence was used for the study of both magmatic zircons that of detrital zircons; analyzes were carried out at the University of Genoa (**Fig.12**).

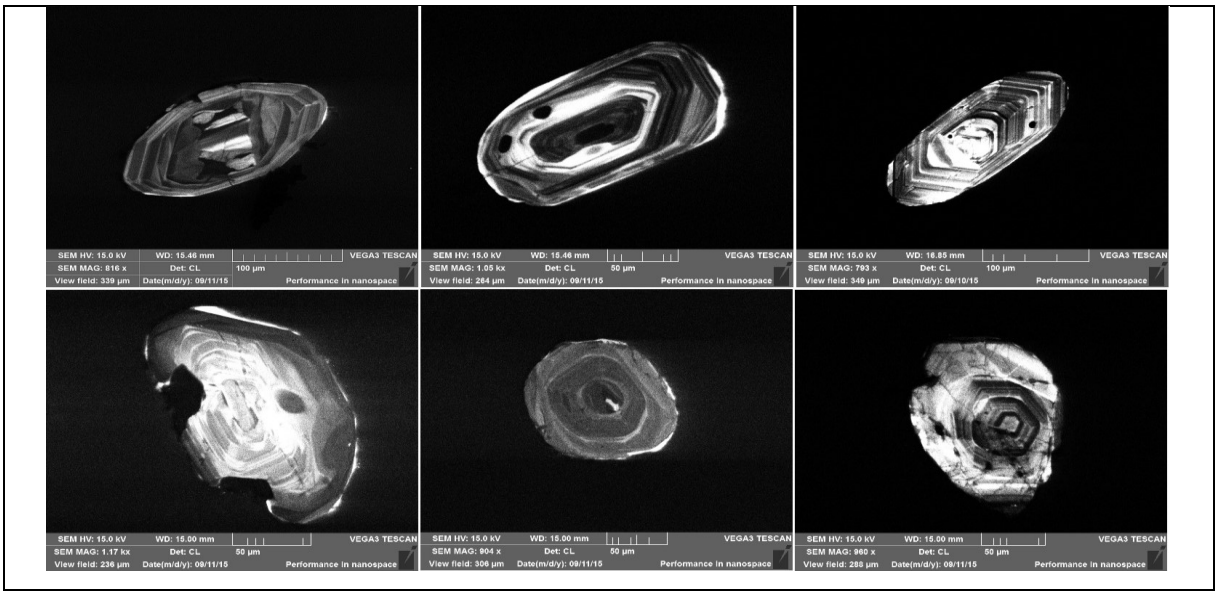

*Figure 12) Zircons CL images (DISTAV,* University of Genoa).

## 2.4.3. Procedures Perfomed

Zircon concentrates were separated from 2-4 kg sample material at the using standard methods. Final selection of the zircon grains for U-Pb dating was achieved by hand-picking under a binocular microscope. Zircon grains of all grain sizes and morphological types were selected, mounted in resin blocks and polished to half their thickness.

Zircons were analyzed for U, Th, and Pb isotopes by LA-SF ICP-MS techniques at the Museum für Mineralogie und Geologie (GeoPlasma Lab, Senckenberg Naturhistorische Sammlungen Dresden),

using a Thermo-Scientific Element 2 XR sector field ICP-MS coupled to a New Wave UP-193 Excimer Laser System (**Fig.13 & 14**).

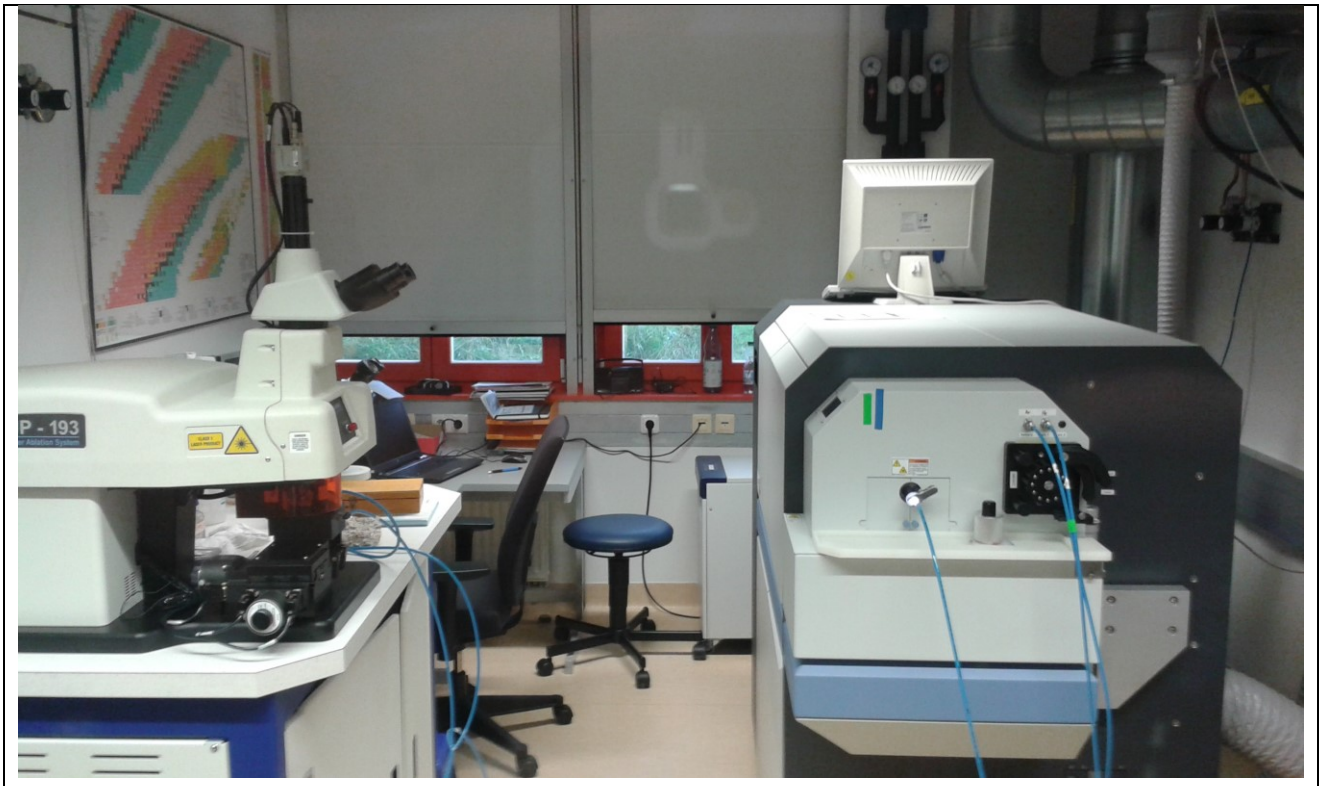


*Figure 13) Laboratory atwith a Senckenberg Natural History Collections Dresden, Head of Department, Museum of Mineralogy and Geology, Section Geochronology NewWave UP-193 ArFexcimer ablation system and a sector-field spectrometer Element XR.*

A teardrop-shaped, low volume laser cell constructed by Ben Jähne (Dresden) and Axel Gerdes (Frankfurt/M.) was used to enable sequential sampling of heterogeneous grains (e.g., growth zones) during time resolved data acquisition. Each analysis consisted of approximately 15 s background acquisition followed by 30 s data acquisition, using a laser spot-size of 25 and 35 µm, respectively.

A common-Pb correction based on the interference- and background-corrected $^{204}$Pb signal and a model Pb composition (Stacey and Kramers, 1975) was carried out if necessary. Raw data were corrected for background signal, common Pb, laser induced elemental fractionation, instrumental mass discrimination, and time-dependant elemental fractionation of Pb/Th and Pb/U using an Excel® spreadsheet program developed by Axel Gerdes (Institute of Geosciences, Johann Wolfgang Goethe-University Frankfurt, Frankfurt am Main, Germany).

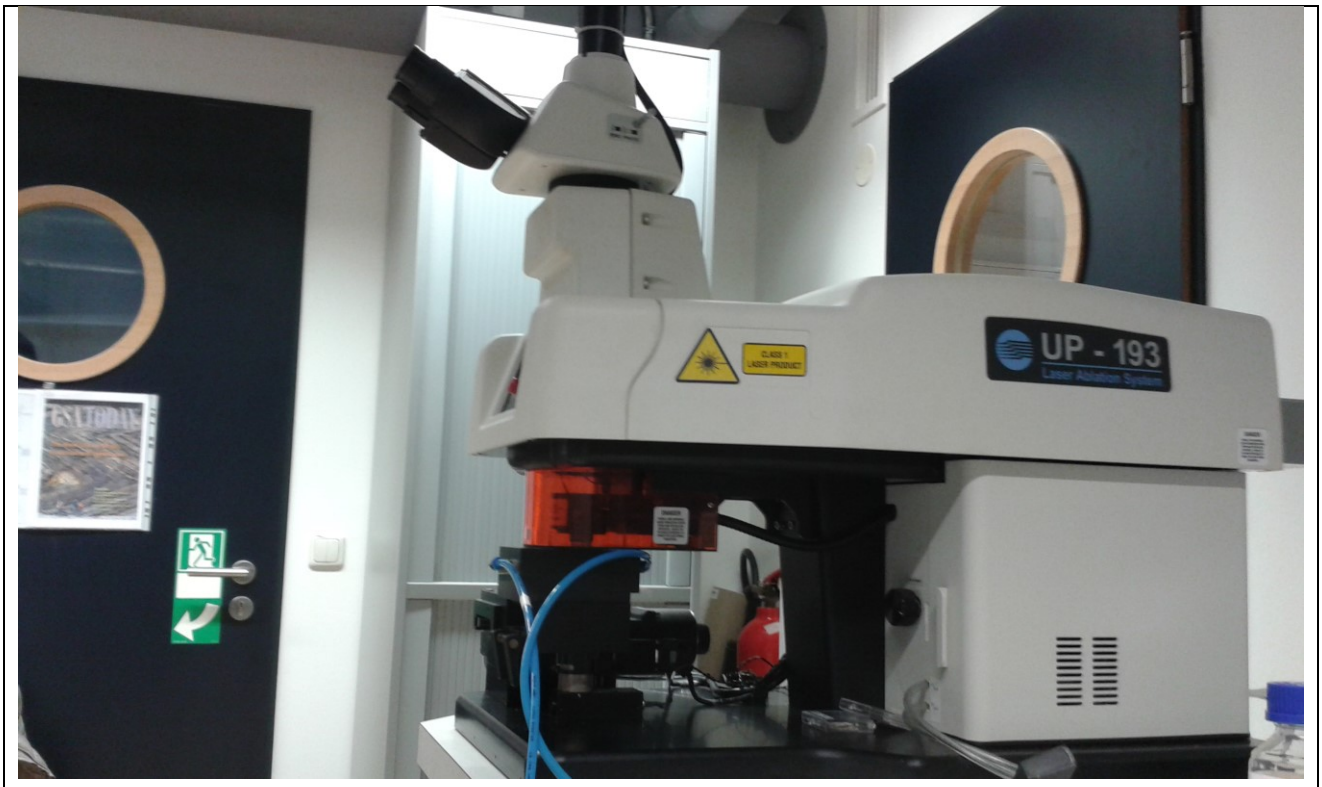


*Figure 14) Laboratory at with a Senckenberg Natural History Collections Dresden, Head of Department, Museum of Mineralogy and Geology, Section Geochronology NewWave UP-193 ArFexcimer ablation system.*

Reported uncertainties were propagated by quadratic addition of the external reproducibility obtained from the standard zircon GJ-1 (~0.6% and 0.5-1% for the $^{207}Pb/^{206}Pb$ and $^{206}Pb/^{238}U$, respectively) during individual analytical sessions and the within-run precision of each analysis. Concordia diagrams (2σ error ellipses) and concordia ages (95% confidence level) were produced using Isoplot/Ex 2.49 (Ludwig, 2001) and frequency and relative probability plots using AgeDisplay (Sircombe, 2004).

The $^{207}Pb/^{206}Pb$ age was taken for interpretation for all zircons >1.0 Ga. For further details on analytical protocol and data processing see Gerdes and Zeh (2006) and Frei and Gerdes (2009). Zircons showing a degree of concordance in the range of 90-110 % in this paper are classified as concordant because of the overlap of the error ellipse with the concordia. Th/U ratios are obtained from the LA-ICP-MS measurements of investigated zircon grains. U and Pb content and Th/U ratio were calculated relative to the GJ-1 zircon standard and are accurate to approximately 10%.

# REFERENCES

Anderson, R. F., Le Huray, A. P., Fleisher, M. Q., & Murray, J. W. (1989). Uranium deposition in Saanich Inlet sediments, Vancouver Island. Geochimica et Cosmochimica Acta, 53(9), 2205-2213.

Bea F (1996) Residence of REE, Y, Th and U in granites and crustal protoliths; implications for the chemistry of crustal melts. J Petrol 37:521-552.

Bowring SA, Williams IS, Compston W (1989) 3.96 Ga gneisses from the Slave Province, Northwest Territories, Canada. Geology 17:971-975.

Bowring SA (1995) The Earth's early evolution. Science 269:1535-1540.

Bowring SA, Erwin DH, Jin YG, Martin MW, Davidek K, Wang W (1998) U/Pb zircon geochronology and tempo of the end-Permian mass extinction. Science 280:1039-1045.

Bowring SA, Williams IS (1999) Priscoan (4.00-4.03 Ga) orthogneisses from northwestern Canada. Contrib Mineral Petrol 134:3-16.

Buick R, Thornett JR, McNaughton NJ, Smith JB, Barley ME, Savage M (1995) Record of emergent continental crust similar to 3.5 billion years ago in the Pilbara craton of Australia. Nature 375:574-575.

Davies, S. J., & Elliott, T. (1996). Spectral gamma ray characterization of high resolution sequence stratigraphy: examples from Upper Carboniferous fluvio-deltaic systems, County Clare, Ireland.

Erdi-Krausz, G., Matolin, M., Minty, B., Nicolet, J., Reford, W., & Schetselaar, E. (2003). Guidelines for Redioelement Mapping Using Gamma Ray Spectrometry Data. International Atomic Energy Agency Publication IAEA-TECDOC-1363, Vienna, Austria.

Gerdes, A., & Zeh, A. (2006). Combined U–Pb and Hf isotope LA-(MC-) ICP-MS analyses of detrital zircons: comparison with SHRIMP and new constraints for the provenance and age of an Armorican metasediment in Central Germany. Earth and Planetary Science Letters, 249(1), 47-61.

Gerdes, A., & Zeh, A. (2009). Zircon formation versus zircon alteration—new insights from combined U–Pb and Lu–Hf in-situ LA-ICP-MS analyses, and consequences for the interpretation of Archean zircon from the Central Zone of the Limpopo Belt. Chemical Geology, 261(3), 230-243.

Gibson GM, Ireland TR (1995) Granulite formation during continental extension in Fiordland, New Zealand. Nature 375:479-482.

Goldstein J., Newbury D.E., Joy D.C., Echlin P., Lyman C.E., Lifshin E. (2003) - Scanning electron microscopy and X-ray microanalysis. Springer Ed., vol. 1, 689 pp.

Götze, J. (2002). Potential of cathodoluminescence (CL) microscopy and spectroscopy for the analysis of minerals and materials. Analytical and bioanalytical chemistry, 374(4), 703-708.

Hall G.E.M., Pelchat J.C. and Loop J. (1990) – Determination of zirconium, niobium, hafnium and tantalum at low levels in geological materials by inductively coupled plasma mass spectrometry. J. Anal. at Spectrom, 5, 339-349.

Hanchar JM, Miller CF, Wooden JL, Bennett VC, Staude J-MG (1994) Evidence from xenoliths for a dynamic lower crust, eastern Mojave desert, California. J Petrol 35:1377-1415.

Herron, M. M., & Matteson, A. (1993). Elemental composition and nuclear parameters of some common sedimentary minerals. The International journal of radiation applications and instrumentation. Part E. Nuclear geophysics, 7(3), 383-406.

Hurst, A. (1990). Natural gamma-ray spectrometry in hydrocarbon-bearing sandstones from the Norwegian Continental Shelf. Geological Society, London, Special Publications, 48(1), 211-222.

Hurst, A., & MlDLOWSKI, A. E. (1994). Characterisation of clays in sandstones: Thorium content and spectral log data. In Transactions of the European Formation Evaluation Symposium, Paper S.

Jarvis K.E. (1990) – A critical evaluation of two sample preparation techniques for low level determination of some geologically incompatible elements by inductively coupled plasma mass spectrometry. Chemical Geology, 83, 89-103.

Lovley, D. R., Phillips, E. J., Gorby, Y. A., & Landa, E. R. (1991). Microbial reduction of uranium. Nature, 350(6317), 413-416.

Ludwig, D. S., Peterson, K. E., & Gortmaker, S. L. (2001). Relation between consumption of sugar-sweetened drinks and childhood obesity: a prospective, observational analysis. The Lancet, 357(9255), 505-508.

Maas R, Kinny PD, Williams IS, Froude DO, Compston W (1992) The Earth's oldest known crust: a geochronological and geochemical study of 3900-4200 Ma old detrital zircons from Mt. Narryer and Jack Hills, Western Australia. Geochim Cosmochim Acta 56:1281-1300.

O'Hara MJ, Fry N, Prichard HM (2001) Minor phases as carriers of trace elements in non-modal crystal-liquid separation processes II: illustrations and bearing on behaviour of REE, U, Th and the PGE in igneous processes. J Petrol 42:1887-1910.

Sawka WN (1988) REE and trace element variation in accessory minerals and hornblende from the strongly zoned McMurry Meadows Pluton, California. Trans Roy Soc Edinburgh: Earth Sci 79:157-168.

Sircombe, K. N. (2004). AgeDisplay: an EXCEL workbook to evaluate and display univariate geochronological data using binned frequency histograms and probability density distributions. Computers & Geosciences, 30(1), 21-31.

Šimíček, D., Bábek, O., & Leichmann, J. (2012). Outcrop gamma-ray logging of siliciclastic turbidites: Separating the detrital provenance signal from facies in the foreland-basin turbidites of the Moravo-Silesian basin, Czech Republic. Sedimentary Geology, 261, 50-64.

Stacey, J. T., & Kramers, 1. (1975). Approximation of terrestrial lead isotope evolution by a two-stage model. Earth and Planetary Science Letters, 26(2), 207-221.

Solar GS, Pressley RA, Brown M, Tucker RD (1998) Granite ascent in convergent orogenic belts: Testing a model. Geology 26:711-714.

Vervoort JD, Patchett PJ, Gehrels GE, Nutman AP (1996) Constraints on early Earth differentiation from hafnium and neodymium isotopes. Nature 379:624-627.

Wilde SA, Valley JW, Peck WH, Graham CM (2001) Evidence from detrital zircons for the existence of continental crust and oceans on the Earth 4.4 Gyr ago. Nature 409:175-178.

# SECOND PART (RESULTS)

- *Radiometric Data*
- *Geochronology*
- *The laconi-Asuni area*
- *The Gadoni area*

# 3. RADIOMETRIC DATA

The Polyphasic deformation and regional metamorphism mask the primary lithologic characters of formations, so lithostratigraphic correlations are very complicated. In the geological survey we utilized natural radioactivity (outcrop gamma-ray spectrometry) which allows us to recognize lithologic formations difficult to identify. This is because some formations have a characteristic gamma-ray signal. Gamma-ray measures give us additional information that fill the deficiency of stratigraphic and lithologic markers in this area. In the study area we performed about 400 measures (**Fig.15**), with a counting time of 120 seconds each. These measures were distributed along the formations in order to identify their specific signal. During the geological survey some formations showed a particular recognizable gamma-ray signal, this signal was very useful to characterize the formations.

| N° | Total[cpm] | K[%] | U[ppm] | Th[ppm] | N° | Total[cpm] | K[%] | U[ppm] | Th[ppm] | N° | Total[cpm] | K[%] | U[ppm] | Th[ppm] | N° | Total[cpm] | K[%] | U[ppm] | Th[ppm] | N° | Total[cpm] | K[%] | U[ppm] | Th[ppm] |
|---|---|---|---|---|---|---|---|---|---|---|---|---|---|---|---|---|---|---|---|---|---|---|---|---|
| 1 | 3738,2 | 0,3 | 6,7 | 9,6 | 41 | 5423,5 | 3,5 | 3,1 | 18,4 | 81 | 4442,4 | 3,3 | 2,4 | 14,5 | 121 | 34950,2 | 1,9 | 16,9 | 247,7 | 161 | 4401,8 | 1,5 | 3,5 | 21,8 |
| 2 | 7958,9 | 4,6 | 8,2 | 24 | 42 | 4191 | 3,8 | 3,4 | 20,3 | 82 | 4382,3 | 2,7 | 3 | 13,7 | 122 | 5642,4 | 3,8 | 3,3 | 17,2 | 162 | 3757 | 2,2 | 3,1 | 12,5 |
| 3 | 1175 | 0,3 | 1,3 | 4,9 | 43 | 7030,7 | 1,2 | 5,9 | 13,3 | 83 | 4971,9 | 3,6 | 3,3 | 13,8 | 123 | 3160,7 | 1,5 | 2,4 | 11,6 | 163 | 5911,3 | 4,3 | 3,4 | 19,6 |
| 4 | 8262,2 | 1,4 | 19,6 | 14,5 | 44 | 9092,8 | 2,9 | 3,5 | 35,3 | 84 | 4536,9 | 2,9 | 2,9 | 12,5 | 124 | 2377,9 | 0,7 | 3,7 | 8,8 | 164 | 6924,7 | 5,4 | 3,3 | 22,3 |
| 5 | 12670,4 | 0,5 | 37,1 | 18 | 45 | 4616,2 | 3,5 | 3,9 | 48,4 | 85 | 4320,9 | 3 | 2,8 | 13,9 | 125 | 3630 | 2,5 | 3,1 | 9,4 | 165 | 1710,1 | 1 | 1,8 | 5,2 |
| 6 | 4374,5 | 0,8 | 8,6 | 12,8 | 46 | 2119,8 | 0,7 | 1,9 | 8,9 | 86 | 4389,1 | 2,4 | 3 | 14,6 | 126 | 3330,6 | 2,4 | 2,2 | 8,6 | 166 | 2634,8 | 1,1 | 3,9 | 8 |
| 7 | 7073,5 | 5 | 4,6 | 22,3 | 47 | 3319,6 | 1,8 | 4,1 | 13,0 | 87 | 6118,3 | 4,1 | 4,7 | 19,9 | 127 | 4838,1 | 2,7 | 4,2 | 16,9 | 167 | 8092,1 | 4,7 | 4,6 | 32,2 |
| 8 | 4923,8 | 4 | 3,3 | 10,3 | 48 | 2355,2 | 3,2 | 3,9 | 13,3 | 88 | 6495,5 | 4,5 | 3,5 | 21,2 | 128 | 5007,6 | 3,4 | 3,8 | 15 | 168 | 7391,3 | 5 | 4,4 | 22,8 |
| 9 | 15306,6 | 0,7 | 45,6 | 15,3 | 49 | 14330,2 | 3,3 | 7,3 | 78,8 | 89 | 7661,9 | 6,3 | 3,7 | 20 | 129 | 3285,1 | 1,6 | 3,2 | 11,7 | 169 | 8423 | 4,4 | 4,4 | 32 |
| 10 | 2016,8 | 0,2 | 3,3 | 5,8 | 50 | 4557,5 | 4,1 | 4,1 | 14,9 | 90 | 6196,9 | 4,7 | 3,9 | 16,9 | 130 | 3898,3 | 1,9 | 3,3 | 13,8 | 170 | 8408,3 | 4,5 | 5 | 32,9 |
| 11 | 21963,3 | 0,8 | 70 | 17 | 51 | 4982,7 | 3,9 | 5,3 | 17,2 | 91 | 6329 | 4,9 | 3,2 | 18,8 | 131 | 9670,7 | 6,7 | 9,1 | 25,5 | 171 | 28050,5 | 5,5 | 12,8 | 166,4 |
| 12 | 8918,5 | 6,6 | 9,1 | 19,3 | 52 | 5245,6 | 3,5 | 4,3 | 15,8 | 92 | 7650,6 | 5,1 | 4,7 | 24,8 | 132 | 3076,7 | 1,7 | 2 | 10,8 | 172 | 32465,8 | 5 | 15,4 | 208,1 |
| 13 | 4159,9 | 1,2 | 5,3 | 14,6 | 53 | 5514,5 | 3,8 | 3,6 | 17,7 | 93 | 5968,7 | 4,3 | 3 | 17,9 | 133 | 4679,8 | 3,6 | 3,9 | 10,4 | 173 | 7903,7 | 4,5 | 3,7 | 24,1 |
| 14 | 6358,2 | 1,3 | 12,7 | 13,4 | 54 | 8056,6 | 7,4 | 3,3 | 20,8 | 94 | 6453 | 4,5 | 3,7 | 21,2 | 134 | 5581,5 | 4 | 3,2 | 15,4 | 174 | 9323,8 | 5,9 | 6,1 | 35,2 |
| 15 | 1654,4 | 0,6 | 2 | 5,1 | 55 | 4346,5 | 1,7 | 5 | 15,7 | 95 | 6995,4 | 5,5 | 4 | 21,6 | 135 | 2720,7 | 1,3 | 2,8 | 8,8 | 175 | 3836 | 0,8 | 3,2 | 19,9 |
| 16 | 8037,5 | 5,7 | 6,2 | 21 | 56 | 5490,4 | 3,9 | 3,6 | 14,1 | 96 | 7010,5 | 4,9 | 3,7 | 21,7 | 136 | 9508 | 7,1 | 6,1 | 23,9 | 176 | 5299,7 | 3 | 4,8 | 18,9 |
| 17 | 4280 | 1,1 | 5,2 | 16,2 | 57 | 4380,2 | 1,9 | 4,4 | 16,3 | 97 | 3443,6 | 3,3 | 1,7 | 7,1 | 137 | 3887,4 | 3,5 | 2,2 | 8,3 | 177 | 10747,9 | 3,4 | 6,3 | 55,2 |
| 18 | 5108,5 | 3,9 | 2,5 | 16,8 | 58 | 6361,6 | 2,2 | 4,9 | 27 | 98 | 3052,9 | 2 | 2 | 9,3 | 138 | 14267,8 | 2,8 | 5,9 | 94 | 178 | 39108,6 | 3,9 | 16,2 | 273,1 |
| 19 | 4355,7 | 2,7 | 2,1 | 15,8 | 59 | 4156,8 | 2,5 | 2,5 | 14,4 | 99 | 639,7 | 0,2 | 1,3 | 1,1 | 139 | 8330,2 | 6,3 | 8,2 | 18,1 | 179 | 44075,5 | 5,5 | 21,6 | 300 |
| 20 | 7447,4 | 5,4 | 5,6 | 22,4 | 60 | 3227,4 | 2 | 2,5 | 9,8 | 100 | 4257,2 | 3,5 | 2,1 | 9,2 | 140 | 3219,6 | 0,6 | 2,4 | 17 | 180 | 37008,5 | 3,8 | 17,9 | 248,7 |
| 21 | 7849 | 6,7 | 5,5 | 17,2 | 61 | 1050 | 0,2 | 2,2 | 1,7 | 101 | 2853,5 | 1,8 | 2,2 | 9,9 | 141 | 5701 | 3,9 | 4,2 | 16,4 | 181 | 65958,1 | 3,7 | 28,9 | 475,4 |
| 22 | 7532,3 | 3,6 | 7,1 | 29,5 | 62 | 6228,6 | 4,3 | 3,4 | 19,2 | 102 | 24615,8 | 2,9 | 10,9 | 171,3 | 142 | 5619,3 | 4,6 | 3,4 | 15,1 | 182 | 66271,1 | 3,5 | 38,2 | 470,1 |
| 23 | 5128,6 | 3 | 3,5 | 20 | 63 | 4809,8 | 2,3 | 3,8 | 17,2 | 103 | 16855 | 2,8 | 6,3 | 110,5 | 143 | 4227,4 | 3,2 | 2,5 | 12,1 | 183 | 70226,9 | 3,1 | 30,5 | 503,5 |
| 24 | 6598,4 | 4,7 | 3,7 | 19,1 | 64 | 7921,1 | 6,1 | 3,3 | 21,8 | 104 | 9930,6 | 2,9 | 5,3 | 57,5 | 144 | 6903,4 | 4,9 | 6,1 | 18,7 | 184 | 3986,9 | 1,3 | 2,2 | 18,5 |
| 25 | 5978 | 4,3 | 2,9 | 18,4 | 65 | 5535,4 | 4,4 | 3,2 | 17,9 | 105 | 19591,4 | 3 | 9,4 | 126,9 | 145 | 4895,7 | 3,7 | 2,6 | 12,7 | 185 | 3404,3 | 3 | 1,9 | 7,6 |
| 26 | 1518 | 0,5 | 1 | 7,7 | 66 | 5587,9 | 4,2 | 3,1 | 16 | 106 | 5550,1 | 3,6 | 2,6 | 20,6 | 146 | 4273,4 | 3,1 | 3,3 | 11,5 | 186 | 3972,5 | 2,1 | 3,1 | 14,6 |
| 27 | 5010,3 | 3,4 | 2,7 | 16,1 | 67 | 5665,2 | 4,3 | 3,2 | 17,9 | 107 | 5411,6 | 3,9 | 3,2 | 15,6 | 147 | 3265,3 | 2,5 | 2,1 | 8,8 | 187 | 1840,9 | 0,6 | 2 | 7 |
| 28 | 4733,5 | 3,1 | 2,4 | 16,9 | 68 | 6068,7 | 4,8 | 3,2 | 17,7 | 108 | 3903,6 | 3,9 | 1,9 | 7,7 | 148 | 5746,8 | 4,1 | 3,5 | 19,6 | 188 | 6568 | 5 | 3,9 | 18,4 |
| 29 | 5357,2 | 3,5 | 3,2 | 17,7 | 69 | 5901,5 | 4,1 | 3,2 | 18,9 | 109 | 5026,8 | 3,9 | 2,4 | 13,8 | 149 | 4300,8 | 2,6 | 3 | 13 | 189 | 5317,4 | 3,7 | 3,8 | 14,4 |
| 30 | 7537,8 | 5,7 | 6,1 | 21,4 | 70 | 5039,1 | 3,9 | 3,9 | 14,3 | 110 | 7495,3 | 5,5 | 3,7 | 22,8 | 150 | 5993,8 | 4,1 | 5,4 | 17,8 | 190 | 4361,3 | 3,3 | 3,6 | 11,8 |
| 31 | 6331,6 | 4,6 | 3,7 | 18,9 | 71 | 6096,1 | 4,4 | 2,9 | 18 | 111 | 2000 | 1,2 | 1,1 | 4,3 | 151 | 6012,4 | 3,5 | 5,8 | 17,9 | 191 | 6093,6 | 4,2 | 2,9 | 21,4 |
| 32 | 5841,5 | 4,2 | 3,5 | 15,1 | 72 | 6793,8 | 4,6 | 4,1 | 24,3 | 112 | 2854,7 | 1,9 | 0,9 | 8 | 152 | 3910,6 | 2 | 3,8 | 13,7 | 192 | 2094,2 | 0,8 | 1,7 | 8,7 |
| 33 | 4836,1 | 2,6 | 2,4 | 16,4 | 73 | 7775,1 | 5,5 | 5,1 | 23,9 | 113 | 2354,5 | 1,7 | 0,9 | 6,3 | 153 | 6213,3 | 1,4 | 11,4 | 16,9 | 193 | 6002,1 | 4,4 | 3,7 | 17,2 |
| 34 | 6296,9 | 4,6 | 3,1 | 19 | 74 | 6120,2 | 4,6 | 4,4 | 18 | 114 | 3923,2 | 2,9 | 1,4 | 12,4 | 154 | 3797,5 | 0,6 | 3,6 | 18,2 | 194 | 4999,9 | 3,1 | 3,2 | 18,2 |
| 35 | 6259,2 | 3,5 | 2,2 | 14,8 | 75 | 6483,7 | 5,4 | 4,4 | 16,8 | 115 | 6707 | 5,4 | 3,3 | 18,2 | 155 | 6327,2 | 3,5 | 4,2 | 25,4 | 195 | 2293,6 | 0,6 | 3,3 | 6,7 |
| 36 | 6456,5 | 3,6 | 5,4 | 21,8 | 76 | 4292,3 | 2,8 | 3 | 14,9 | 116 | 5560 | 3,9 | 3,4 | 15,5 | 156 | 4429,5 | 1,1 | 5,9 | 15,8 | 196 | 7659,7 | 2,5 | 14 | 17,6 |
| 37 | 7512,5 | 5,5 | 4,7 | 22,8 | 77 | 4144,7 | 2,8 | 2,4 | 13 | 117 | 5597,2 | 4,2 | 2,9 | 19,4 | 157 | 14220,2 | 4,8 | 6,5 | 76,8 | 197 | 2165,6 | 0,7 | 2,6 | 8,2 |
| 38 | 3706,3 | 2,5 | 1,9 | 11,8 | 78 | 3800,3 | 2,4 | 3,9 | 11,6 | 118 | 11664,3 | 4 | 5,2 | 65,7 | 158 | 10221,6 | 4,7 | 6,3 | 45,6 | 198 | 4609 | 0,4 | 6,7 | 22,7 |
| 39 | 9485,2 | 4,4 | 15,9 | 18,6 | 79 | 3774,1 | 2,3 | 2,3 | 10,5 | 119 | 5867,5 | 4 | 2,8 | 18,5 | 159 | 8280,7 | 0,7 | 20,9 | 16 | 199 | 4436,6 | 1 | 4,1 | 21,3 |
| 40 | 9060,6 | 1,4 | 6,5 | 52,5 | 80 | 4337,6 | 2,7 | 3,5 | 12,9 | 120 | 29351,5 | 2,8 | 11,9 | 201,5 | 160 | 6400,4 | 3,9 | 4,4 | 24,5 | 200 | 3291,4 | 0,4 | 3,8 | 16,8 |

*Figure 15) Field gamma-ray spectrometry data in the study area.*

## 3.1. MEANA SARDO UNIT

Most of the metasedimentary formations within the Meana Sardo Unit (Carmignani et al. 1982) are distinguishable on palaeontological bases and the volcanic ones exhibits peculiar textural and mineralogical features, still evident despite the deformation, hence the gamma ray values of these rocks were used as benchmarks for correlations with the nappes bearing more severe metamorphism and deformation, the GRS response allows us showed meaningful differences between the Orroeledu Fm (ORRa,b) and the Scisti a Graptoliti Fm (SGA and SGAa), however, in a less obvious way the MSVc, MSVb and the SVI formations have characteristic gamma-ray signals as well.

**3.1.1 Arenarie di San Vito Fm (SVI),** (Calvino, 1959) is characterized by middle values of total counts (2800 total cpm). This Formation shows average values of Th similar 13 ppm, U similar 4 ppm and K close to 2,5%. This Formation emerges in a very restricted area, for this in statistical terms is not important.

**3.1.2 Monte Santa Vittoria Fm (MSVa,b,c)** (Oggiano et al., 2010) is composed of metavolcanites, metagreywackes, metaepiclastites and metaconglomerates. This volcanic succession shows middle values of Th reaching 10 ppm whit low values of 2-3 K % in the basic metavolcanites and 4-5 K % in the rhyolitic metavolcanites. The rhyolitic metavolcanites shows values of Th reaching 15 ppm (**Fig.16**). The middle total counts ranging from 3300 cpm in the basic metavolcanites to 5400 total cpm in the rhyolitic metavolcanites.

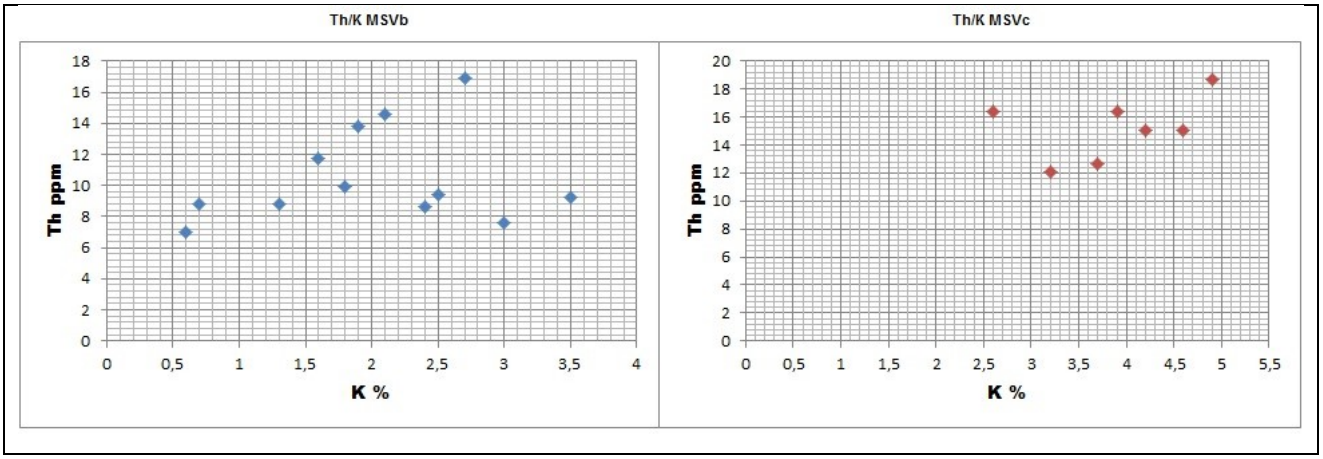


*Figure 16) Th/K in the Monte Santa Vittoria Fm: (with blue MSVb and with red MSVc).*

**3.1.3 Orroeledu Fm (ORRa,b)** (Bosellini & Ogniben, 1968) consists of fine-to coarse-grained lithic wackes. This sedimentary succession shows the highest values of Th with maximum of 503,5 ppm. These high values correspond to enrichement in heavy minerals deposited as thin strata ( mm to cm) in a nearshore environment. In the coarse-grained facies of the ORRa, heavy minerals are composed mainly of titaniferous phases (rutile, pseudo-rutile, anatase) whether in the fine-grained facies of the ORRb, zircon and primarily monazite (represented by Zr and Ce+La respectively) are more abundant. The ORRa shows a relatively low radioactivity, the middle values of total counts is of 6500 total cpm;(up to 14267 total cpm, corresponding to 94 Th ppm and 5,9 U ppm) (**Fig. 15 & 17**), whereas the ORRb is characterized by an increase of radioactivity (up to 70226 total cpm, 503,5 Th ppm and 30,5 U ppm) (see measure 183 in **Fig.15**). The average values of total counts of ORRb is of 19100 total cpm, 118 Th ppm, 9 U ppm and 4 K %. This formation is comparable to the Punta Serpeddì Fm (Loi et al., 1992) outcropping mostly in the Sarrabus area of Sardinia, where the high Th gamma-ray response is due to the presence of zircon and monazite (Pistis et al., 2015).

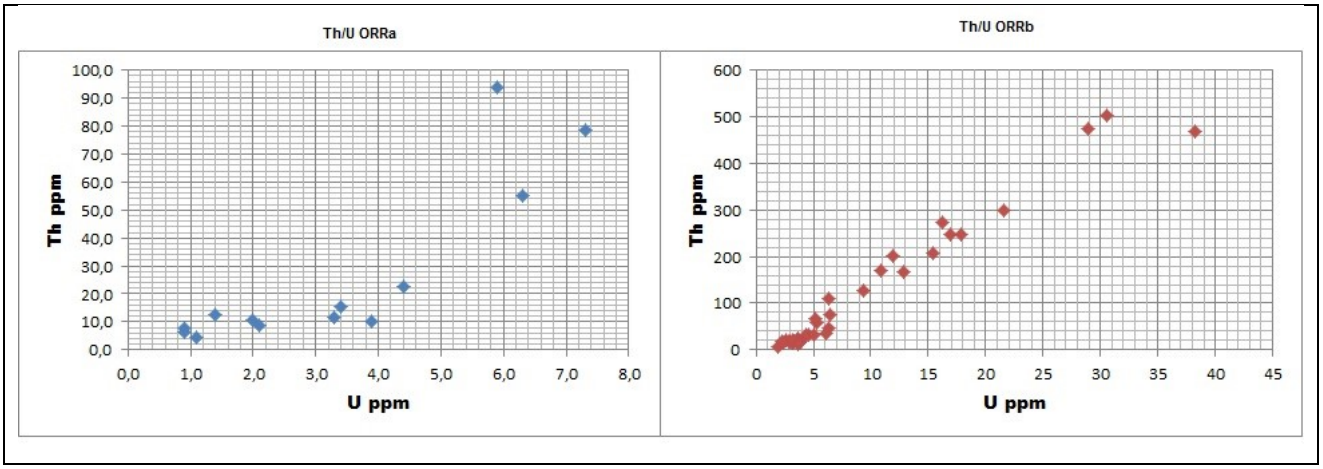


*Figure 17) Th/U in the Orroeleddu Fm: (with blue ORRa and with red ORRb).*

**3.1.4 Black Shales Formation (SGAa,b)** (Scisti a Graptoliti Fm; Corradini et al., 1998), is subdivided in two members. SGAa is made up of meta-limestones showing low values of total counts, U, Th and K (**Fig.18**). This values are 4 to 6 times lower than the average crustal abundances. The middle values of total counts of SGAa is of 2100 total cpm. SGAb, composed of black shales, is characterized by an increase of radioactivity (up to 21963 total cpm, 70 U ppm), this

values are 25 to 35 times high than the average crustal abundances (see measure 11 in **Fig.15**). The middle values of total counts of SGAb is of 7700 total cpm.

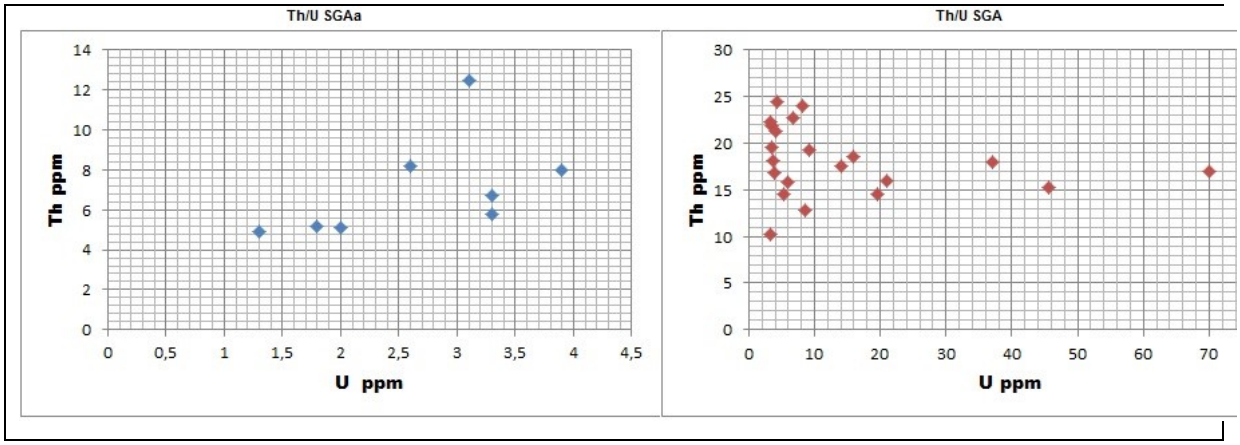


*Figure 18) Th/U in the Scisti a Graptoliti Fm: (with blue SGAa and with red SGA).*

## 3.2. BARBAGIA UNIT

In the Gennargentu area the differences between similar metamorphic terrigenous formations, can hardly be recognized, the gamma ray survey was performed tentatively. In order to correlate these units with the Meana and Sarrabus units.

**3.2.1 Gray Phyillites of Gennargentu (PGT)** ("Postgotlandiano" Vai & Coccozza, 1974), is made up of meta-pelites and quartzites characterized by middle values of total counts (4,400 total cpm). This Formation shows values of Th reaching 14 ppm, 3U ppm and 3 K %. The quartzites member shows values of Th reaching 11 ppm, 2 U ppm and 2 K % (**Fig.19**). With total count of 3,100 total cpm.

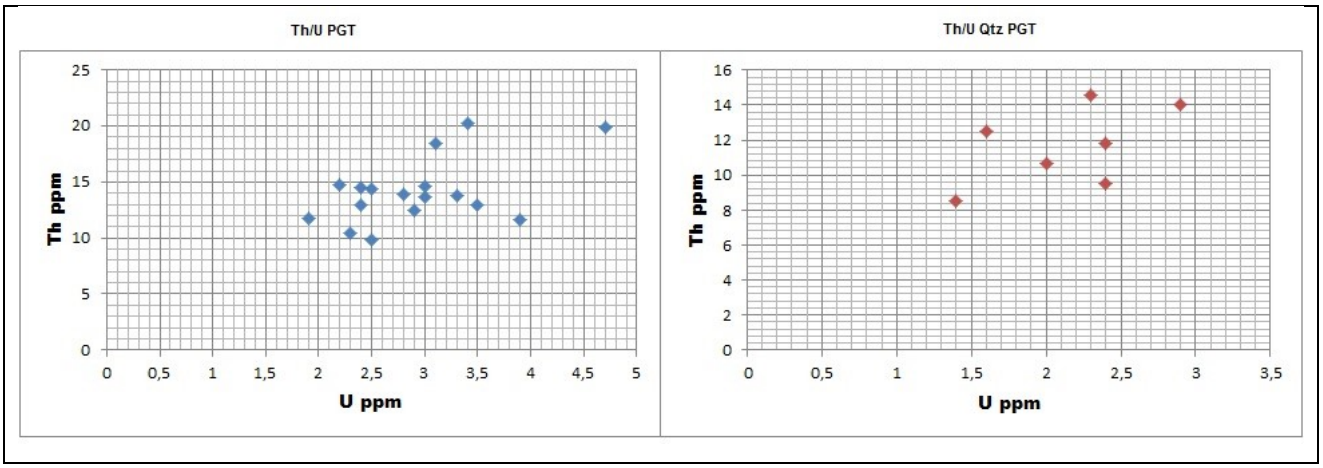


*Figure-19) Th/U in the Gray Phillites Fm: (with blue PGT and with red Qtz).*

Different values were obtained in a wide portion of metasandstones and quartzites of a tectonic unit, namely the Corr'e Boi Unit (Dessau et al., 1982) also pertaining to the Barbagia units. This unit contains a huge succession of quartzite and overlaps the Siluro Devonian black phyllites and marbles through a tectonic contact. For this reason was attributed to The basal portion of the Gray Phyllites of Gennargentu and tentatively correlated to the San Vito Fm. The values unexpectedly were as high as those found in the Upper Ordovician Orroeledu Fm (Qtz CORR) with a good deal of measures in the range of 243 Th ppm, 32 U ppm and 2.5 K% (**Fig.20**).

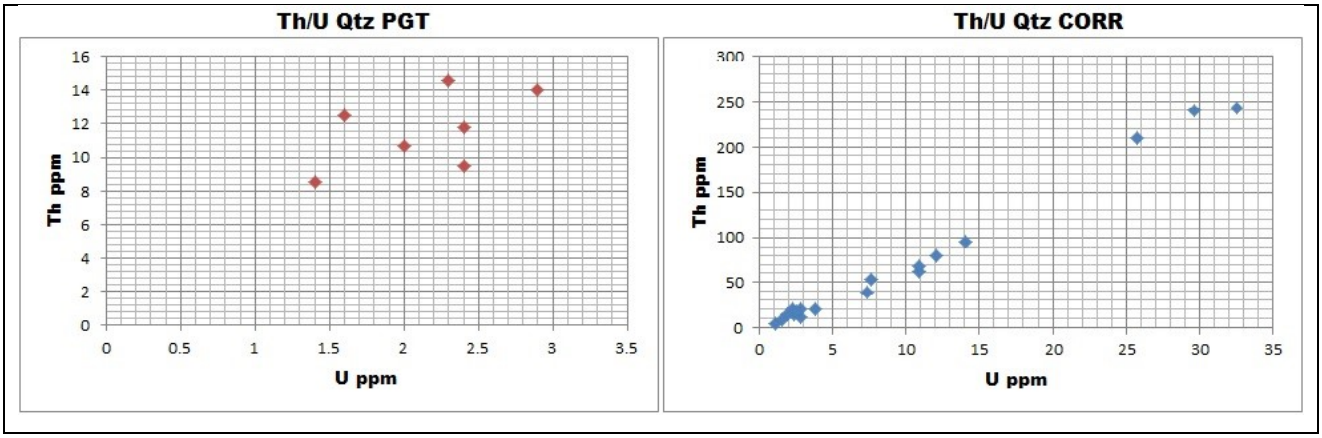


*Figure-20) Th/U in the Gray Phillites Fm and Corr'e Boi : (with red Qtz PGT and with blue Qtz CORR)*

## 3.3. DISCUSSION

The Orroeledu Fm (ORRa,b) and the Scisti a Graptoliti Fm (SGA and SGAa) yielded characteristic signals: the SGAb values of 14.1 U and 18.1 Th have a high U/Th ratio, 0.78 (**Fig.21**), typical of sedimentary reducing environment where primary uranium was up taken by carbonaceous matter in the form of $U^{4+}$. In the same way also the signal of MSVc, MSVb and the SVI formations have characteristic gamma-ray signals. Particularly MSVb (mostly meta-andesites) and MSVc (acidic metavolcanites) differ for the K content meaning full higher in the acidic terms ( i.e 2% vs 5 %).

The Orroeledu Fm gave an outstanding maximum of total cpm ( i.e 70226) with U values of 30,5 ppm and Th values of 503.5 ppm . Here the U/Th ratio maximum is 0.06 (average 0.08) (**Fig.21**) hence one order of magnitude lower than that of the SGA . The obvious explanation is that the Orroeledu Fm retains clastic phases bearing U Th, and possibly REE, such as monazite zircons and allanite. The occurrence of K 4% testifies for an original arkosic composition of fine sediments.

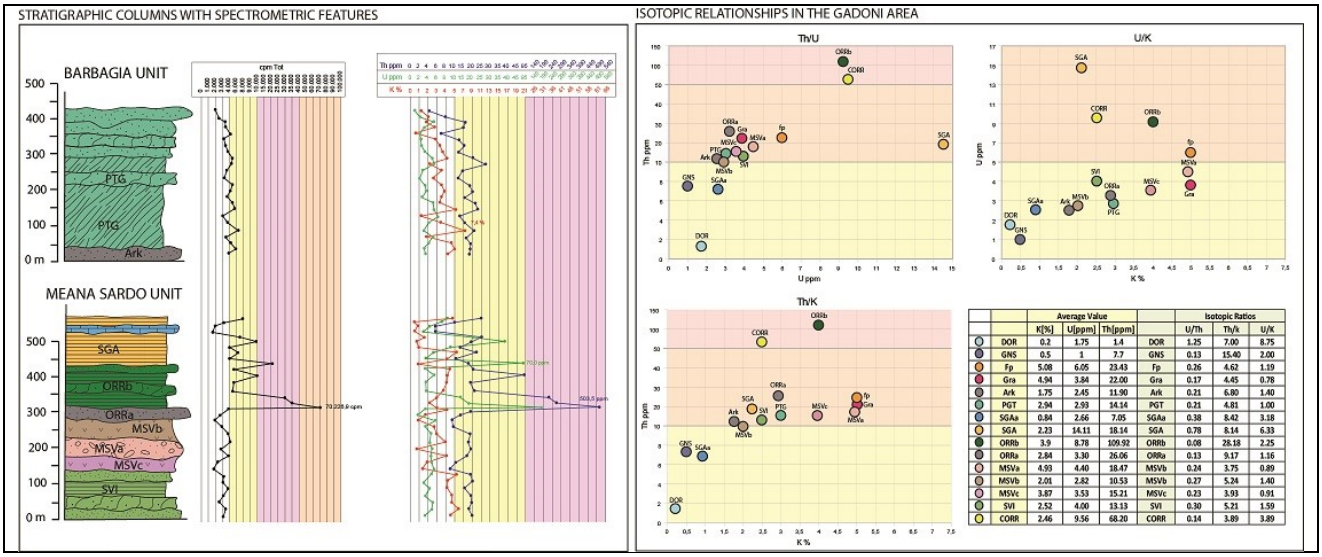


*Figure 21) Stratigraphic columns with spectrometric features and isotopic relationships in the Gadoni area.*

The Barbagia Unit shows quite uniform values in the Gennargentu Gray Phyllites. The U/Th ratio of 0.2 (**Fig.21**) close to that of the GLOSS (Plank & Langimur, 1998) and Th values of 14 ppm when plotted in the diagram of Hawkesworth et al 1997 match the typical orogenic wedge metasediments.

# REFERENCES


Bosellini, A., & Ogniben, G. (1968). Ricoprimenti ercinici nella Sardegna centrale. Annali dell'Universita` di Ferrara, 1, 1–15.

Calvino, F. (1959). Lineamenti strutturali del Sarrabus-Gerrei (Sardegna sud-orientale). Bollettino del Servizio Geologico d'Italia, 81(4–5), 489–556.

Carmignani, L., Minzoni, N., Pertusati, P. C., & Gattiglio, M. (1982). Lineamenti geologici principali del Sarcidano-Barbagia di Belvı`. In L. Carmignani, T. Cocozza, C. Ghezzo, P. C. Pertusati & C. A. Ricci (Eds.), Guida alla Geologia del Paleozoico Sardo (pp. 119–125). Guide Geologiche Regionali. Societa` Geologica Italiana.

Cocozza, T., Jacobacci, A., Nardi, R., & Salvadori, I. (1974). Schema stratigrafico-strutturale del Massiccio Sardo-Corso e minerogenesi della Sardegna. Memorie della Societa` Geologica Italiana, 13, 85–186.

Corradini, C., Ferretti, A., & Serpagli, E. (1998). The Silurian and Devonian sequence in SE Sardinia. Giornale di geologia, 60(ECOS VII - special issue), 71–74.

Dabard, M. P., Loi, A., Paris, F., Ghienne, J. F., Pistis, M., & Vidal, M. (2015). Sea-level curve for the Middle to early Late Ordovician in the Armorican Massif (western France): Icehouse third-order glacio-eustatic cycles. Palaeogeography, Palaeoclimatology, Palaeoecology, 436, 96-111.

Dessau, G., Duchi, G., Moretti, A., & Oggiano, G. (1982). Geologia della zona valico di Correboi (Sardegna centro-orientale); Rilevamento, tettonica, giacimenti minerari. Bollettino della Società Geologica Italiana, 101(4), 497-522.

Loi, A., Barca, S., Chauvell, J. J., Dabard, M. P., & Leone, F. (1992). Analyse de la se´dimentation post-phase sarde: le de´pots initiaux a` placers du SE de la Sardaigne. Comptes Rendus de l'Acade´mie des Sciences de Paris, 315, 1357–1364.

Oggiano, G., Gaggero, L., Funedda, A., Buzzi, L., & Tiepolo, M. (2010). Multiple early Palaeozoic volcanic events at the northern Gondwana margin: U-Pb age evidence from the Southern Variscan branch (Sardinia, Italy). Gondwana Research, 17(1), 44–58. doi:10.1016/j.gr.2009.06.001

Pistis, M., Loi A., & Dabard M.P. (2015). Influence of sea-level variations on the genesis of palaeoplacers, the examples of Sarrabus (Sardinia, Italy) and the Armorican Massif (Western France). Comptes Rendus Geoscience (in press).

Plank, T., & Langmuir, C. H. (1998). The chemical composition of subducting sediment and its consequences for the crust and mantle. Chemical geology, 145(3), 325-394.

Vai, G. B., & Cocozza, T. (1974). Il" Postgotlandiano" Sardo, unita'sinorogenica ercinica. Bollettino della Societa Geologica Italiana, 93(1), 61-72.

# 4. GEOCHRONOLOGY

This part presents the results of laboratory analyses on zircons extracted from samples collected in the study and neighboring area. Sampling was performed on the Gray Gennargentu Phillites "Postgotlandiano" (Vai et al., 1974). The S.Vito Fm. in order to compare the unknown "Postgotlandiano" and the S.Vito formation of the Meana Unit. In fact this formation was referred to Middle Cambrian-Lower Ordovician (pre-Sardic Phase) on the base of achritarc associations. One more sample derives a key intrusion mapped in the mineralized Gadoni district. The zircons were analysed at the Senckenberg Natural History Collections of Dresden.

## 4.1. SAMPLE LOCATION

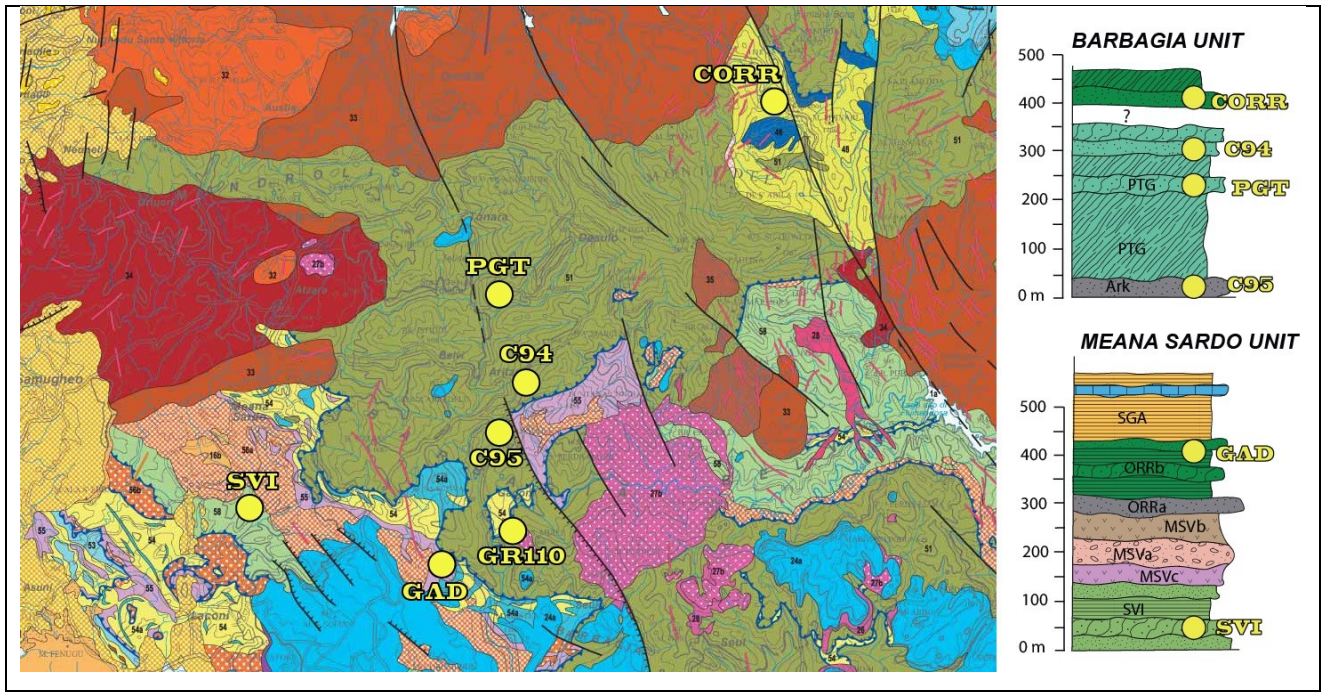


*Figure 22) Sample location (Geological Map Of Sardinia 1:250.00 Carmignani et al., 2008).*

Four samples belong to the area of the Internal Nappe (**Fig.22 & 23**),: three were taken from metaquartzites, metasiltstons, metasandstones deposit (PGT, C94 and CORR) and one from metaquartzites and metarkose sediment (C95). These four samples are included in the Barbagia Units. Two samples belong to the Meana Sardo Unit: one to a meta-quartzarenite horizon in the Orroeledu formation (GAD), the other to a metagraywacke level of the Arenarie di S.Vito

Formation (SVI). The sample from the late Variscan magmatic Complex consist of granodiorites derives from an unknown granodiorite which cross close to the ore-bodies of Funtana Raminosa (GR110).

| NAME | FORMATION | LITOLOGY | COUNTRY | GEOGRAPHIC COORDINATES |
|---|---|---|---|---|
| **PGT** | Gray Phyillite Fm ("Postgotlandiano" Auct.) | Metaquartzites, Metasiltstones, Metasandstone, | Italy, Sardinia, Barbagia | 39.988339N 9.187507E |
| **C95** | Gray Phyillite Fm ("Postgotlandiano" Auct.) | Metaquartzites, Metarkoses, | Italy, Sardinia, Barbagia | 39.938174N 9.196404E |
| **C94** | Gray Phyillite Fm ("Postgotlandiano" Auct.) | Metaquartzites, Metasiltstones, Metasandstone, | Italy, Sardinia, Barbagia | 39.955669N 9.205223E |
| **CORR** | Gray Phyillite Fm ("Postgotlandiano" Auct.) | Metaquartzites, Metasiltstones, Metasandstone, | Italy, Sardinia, Barbagia | 40.082364N 9.347779E |
| **SVI** | Arenarie di S.Vito Fm | Metasandstones, Metasiltstones | Italy, Sardinia, Barbagia | 39.904755N 9.051216E |
| **GAD** | Orroeledu Fm | Metarkoses, Metasiltstone, Metagraywackes | Italy, Sardinia, Barbagia | 39.883571N 9.159598E |
| **GR110** | Late Paleozoic Magmatism | Granodiorites, | Italy, Sardinia, Barbagia | 39.897074N 9.195663E |

*Figure 23) Samples collected in the Palaeozoic basement of Sardinia .*

## 4.2. BARBAGIA UNIT

The Barbagia Units are considered as inner nappes within the orogenic wedge of the Variscan orogeny of Sardinia.. The primary sedimentary feature are almost completely obliterated, as the deformation and the metamorphic grade id sensibly higher with respect that affecting the external nappe.

## 4.2.1. PGT SAMPLE

Is made up of irregular levels of micaceous sandstones, quartzites, phyllite and quartz-phyllites in centimetric to millimetric level transposed along the regional S2 foliation (**Fig.24**).

*Figure 24) Micaceous sandstones, quartzites, phyllite and quartz phyllites.*

### U-Pb isotope

One hundred and eighteen zircon from PGT sample have been analysed and the results reported in the Concordia diagram (Wheterill, 1956) (**Fig.26**). Sixty-three zircons are concordant. The age spectra span between 550 Ma and 2800 Ma. The minimum age is 559±15 Ma; the average age is 1259 Ma and the maximum age is 2816±47 Ma (**Fig.25**).

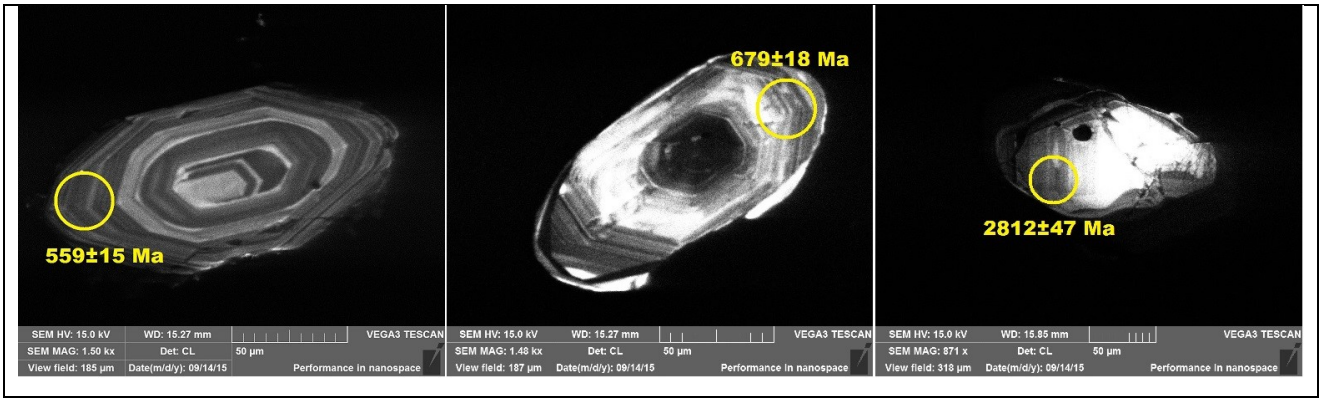


*Figure 25) CL images and U-Pb ages from the PGT sample.*

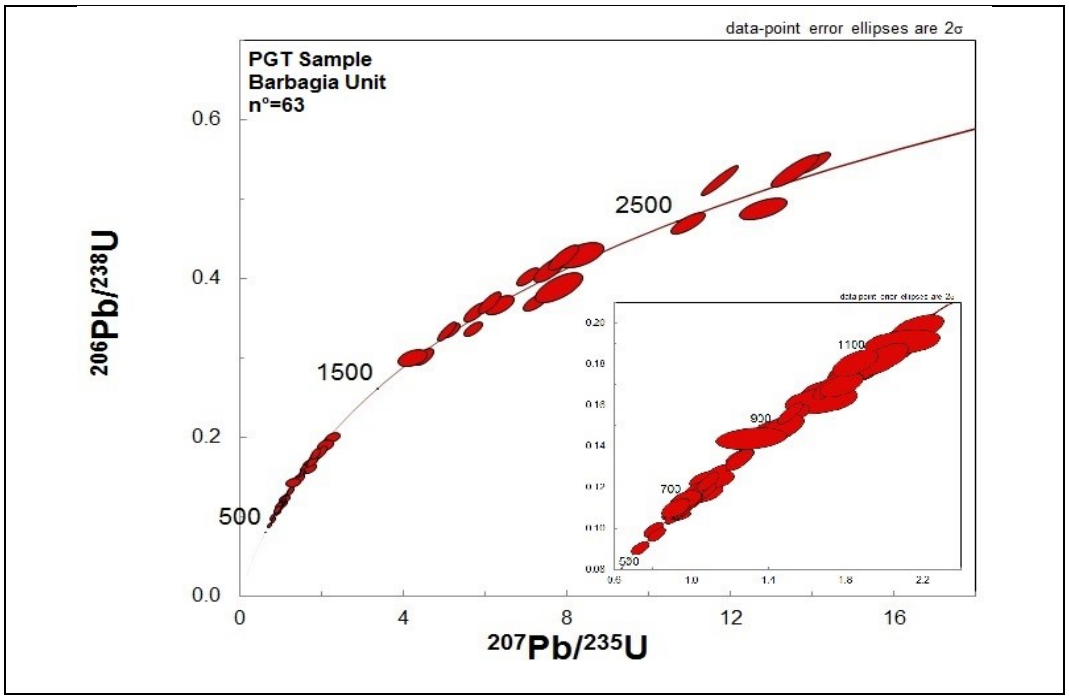


*Figure 26) U-Pb ages from the PGT sample.*

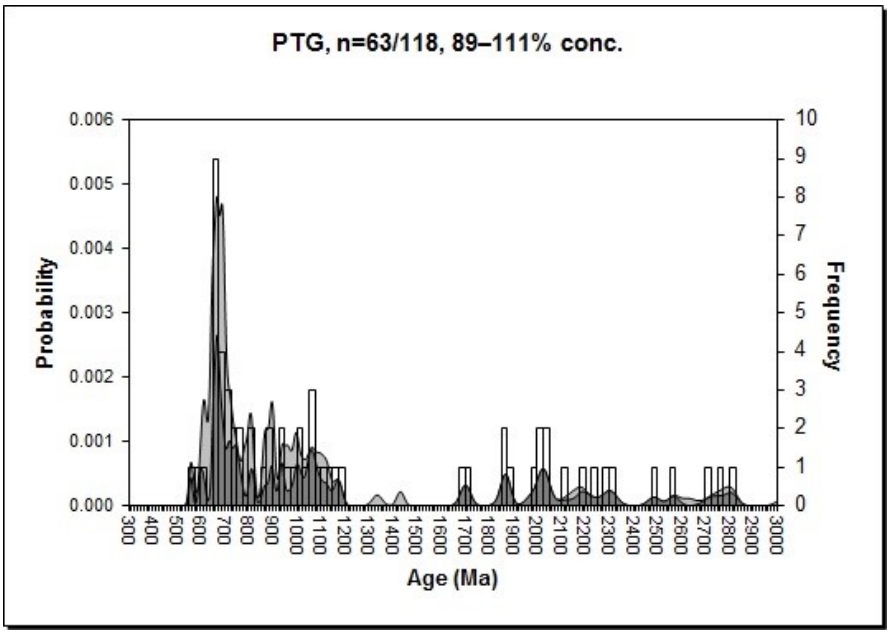


*Figure 27) Distribution by PGT sample. The histogram shows a polymodal distribution of ages, with main populations between 559 and 2812 Ma.*

The frequency histogram shows a polymodal distribution with two main populations with peaks at 669 and 1061 Ma; A third minor population has ages between 2487 and 2812 Ma (**Fig.27**).

### 4.2.2. C95 SAMPLE

Is made up of a succession of irregular levels of metagreywackes and metarkoses with bimodal grain size distribution; is intercalated in the Gray Phyillite of Gennargentu Fm (Pertusati, P. 2002) (**Fig.28**).


*Figure 28) Metagreywackes and metarkoses.*

### U-Pb isotope

One hundred and eighteen zircon from C95 sample have been analysed and the results reported in the Concordia diagram (Wheterill, 1956) (**Fig.30**). Eghty-three zircons are concordant; age spectra span between 550 Ma and 2700 Ma. The minimum age is 576±15 Ma; the average age is 925 Ma and the maximum age is 2658±61 Ma (**Fig.29**).


*Figure 29) CL images and U-Pb ages from the C95 sample.*

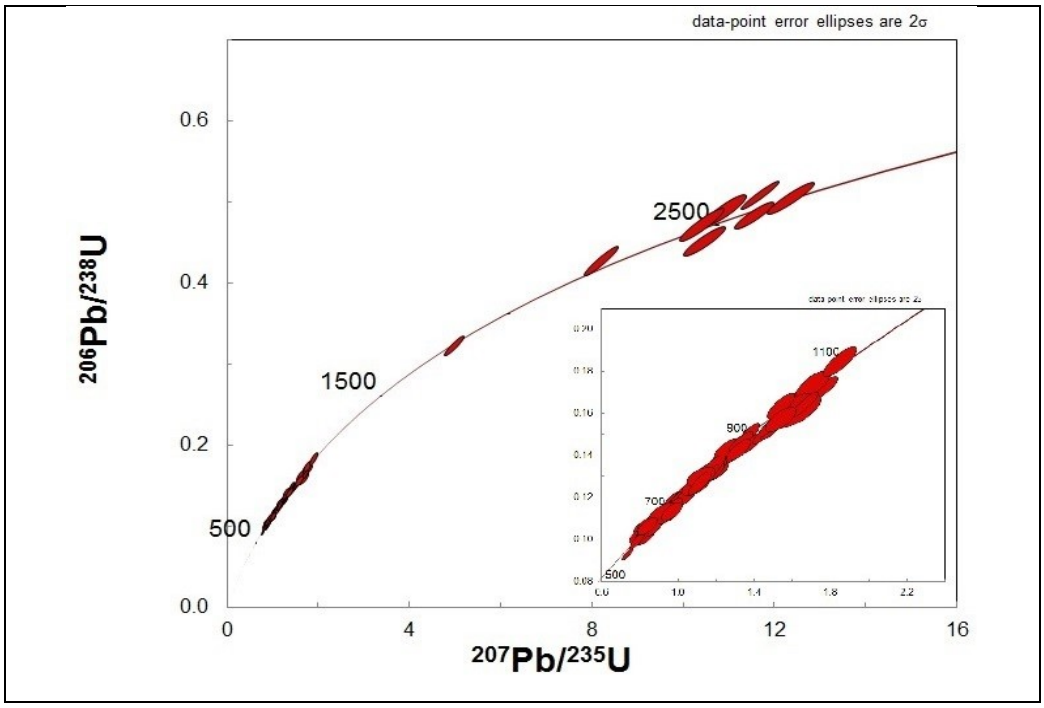


*Figure 30) U-Pb ages from the C95 sample.*

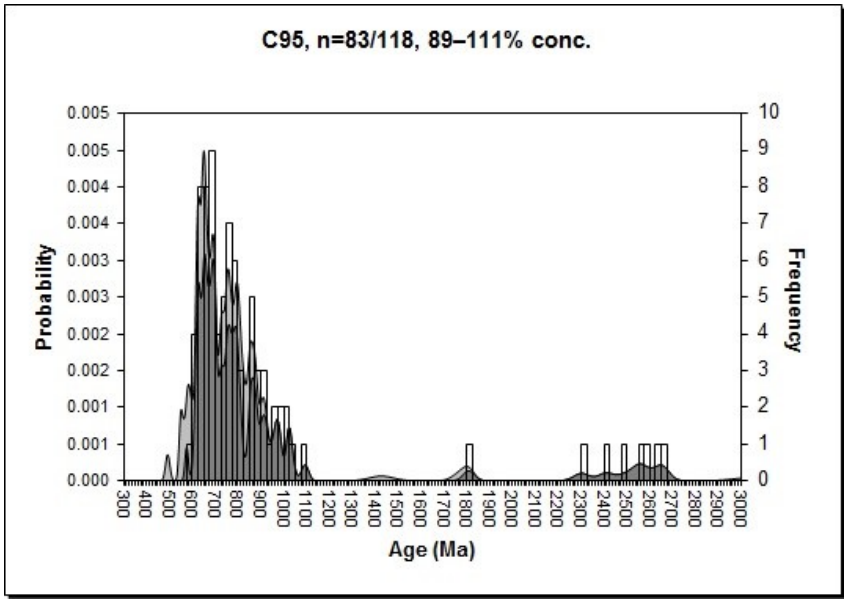


*Figure 31) Distribution by C95 sample. The histogram shows a polymodal distribution of ages, with main populations between 576 and 2812 Ma.*

The frequency histogram (**Fig.31**) showing a polymodal distribution with two main populations with peaks at 691 and 865 Ma and a third minor population with ages between 1809 and 2658 Ma.

### 4.2.3. C94 SAMPLE

Consist of an alternation of transposed levels of micaceous sandstone, quartzite, phyllite and quartz phyllites (**Fig.32**).

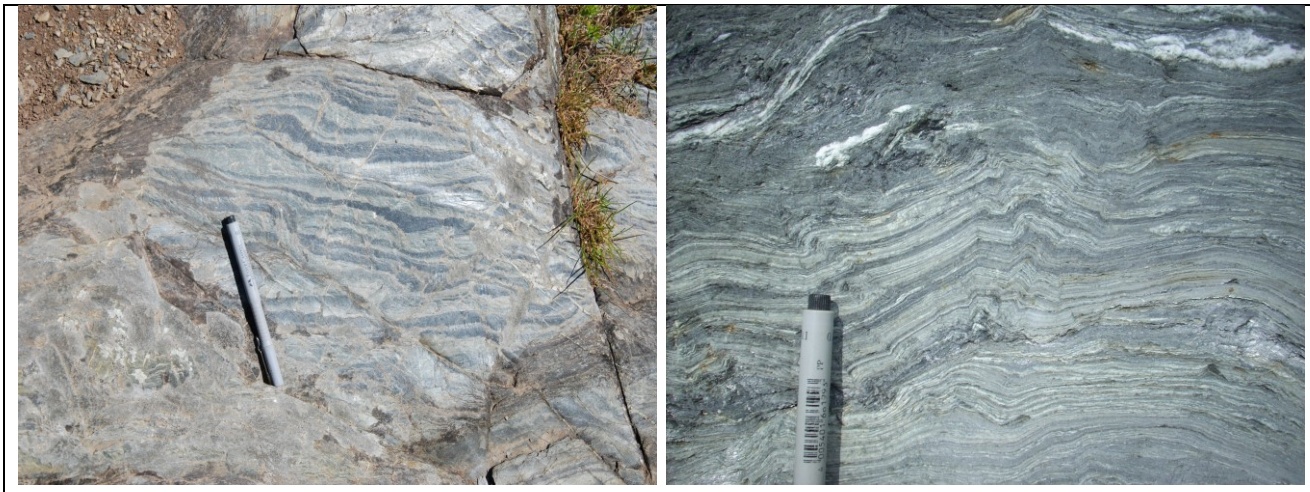

*Figure 32) Quartzitse, phyllites and quartz phyllites.*

**U-Pb isotope**

One hundred nineteen zircon from C94 sample have been analysed and the results reported in the Concordia diagram (Wheterill, 1956) (**Fig.34**). Eighty zircons are concordant. The age spectra span between 500 Ma and 3000 Ma. The minimum age is 519±14 Ma; the average age 910 Ma and the maximum age 2963±70 Ma (**Fig.33**).

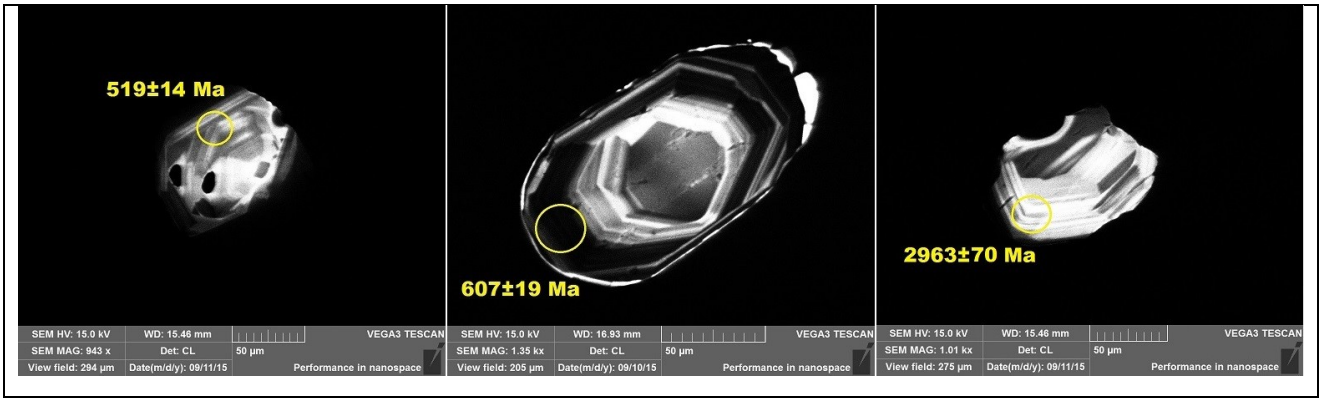


*Figure 33) CL images and U-Pb ages from the C94 sample.*

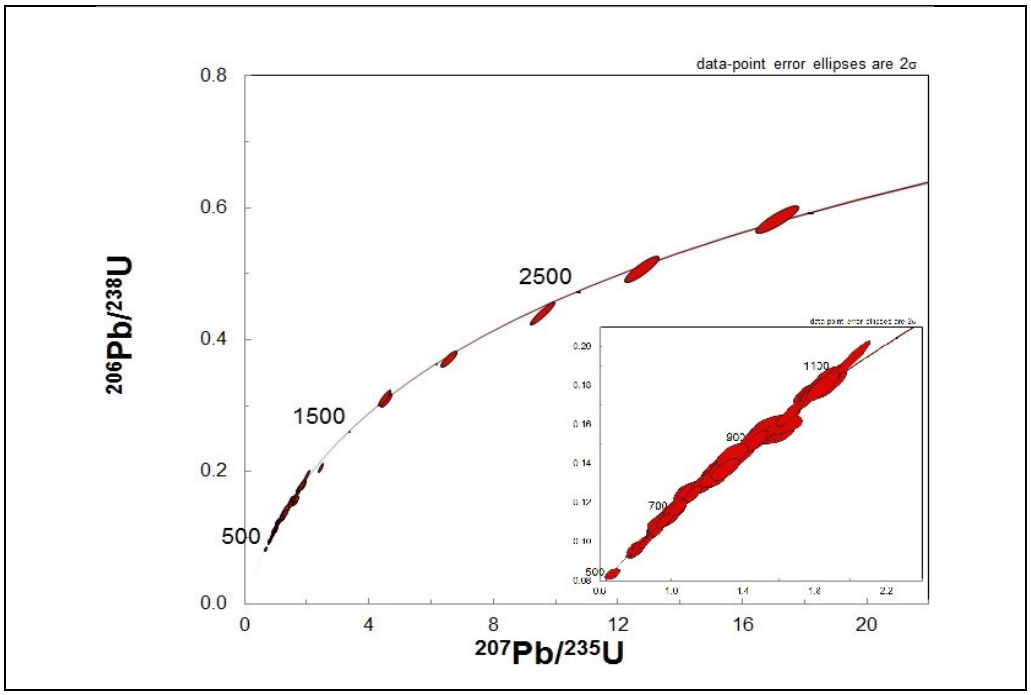


*Figure 34) U-Pb ages from the C94 sample.*

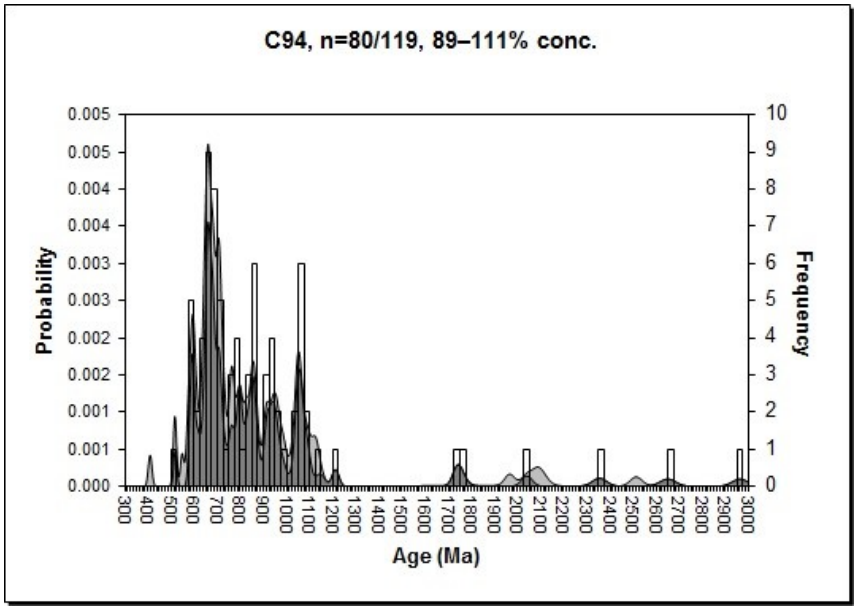


*Figure 35) Distribution by C94 sample. The histogram shows a polymodal distribution of ages, with main populations between 519 and 2963 Ma.*

The frequency histogram (**Fig.35**) shows polymodal distribution with three main populations with peaks at 662, 853 and 1055 Ma and a fourth minor population with ages between 1744 and 2963 Ma.

## 4.2.4. CORR SAMPLE

Consist of an alternation of micaceous sandstones, quartzites, phyllite and quartz phyllites. Even though the original bedding is heavily transposed the primary sedimentary differentiation is still preserved I the limbs of some isoclinal folds (**Fig. 36**).

*Figure 36) Micaceous sandstones and quartzites.*

### U-Pb isotope

One hundred twelve zircons from CORR sample have been analysed and the results reported in the Concordia diagram (Wheterill, 1956) (**Fig.38**). Sixty-eight zircons are concordant. The age spectra pan between 400 Ma and 2600 Ma. The minimum age is 437±12 Ma; the average age is 925 Ma and the maximum age is 2621±86 Ma (**Fig.37**).

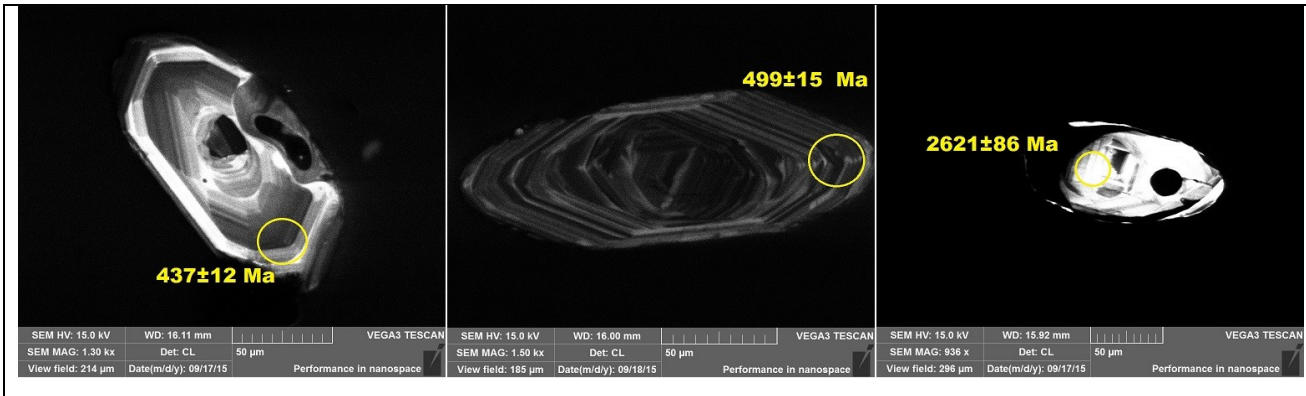


*Figure 37) CL images and U-Pb ages from the CORR sample.*

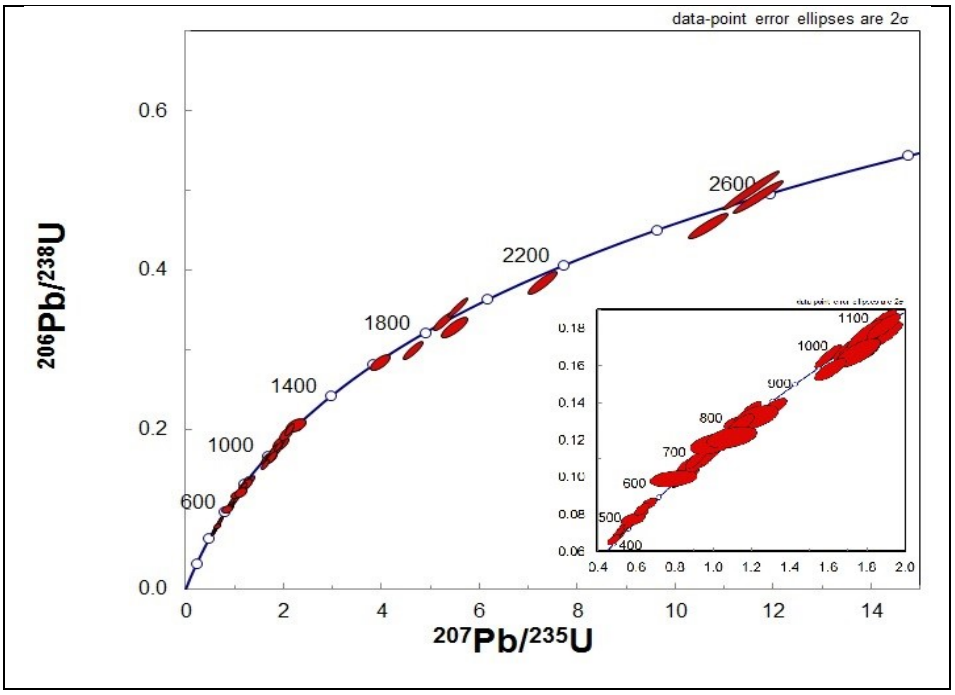


*Figure 38) U-Pb ages from the CORR sample.*

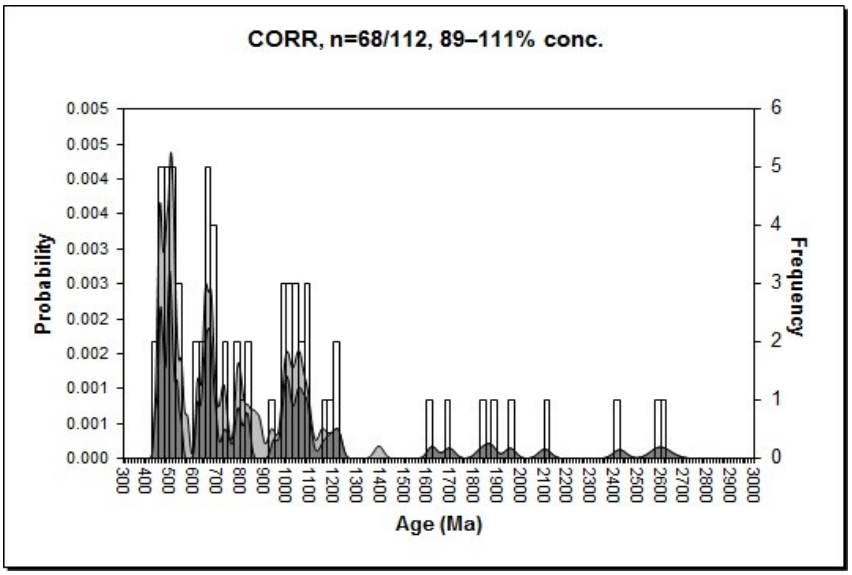


*Figure 39) Distribution by CORR sample. The histogram shows a polymodal distribution of ages, with main populations between 437 and 2621 Ma.*

The frequency histogram (**Fig.39**) shows a polymodal distribution with three main populations with peaks at 461-500, 667, 1000-1054 Ma and a fourth minor population with ages between 1623 and 2621 Ma.

## 4.3. MEANA SARDO UNIT

The Meana Sardo unit consists of two main megasequences: the first is the metapelitic-metarenaceous S.Vito formation, which predates the Sardic Phase and the other is the transgressive sequence spanning from the upper Ordovician to the Devonian. This latter sequence starts with the Orroeledu Fm. which consists of metasandstone an minor metasiltite.

### 4.3.1 (SVI SAMPLE)

This sample is an alternation of transposed levels with variable thickness (millimeter to centimeter in thickness) of fine quartz-feldspathic sandstones, gray-green mudstones and siltstones (**Fig.40**).

*Figure 40) Sandstones, and quartz-feldspathic sandstones.*

**U-Pb isotope**

One hundred and fifteen zircon from SVI sample have been analysed and the results reported in the Concordia diagram (Wheterill, 1956). Sixty-six zircons are concordant. The age spectra is span between 500 Ma and 3000 Ma. The minimum age is 539±23 Ma; the average age is 1210 Ma and the maximum age is 2968±99 Ma (**Fig.41**).

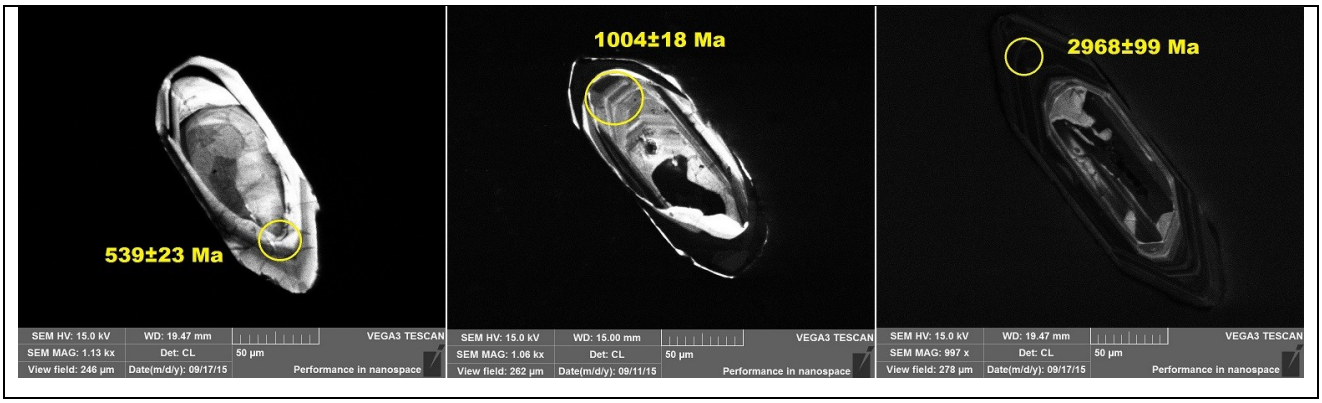


*Figure 41) CL images and U-Pb ages from the SVI sample.*

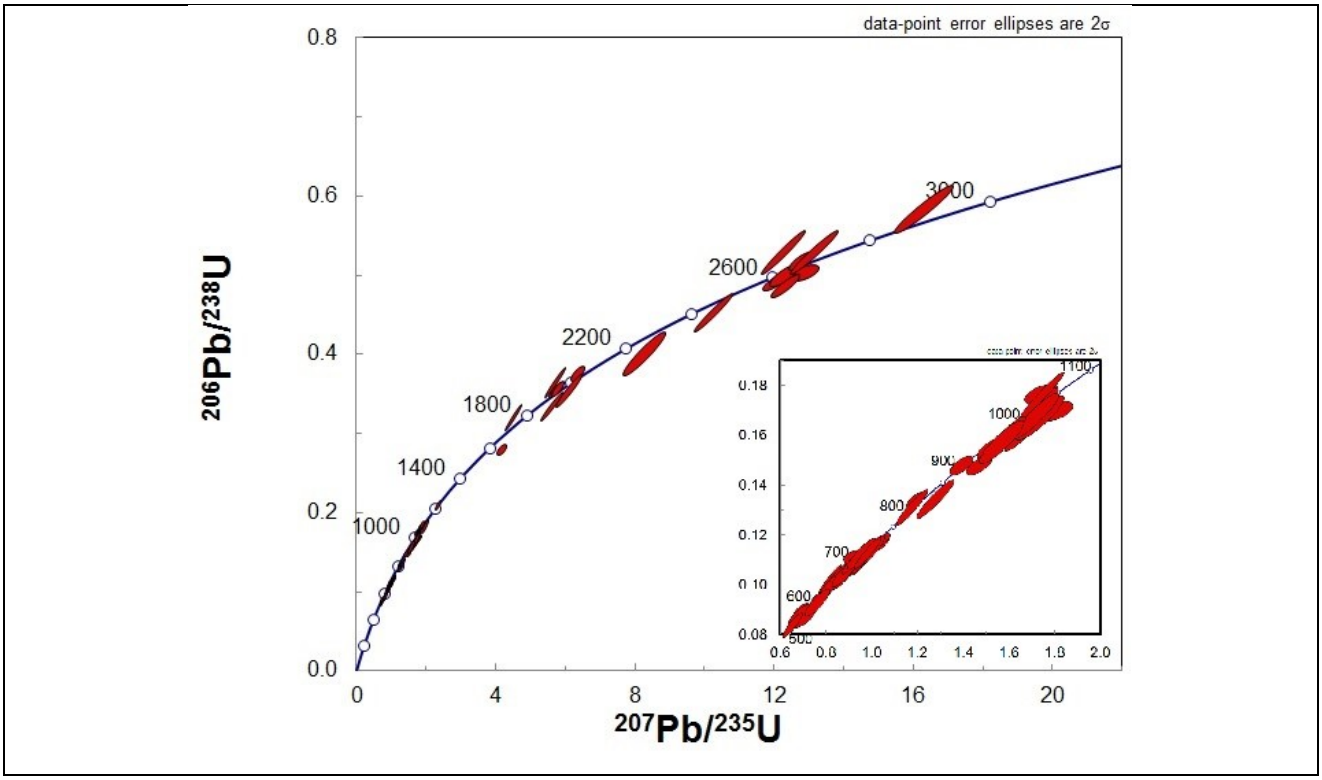


*Figure 42) U-Pb ages from the SVI sample.*

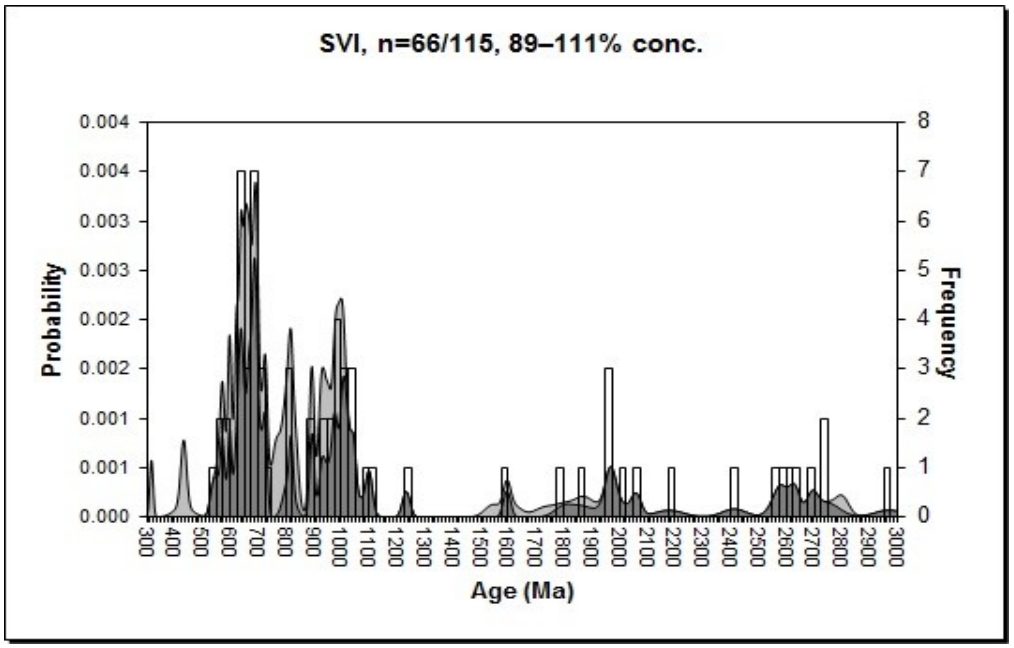


*Figure 43) Distribution by SVI sample. The histogram shows a polymodal distribution of ages, with main populations between 539 and 2968 Ma.*

The frequency histogram (**Fig.43**) showing a polymodal distribution with two main populations with peaks at 688, and 1008 Ma and a third minor population with ages between 1816 and 2968 Ma.

### 4.3.2 (GAD SAMPLE)

It consists of alternations metasandstones, arkose, phyllites and metasiltstones with sericitic-cloritic matrix (**Fig.44**). In the coarse-grained facies, tappears millimetric levels, which in thin section resulted made of heavy minerals mainly of titaniferous (rutile, pseudo-rutile, anatase), whereas the fine-grained facies contain similar levels made by detrital zircon and monazite responsible for the aforementioned high radioactivity values. The high quantity of zircons of this sample was worthy of a typology study.

*Figure 44) Metasandstones, arkose, phyllites and metasiltstones.*

### 4.3.2.1 TYPOLOGICAL STUDY OF ZIRCONS (GAD sample)

The typological study of zircons is useful in recognize the source that contribute to the detrital supply of sedimentary basins. The recognition of the source areas allows paleogeographical reconstruction and, within an orogenic building, the provenance of superposed tectonic units. The studies of Pupin around the years 70-80ies have shown that the morphology is closely tied to the physical-chemical conditions of the environment of crystallization (Pupin 1980). Most of Samples taken in the Gennargentu area not suitable for typological studies due to the scarce abundance and to the strong elaboration (roundness), which undermines this kind of study.

Hundred zircons were observed, of these 22 were not identified, because broken, opacified, oxidized and rounded. Only zircons with sharp faces and straight edges were determined. Some morphotypes (S1, S2 and S3 types) have inherited cores that match and exhibit canals, bubbles,

solid inclusions and growth gaps. The distribution of these zircon in the typology scheme (Pupin 1980) spreading the left side (**Fig.45**).

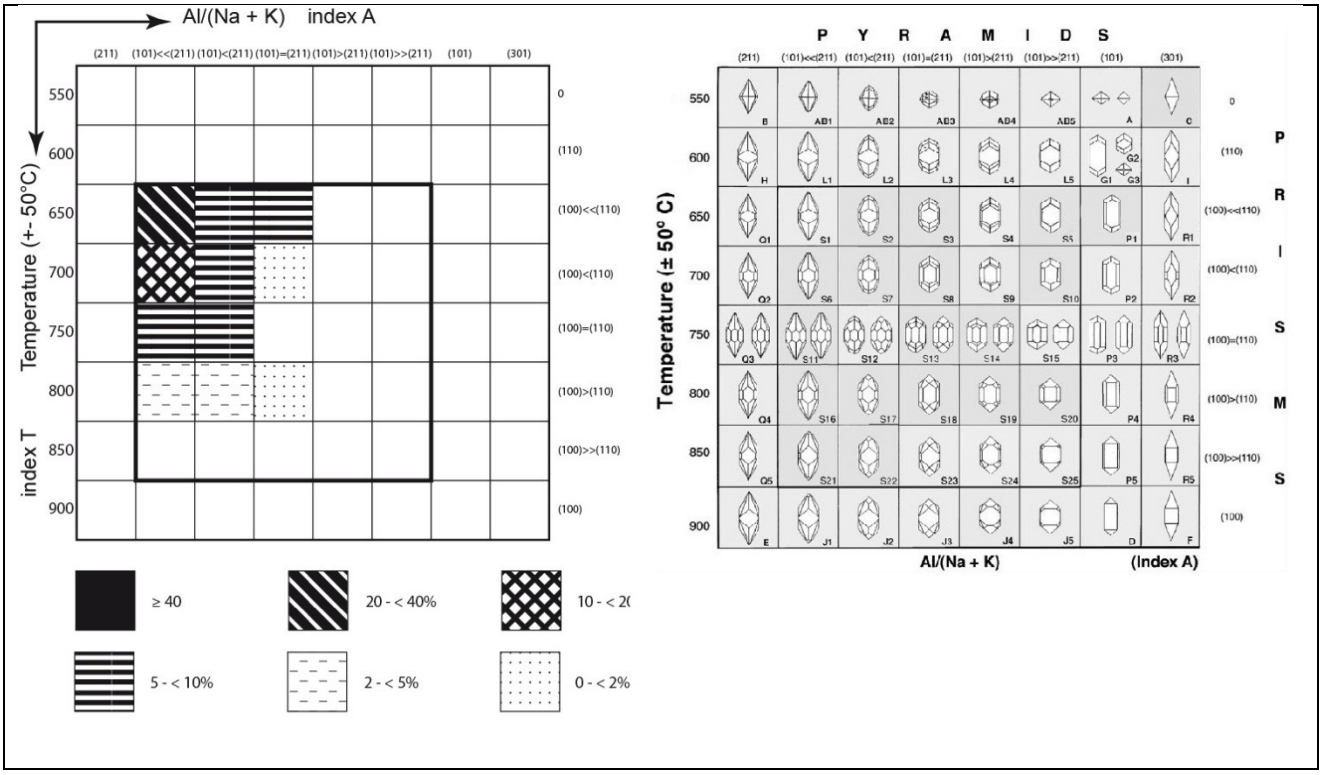


*Figure 45) Type of zircon in the Orroeledu Formation (Gadoni).*

Prism (110) and (211) dominate in the analysed population, which are typical of calc-alkaline volcanic series with aluminous component referable to crustal assimilation. This is in good agreement with the zircon typology gf the Mid-Ordovicia " Porfidi Grigi auct" in the Sarrabus Unit ( Loi & Dabard 1997) . This similarity led to consider the metasediment that yielded the GAD population as the product of the dismantling of the Andean type volcanic arc supposed in the north Gondwana margin (Gaggero et al 2012).

## U-Pb isotope

One hundred and eighteen zircon from GAD sample have been analysed and the results reported in the Concordia diagram (Wheterill, 1956) (Fig.48). Forty-seven zircons are concordant. The age spectra is span between 400 Ma and 800 Ma. The minimum age is 435±12 Ma; the average age is 494 Ma and the maximum age is 744±24 Ma (**Fig.47**).


*Figure 47) CL images and U-Pb ages from the GAD sample.*

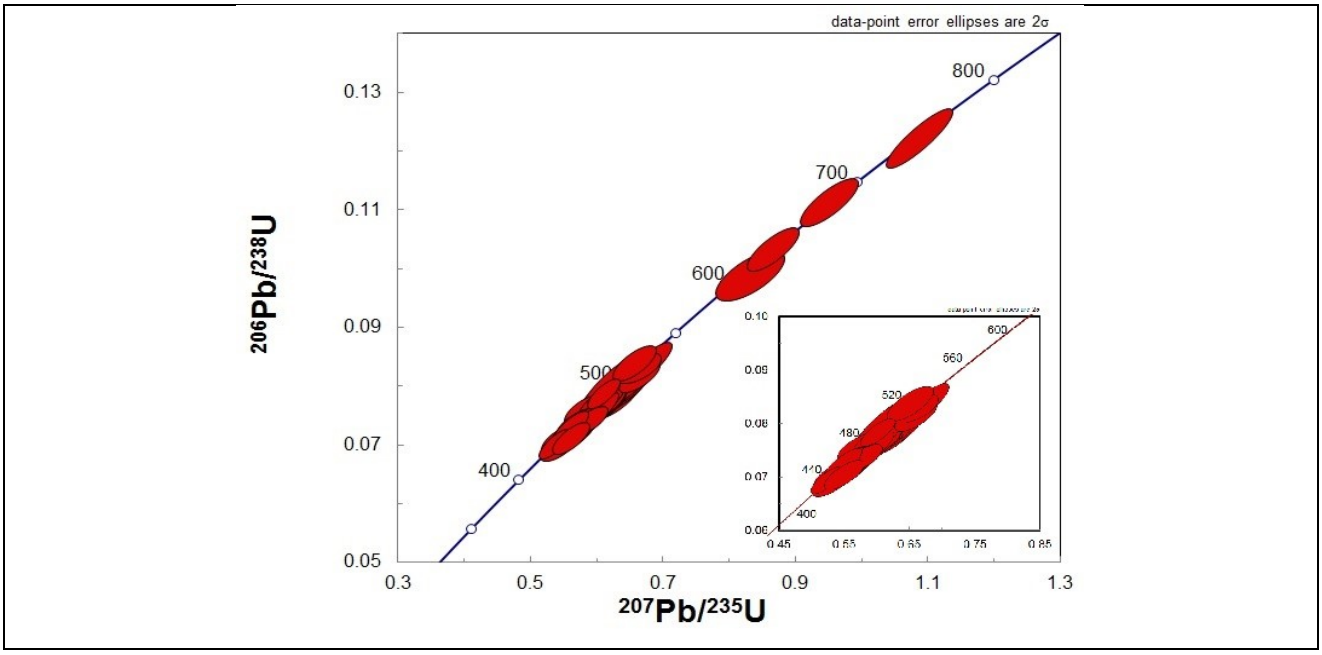


*Figure 48) U-Pb ages from the GAD sample.*

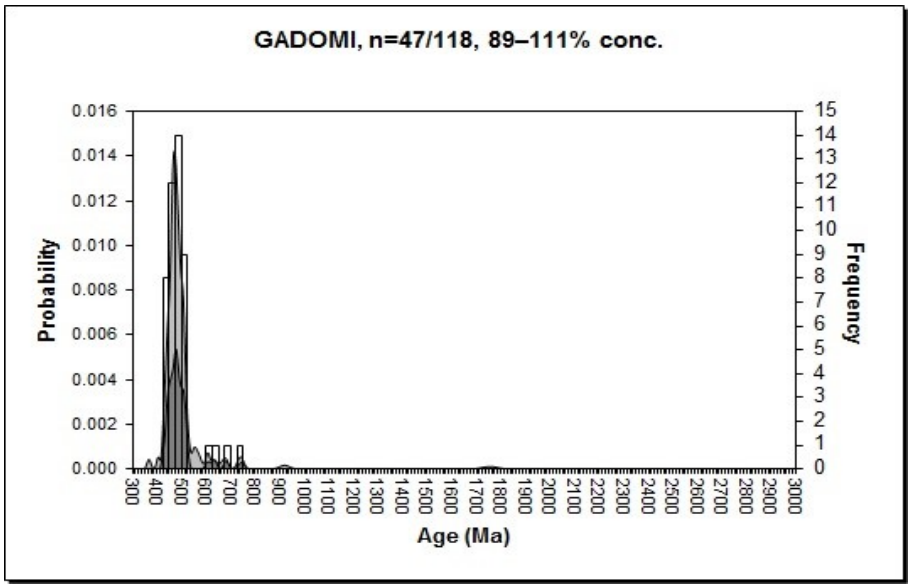


*Figure 49) Distribution by SVI sample. The histogram shows a polymodal distribution of ages, with main populations between 435 and 744 Ma.*

The frequency histogram (**Fig.49**) shows a polymodal distribution with one main populations with peaks at 477 Ma and a fourth minor population with ages between 608 and 744 Ma.

## 4.4 (GR110 SAMPLE)

It consists of the intrusive bodies are represented by granodiorites; the granodiorite is fine to medium grained rock with weak oriented texture marked by biotite crystals (**Fig.50**).

*Figure 50) Granodiorites in the Gadoni area.*

## U-Pb isotope

Fifty-four zircon from GAD sample have been analysed and the results reported in the Concordia diagram (Wheterill, 1956) (**Fig.52**). Twelve zircons are concordant; the age is 299±3 Ma. The core yeld ages of 591±17 and 593±17 Ma (**Fig.51**).

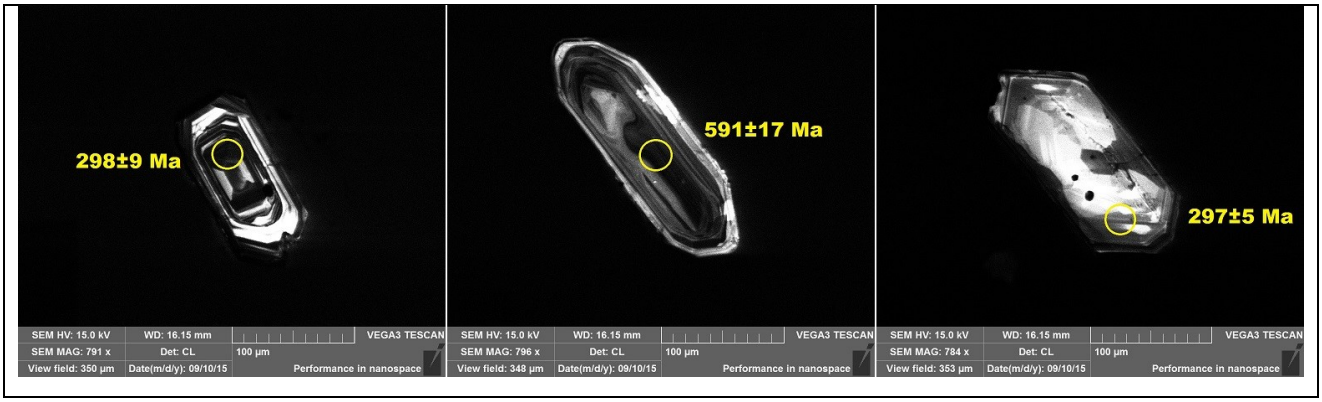


*Figure 51) CL images and U-Pb ages from the GR110 sample.*

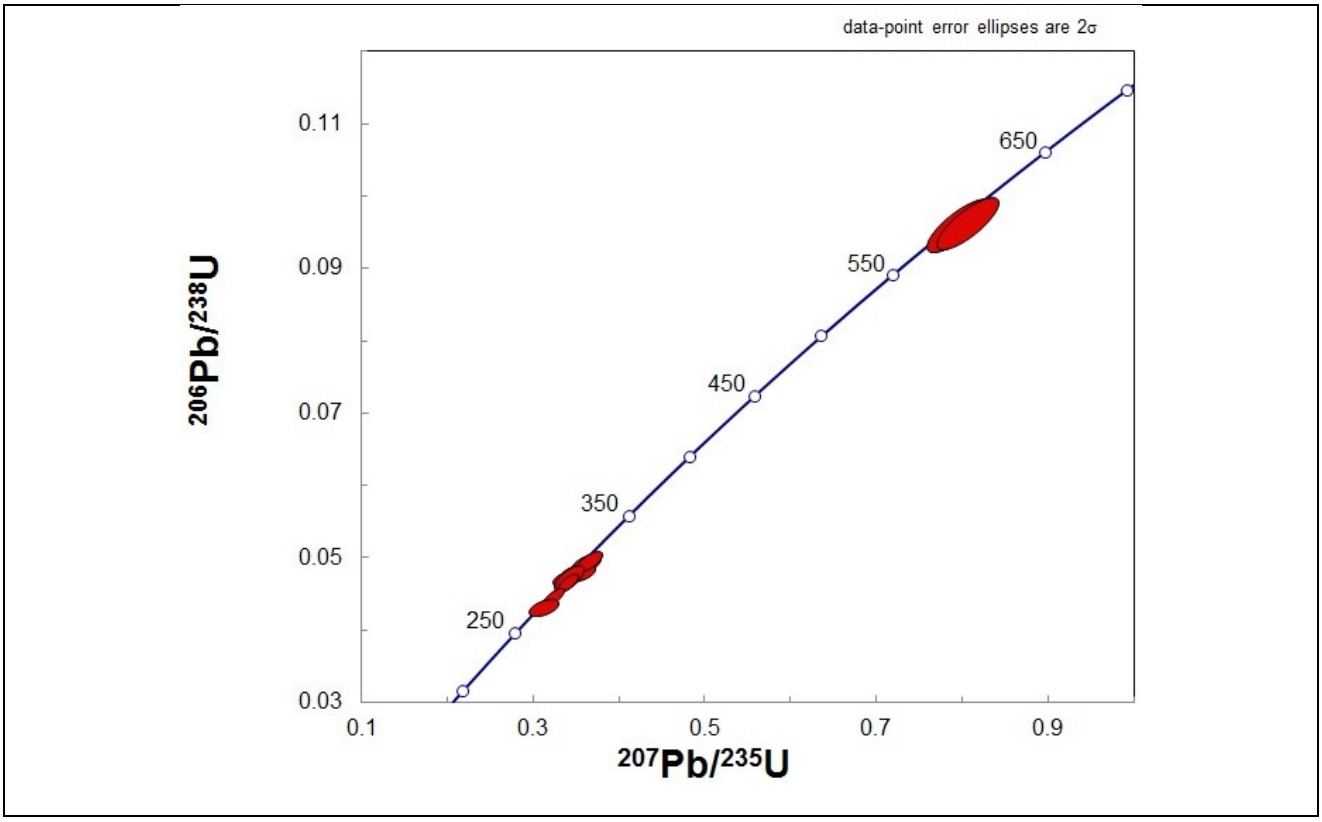


*Figure 52) U-Pb ages from the GR110 sample.*

## 4.5 DISCUSSION

### 4.5.1 PALAEOZOIC DETRITAL SAMPLES IN THE BARBAGIA UNIT

All samples show a small, but not negligible, input of Archean population (> 2500 Ma): PGT wich is higher in the "Postgotlandiano" auct. PGT 6,45%; C95 4,87%; C94 2,5% and CORR 3,03%. The Paleo-proterozoic input (1600-2500 Ma) especially in the PGT and CORR sample is decidedly important: PGT 25,80%; CORR 10,60% C95 4,87%; C94 5,00% (**Fig.53**). All samples lack of Middle Mesoproterozoic input (1200-1600 Ma) probably during this interval the feeding areas did not experienced any igneous activity.

The Grenvillian population (±Stenian 1000-1200 Ma) is well expressed in all the samples with higher frequences in PGT, C94 and CORR samples; PGT and CORR 16,12%, 16,25 and 25,75% wit low presence in the C95 (6,09%).

The Tonian population (8500-1000 Ma) have been found in C94,C95, and PGT; 20%, 19,51% and 9,67% respectively.

The Cryogenian contribute (635-850 Ma) of is decidedly the highest. Samples C95 and C94 reach the 54,87% and 46,25% respectively; PGT and CORR 35,48% and 25,75%. The main peak falls within 660-670 Ma and represents the dominant signal in the Neoproterozoic populations (**Fig.53)**.

The Ediacaran population referable to the Panafrican Orogenic Cycle is well represented only in the samples C95 and C94 with (around of 10-11% of the total populations). Nevertheless this population does not show any pronounced peak. Samples PGT and CORR have lower values, 4.83% and 4.54% respectively.

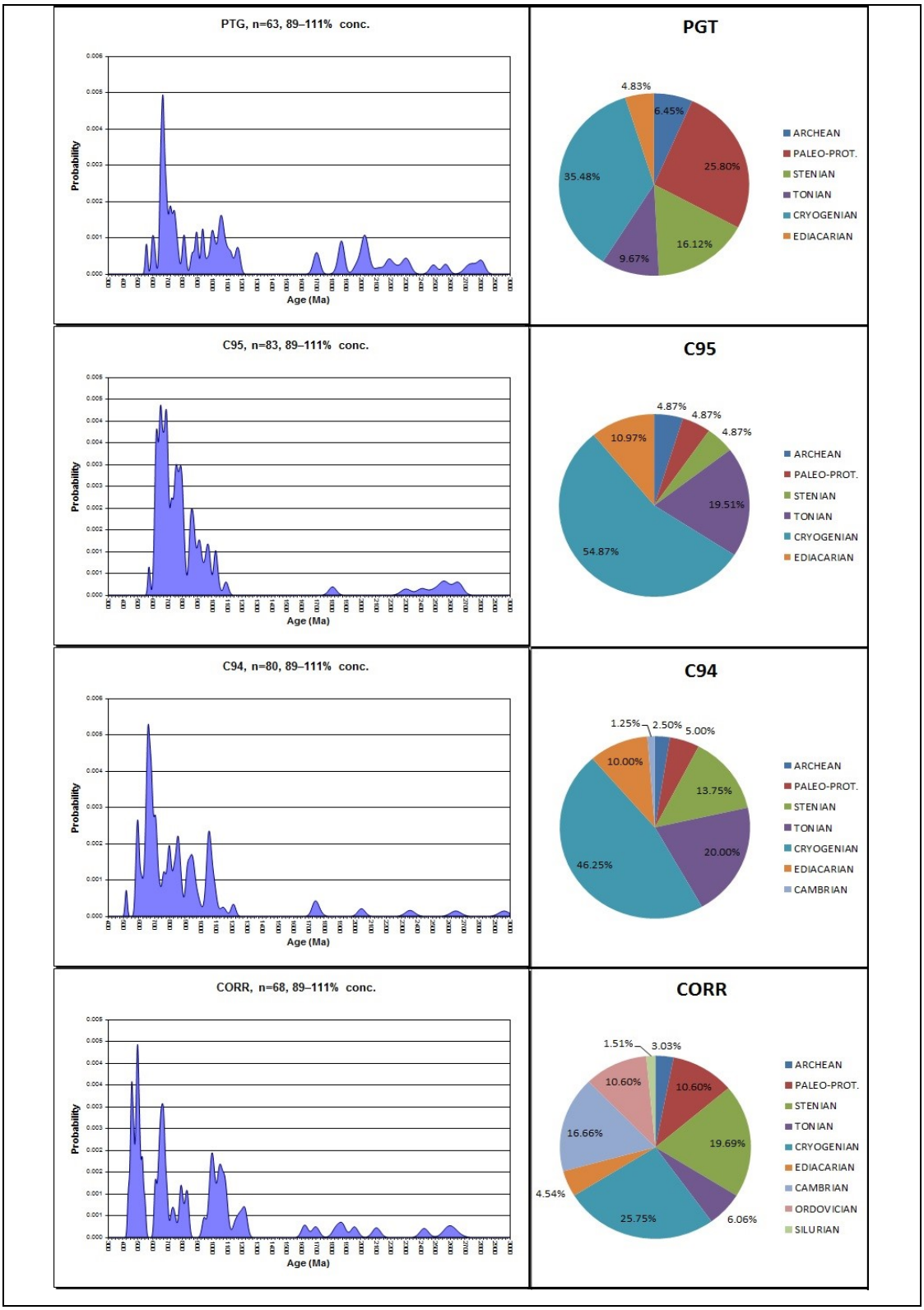


*Figure 53) Histogram frequency for the PGT, C95,C94 and CORR samples and density population. with related percentage of the samples.*

Zircon populations younger than Ediacaran have been found only in CORR with 10.60% of total abundance; this suggests that an Ordovician magmatism with main peak at 460-470 Ma contributed to the detrital provenance of this sediments. This eventuality is in good agreement whith the short-lived Middle Ordovician Andean-type arc that affected the north Gondwana margin (Oggiano et al., 2010). In the CORR sample the average age of Ordovician zircons is 459,6± 6,9 Ma (**Fig. 54**).

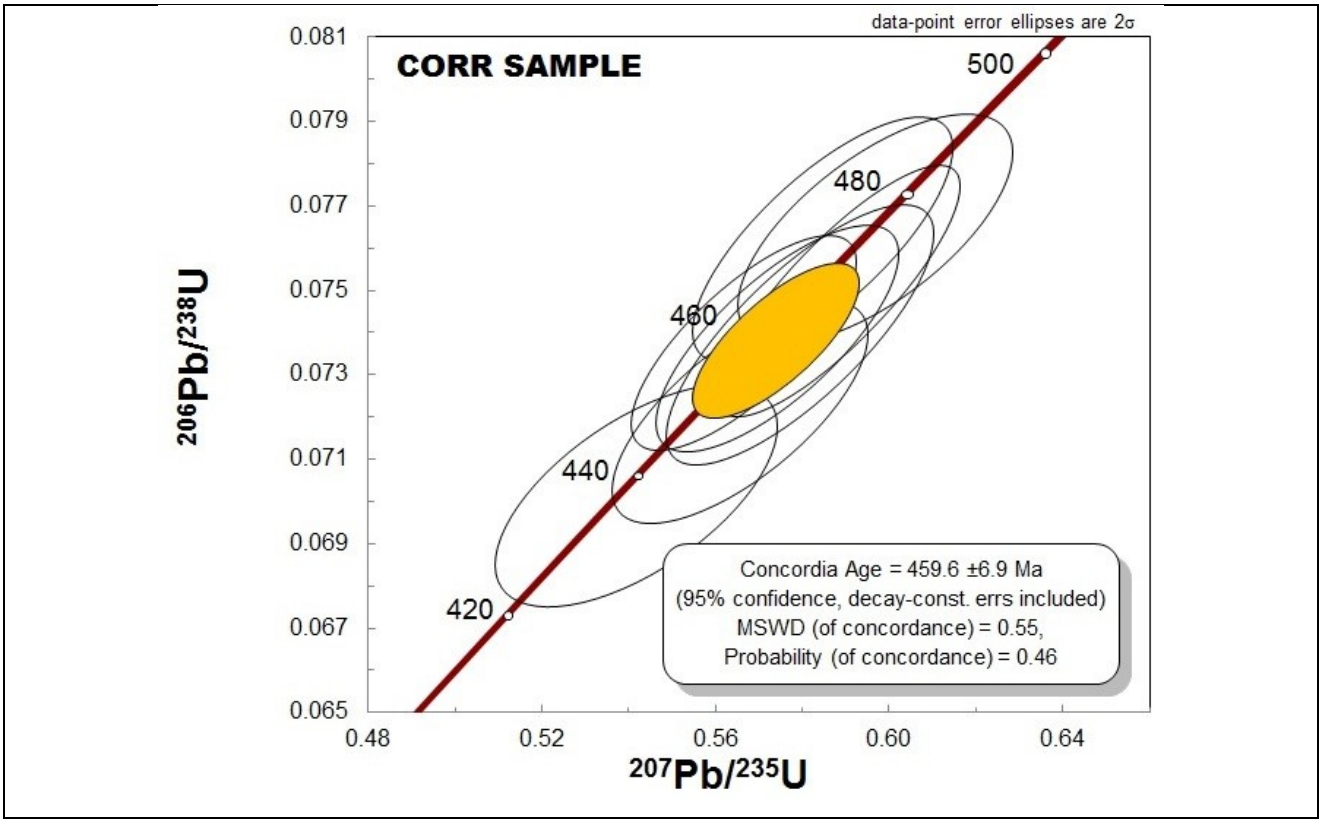


*Figure 54) Concordia diagram (Wetherill, 1956) with concordant age from the CORR sample (the volcanic Middle Ordovician cycle).*

## 4.5.2 PALAEOZOIC DETRITAL SAMPLES IN THE MEANA SARDO UNIT

Two sedimentary samples from were picked in the Meana Sardo Unit from as much formations previously dated on palaentological bases or by sure correls: sample SVI from the S.Vito Fm., sample GAD from the Orroeledu Fm. As before stated the S. Vito Fm (Calvino, 1959). is dated to Mid-Cambria-Lower Ordovician on the base of acritatcs, whereas the Orroeledu Fm. is correlated, with good confidence, to the Rio Cannoni Shales retaining of Upper Ordovician fossil associations (Naud, 1979).

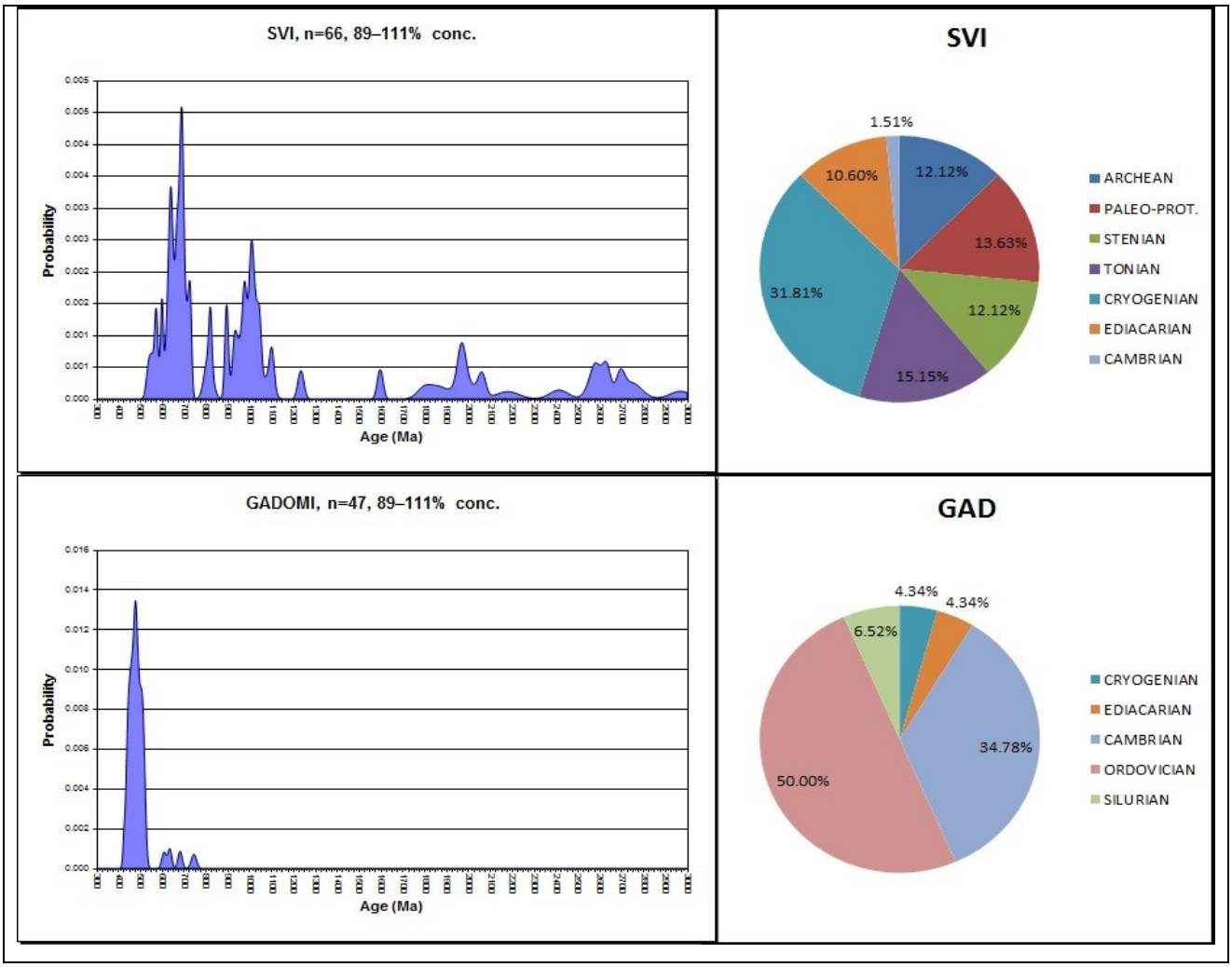


*Figure 55) Histogram frequency for the SVI samples and population density with related percentage of the same samples.*

Archean and Paleo-proterozoic population is only present in the SVI sample, whereas it is absent in the GAD sample. The SVI sample shows a 12.12% of Archean zircons and 13,63% of Paleo-Proterozoic zircons, and lacks of Middle Mesoproterozoic input (1200-1600 Ma). The Grenvillian population (980-1250 Ma) is well expressed with a population peak around 1008 Ma (18,12%). The Cryogenian presence (635-850 Ma) has the most abundant presence with 31,81% of the total population (**Fig.54**). A meaningful presence is also expressed by the Ediacarian population, which reaches 10,6 % 0f the total population. The contribute of Cambrian zircons is quite negligible, in the range of 1%.

In the GAD sample all the Precambrian population is reduced to a few (4) Neoproterozoic zircons of Cryogenian and Ediacarian ages respectively. Almost the whole population is bracketed within the Cambrian-Ordovician interval. Specifically 34% derive from Cambrian rocks and 50% from Ordovician. A little population (6,5%) exhibits an age which straddles the Ordovician-Silurian boundary.

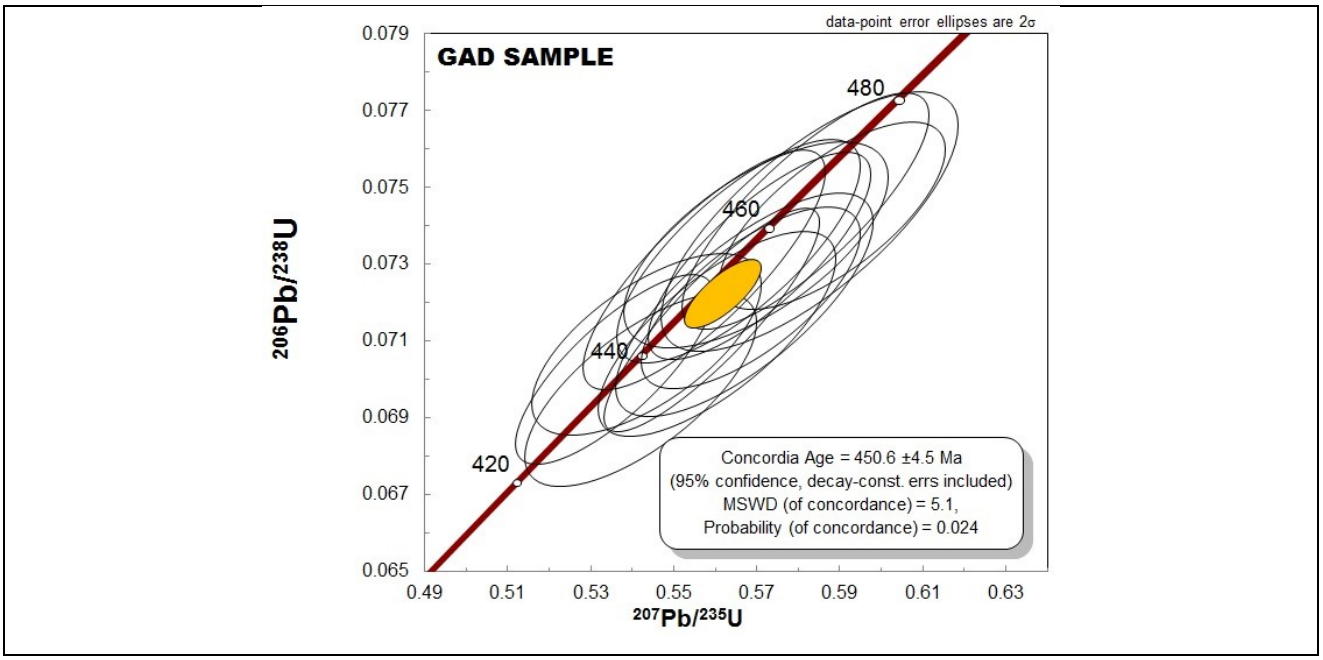


*Figure 56) Concordia diagram (Wetherill, 1956) with concordant age from the GAD sample (the volcanic Middle Ordovician cycle).*

The Ediacaran populations in the SVI sample is around 10.60%, while it has a small presence of the Cambrian population (1,51%). The Gad samples is composed mainly of the Cambrian and

Ordovician populations, with percentages of 34,78% and 50%; in this samples is recognizable the Ordovician magmatism that shows the main peak at 477 Ma. The Middle Ordovician cycle (~ 465 Ma, Gaggero et al. 2012), here obtained by the U-Pb age in GAD sample, gives a mean age of 450,6± 4,5 Ma (**Fig.56**).

## 4.5.3 MAGMATIC LATE PALAEOZOIC SAMPLES

In Sardinia the intrusions, constitutive of the C-S Batholith emplaced from 320 to 285 Ma (Casini et al. 2015). The ages of the U2 intrusions, mostly monzogranites and subordinate granodiorites range between 320 and 300 Ma whereas the U3 represented by Leucogranites and minor basic bodies emplaced around 290 Ma (Cocherie et al. 205). The U-Pb age obtained in fine grained granodiorite with mafic enclaves (GR110 sample) , is of 299± 3 Ma (**Fig-57**). Hence this intrusion is referable to the U2 intrusions that herefore referable to ages of the intermediate to acid intrusions range (305 and 300 Ma).

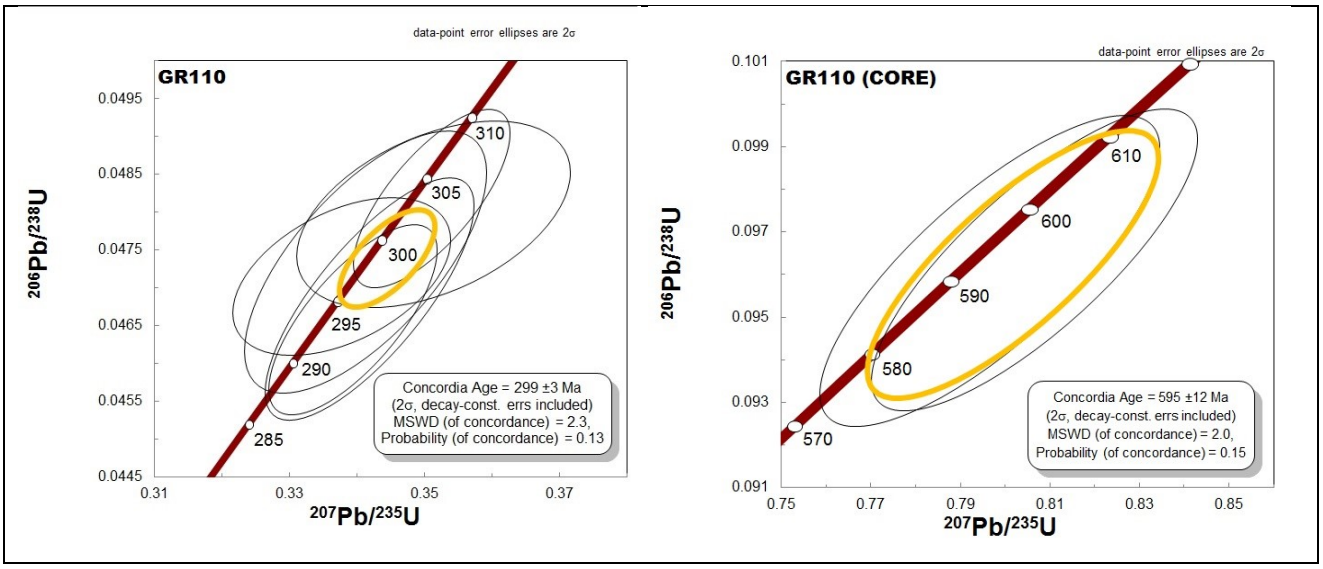


*Figure 57) Concordia diagram (Wetherill, 1956) with concordant age from the GR110 sample.*

# REFERENCES


Calvino, F. (1959). Lineamenti strutturali del Sarrabus-Gerrei (Sardegna sud-orientale). Bollettino del Servizio Geologico d'Italia, 81(4–5), 489–556.

Casini, L., Cuccuru, S., Maino, M., Oggiano, G., Puccini, A., & Rossi, P. (2015). Structural map of Variscan northern Sardinia (Italy). *Journal of Maps*,*11*(1), 75-84.

Gaggero, L., Oggiano, G., Funedda, A. & Buzzi, L., 2012. Rifting and arc-related early Paleozoic volcanism along the North Gondwana margin: geochemical and geological evidence from Sardinia (Italy). The Journal of Geology.

Loi A. & Dabard M.P. (1997) - Zircon typology and geochemistry in the palaeogeographic reconstruction of the Late Ordovician of Sardinia (Italy). Sedimentary Geology: 112, 263-279, Amsterdam.

Naud, G. (1979). Les shales de Rio Canoni, formation-repe`re fossilife`re dans l'Ordovicien supe´rieur de Sardaigne orientale. Conse´quences stratigraphiques et structurales. Bulletin de la Socie´te´ ge´ologique de France, 21(2), 155–159.

Oggiano G., Gaggero L., Funedda A., Buzzi L. & Tiepolo M. 2010. Multiple early Paleozoic volcanic events at the northern Gondwana margin: U–Pb age evidence from the Southern Variscan branch (Sardinia, Italy). Gondwana Research 17, 44–58.

Pertusati, P. C., Sarria, E., Cherchi, G. P., Carmignani, L., Barca, S., Benedetti, M., ... & Pintus, C. (2002). Note Illustrative della Carta Geologica d 'Italia alla scala 1: 50.000, Foglio 541 Jerzu.

Pupin JP (1980) Zircon and granite petrology. Contrib Mineral Petrol 73:207-220

Vai G.B. & Cocozza T. (1974) - Il "Postgotlandiano" sardo, unità sinorogenica ercinica. Boll. Soc. Geol. It.: 93, 61-72, Roma.

Wetherill, G. W. (1956). Discordant uranium-lead ages, I. Eos, Transactions American Geophysical Union, 37(3), 320-326.

# 5. THE LACONI-ASUNI AREA

In the southern part of the study area they are well represented the nappes with the lower metamorphic grade and less complex deformation, hence the geological surveys and mapping began around Laconi-Asuni where the Cambrian-Devonian succession is well exposed and decipherable also thanks to a still preserved fossil record including acritarchs. The works on this area has been published in 2014 on the Journal of map and is reported in the followings. The main aspect of this area is a regional structure known as the Flumendosa Antiform.

**Journal of Maps**
Publication details, including instructions for authors and subscription information:
http://www.tandfonline.com/loi/tjom20

# Geology of the Variscan basement of the Laconi-Asuni area (central Sardinia, Italy): the core of a regional antiform refolding a tectonic nappe stack

Antonio Funedda[a], Mattia Alessio Meloni[b] & Alfredo Loi[a]
[a] Dipartimento di Scienze chimiche e geologiche, University of Cagliari, Cagliari, Italy
[b] Dipartimento di Scienze della Natura e del territorio, University of Sassari, Sassari, Italy
Published online: 17 Jul 2014.

**To cite this article:** Antonio Funedda, Mattia Alessio Meloni & Alfredo Loi (2014): Geology of the Variscan basement of the Laconi-Asuni area (central Sardinia, Italy): the core of a regional antiform refolding a tectonic nappe stack, Journal of Maps, DOI: 10.1080/17445647.2014.942396
**To link to this article:** http://dx.doi.org/10.1080/17445647.2014.942396

Journal of Maps, 2014

http://dx.doi.org/10.1080/17445647.2014.942396

# GEOLOGY OF THE VARISCAN BASEMENT OF THE LACONI-ASUNI AREA (CENTRAL SARDINIA, ITALY): THE CORE OF A REGIONAL ANTIFORM REFOLDING A TECTONIC NAPPE STACK

**Antonio Funedda[a]*, Mattia Alessio Meloni[b] and Alfredo Loi[a]**

[a]*Dipartimento di Scienze chimiche e geologiche, University of Cagliari, Cagliari, Italy;* [b]*Dipartimento di Scienze della Natura e del territorio, University of Sassari, Sassari, Italy*

*(Received 7 March 2014; resubmitted 24 June 2014; accepted 3 July 2014)*

The study area extends in central Sardinia between the coordinates 8856′00″/39855′00″ (NW corner) and 9803′00″/39850′00″ (SE corner). It forms part of the Sardinian Variscides that are characterized here by the western-most aspect of a regional structure known as the Flumendosa Antiform, which runs ENE-trending for more than 50 km along its axis. It represents the envelopment of several, upright km-scale minor folds that refold the different tectonic units of the Variscan Nappe zone characterized by a number of isoclinal folds, with axial plane foliation and thick ductile shear zones. The antiform is in turn deformed by lateorogenic extensional structures, namely asymmetric folds and narrow, low angle ductile shear zones that generally reactivate earlier collisional structures. The 1:12,500 scale map completes the mapping of this important regional structure, meaning that a detailed survey of the entire mega-structure is now available. This enables more detailed structural analyses of poly-deformed areas in low-grade metamorphic conditions to be conducted, given the robust knowledge available of the lithostratigraphic succession and the geometric and kinematic outlines.

**Keywords:** Variscan orogenesis; north-Gondwana; regional antiform; Nappe zone; polyphasal deformation; structural map

## 5.1. Introduction

The study area is one of the key sites where 35 years ago the geology of the Nappe zone of the Sardinian branch of the Variscan chain began to be discovered (Carmignani et al., 1994; Carmignani, Oggiano et al., 2001, and references therein) (**Figure 58**). Until then, the Variscan basement of SE Sardinia had been regarded as an indistinguishable succession of low-grade metamorphic rocks (Cocozza, Jacobacci, Nardi, & Salvadori, 1974). During the 1970s and 1980s, geological mapping (in detail for the first time) performed by Carmignani, Minzoni, Pertusati, and Gattiglio (1982) allowed the detection of a number of tectonic structures affecting several formations of different lithostratigraphic units. These authors produced an innovative map (**Figure 59)**, although not all of the geological framework of the Variscan belt in Sardinia was clear and there were still many uncertainties about both the lithostratigraphy and deformational structures. Indeed, after taking the first step towards mapping the area, and given the difficulties faced in getting deeper into unravelling its structures, the authors chose to turn their interest to different zones, although they did apply some key knowledge they acquired on the lithostratigraphic successions to the new zones. We now return to the Laconi-Asuni area to present the final results of that work, integrating the knowledge discovered over the last three decades in the rest of the Sardinian Variscan basement. Several maps have recently been published in this part of the Nappe zone, some of which were produced for the Italian geological survey: Foglio 541-Jerzu (Pertusati et al., 2002); Foglio 549-Muravera (Carmignani, Conti et al., 2001); Foglio 548-Senorbı` (Funedda, Carmignani, Pertusati, Forci et al., 2011); Foglio 540-Mandas (Funedda, Pertusati et al., 2011); and two others (Funedda, Naitza et al., 2011; Musumeci et al., 2014). The present map (see Main Map) completes the geological mapping of the entire Flumendosa Antiform (**Figure 60**) at a detailed scale (generally between 1:10,000 and 1:25,000). This suite of maps shows a model of an antiformal nappe stack that occurred throughout repeated shortening phases involving a foreland during the continental collision between some parts of the peri north-Gondwana terranes (Armorica Terranes Assemblage or Galatian according to von Raumer, Bussy, Schaltegger, Schulz, &

Stampfli, 2012) and the southern part of the Laurussia paleo-continent that gave rise to the South Variscan Realm (Rossi, Oggiano, & Cocherie, 2009).

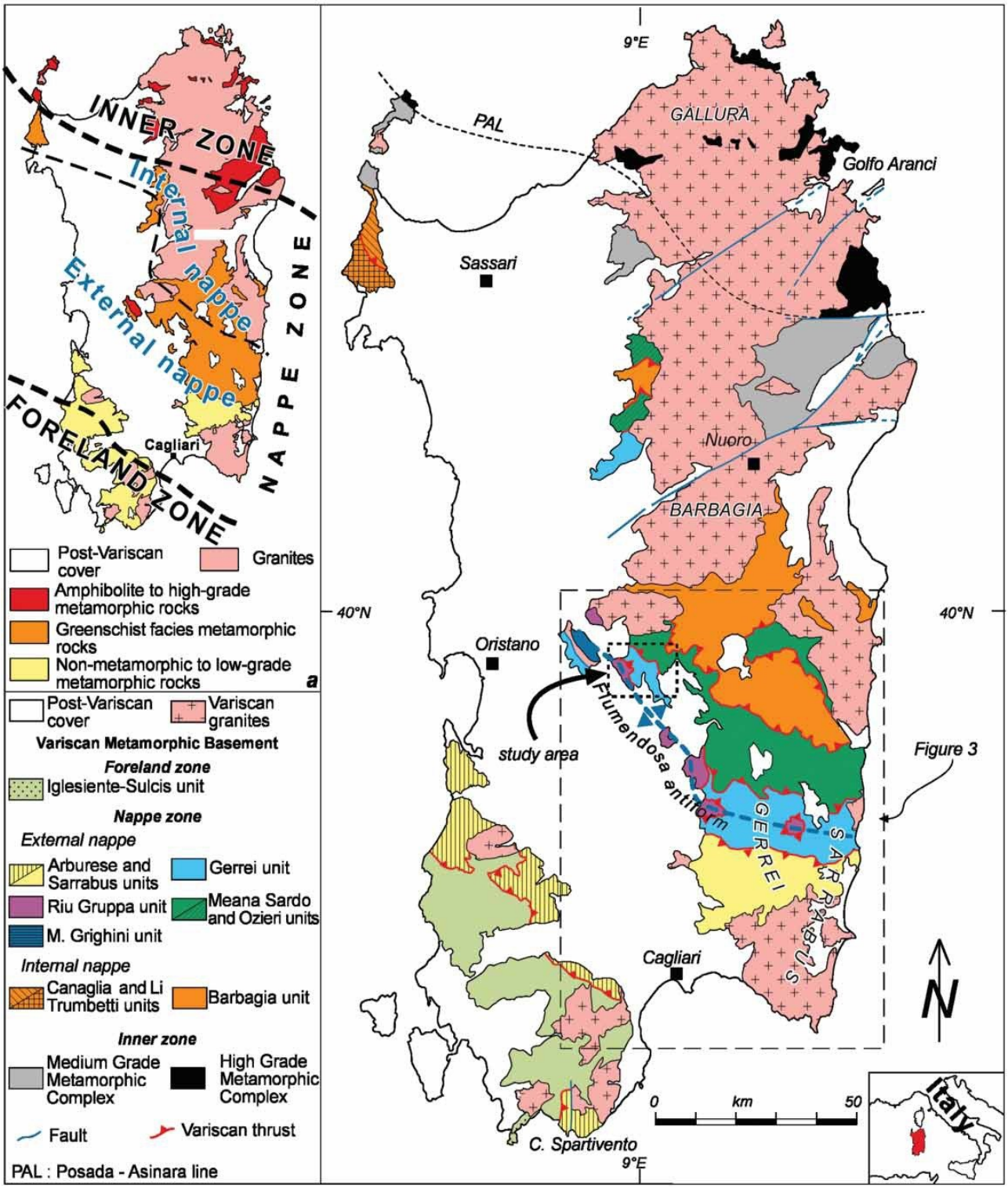


*Figure 58) Structural sketch map of the Variscan basement in Sardinia;*

*(a) Variscan tectono metamorphic zones.*

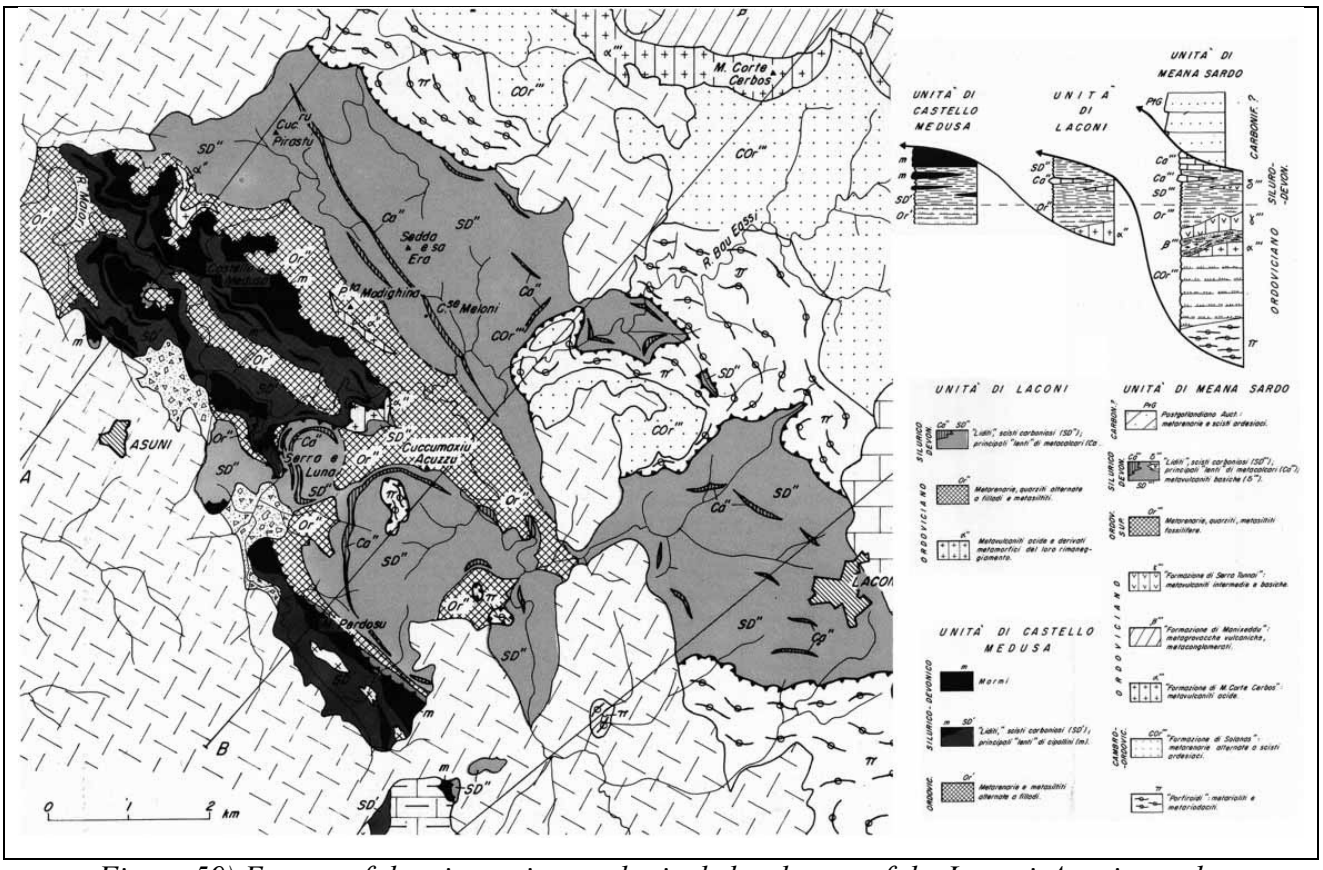


*Figure 59) Extract of the pioneering geological sketch map of the Laconi-Asuni area by Carmignani, Minzoni et al. (1982).*

## 5.2. Geological outline

The study area is located along the north-western end of the Flumendosa Antiform, which is one of the main regional features in central-south Sardinia that is related to the late Variscan collision. There, the erosion permits the outcrop of a nappe stack composed of several tectonic units emplaced by a general tectonic transport the 'top-towards-SSW' that were internally strongly deformed in a low-grade metamorphic environment and were subsequently refolded all together in huge antiforms and synforms. From the bottom, the mapped tectonic units are: the Rio Gruppa Unit (also known as the Castello Medusa Unit), the Gerrei Unit (in this area, the Arcu de su Bentu sub-unit) and, at the top, the Meana Sardo Unit. The antiform gently dips towards the ESE, therefore in the western part crops out the lowest part of the nappe stack. The detection of wide ductile shear zones among the three tectonic units that developed during the collisional phase outlined a different architecture and

different lithostratigraphic successions with respect to what was formerly known. The map therefore represents a clear improvement on the previously available structural sketch map.

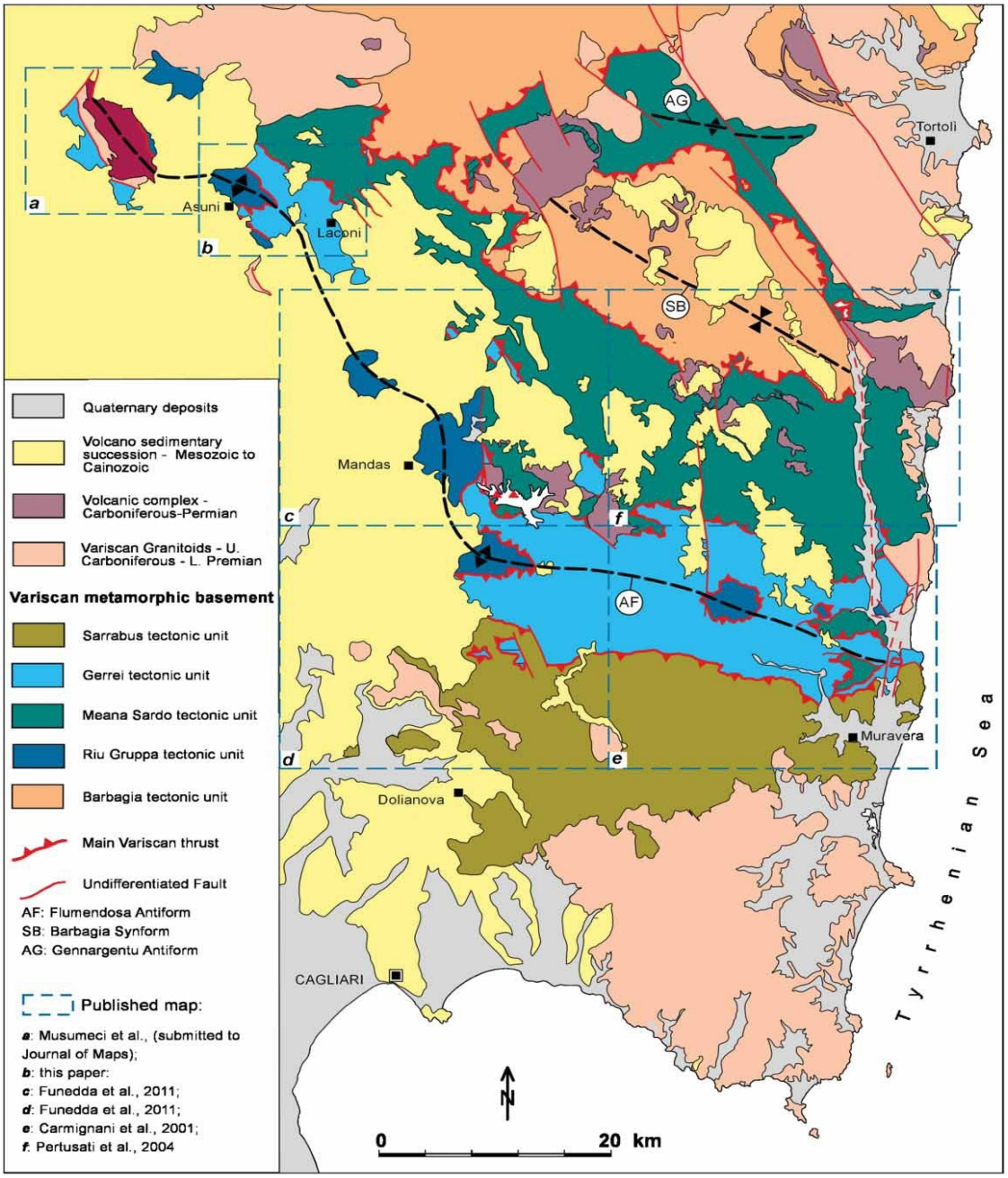


*Figure 60) Tectonic sketch map of the south-central Sardinia Variscan basement; the blue dashed boxes indicatethe location of published geological maps that cover all of the regional Flumendosa Antiform.*

## 5.3. Stratigraphic outline

All of the tectonic units that made up the Nappe zone have in common a similar lithostratigraphic succession (from the Middle Cambrian to the Early Carboniferous), which was involved in the Variscan orogenesis and metamorphosed in lower green-schist facies (**Figure 61**). Very few fossils have been found in the Rio Gruppa Unit. However, based on their lithostratigraphic features, the different formations are easily correlated with the ones dated in the Gerrei,Meana Sardo and Sarrabus units. From the bottom to the top, the succession comprises:

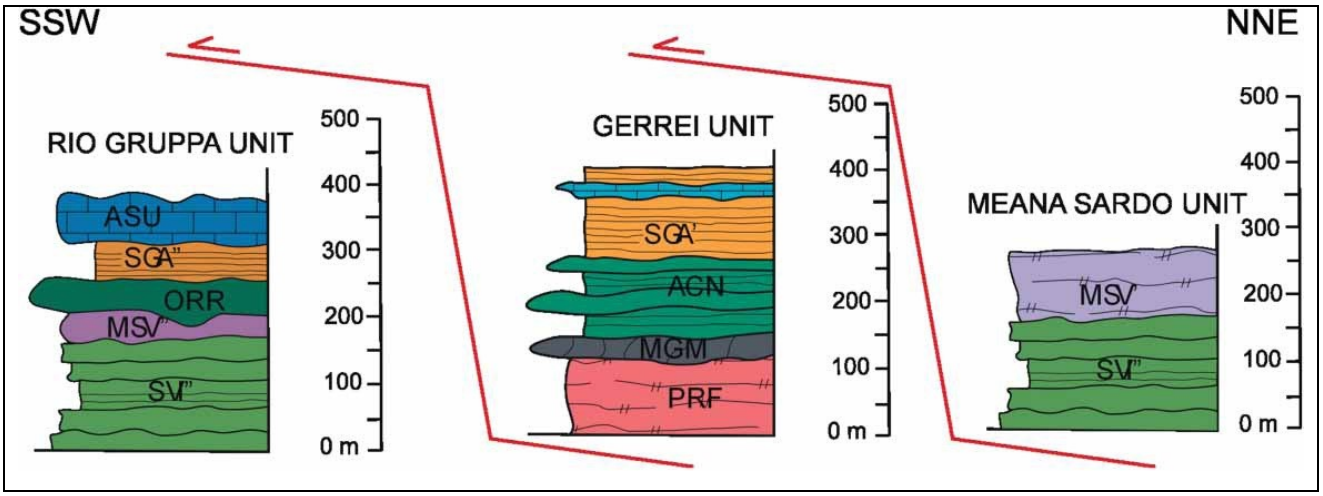


*Figure 61) Schematic lithostratigraphic columns of the Variscan tectonic units in the Laconi-Asuni area*.

- A siliciclastic succession (Arenarie di San Vito, Calvino, 1959) that consists of prevailing metasandstones and metasiltstones. The occurrence of widespread storm deposits and the recent discovery of a trilobite association in the Sarrabus tectonic Unit (Gnoli & Pillola, 2002; Pillola & Leone, 1997) indicate a deposition in a littoral environment, rather than in a deep water turbidite system as previously reported; the age of the succession is from the Middle Cambrian to the Early Ordovician (Naud & Pittau Demelia, 1987).

- A volcanic complex where it is possible to distinguish different volcanic facies interlayered with epiclastic deposits; they are generally metandesites (Monte Santa Vittoria Formation) and rhyolitic to dacitic metaignimbrites, with a porphyric texture for the phenocrysts of Kfeldspar and quartz (Porfiroidi Formation), all with a calcalkaline geochemistry. The age is now commonly stated to be about 460 Ma (Middle -Late Ordovician) based on radiometric analyses (Cruciani,

Franceschelli,Musumeci, Spano, & Tiepolo, 2013; Dabard, Chauvel, & Loi, 1994; Gaggero, Oggiano, Funedda, & Buzzi, 2012; Loi & Dabard, 1997; Oggiano, Gaggero, Funedda, Buzzi, & Tiepolo, 2010; Pavanetto et al., 2012).

- A changing upwards succession from mainly siliciclastic at the bottom to carbonate at the top as follows:(i) quarzites, metagreywackes and metarkoses (Metarcose di Gennamesa, Carmignani, Conti et al., 2001) that are Late Ordovician in age; (ii) then, fossiliferous metasiltstones and rare metalimestones (Orroeledu Formation in the Meana Sardo Unit, Bosellini & Ogniben, 1968; Punta Serpeddı` Formation in the Sarrabus Unit, Loi, Barca, Chauvell, Dabard, & Leone, 1992; Rio Canoni shale in the Gerrei Unit, Naud, 1979) that are Late Ordovician in age; (iii) in turn, these formations are covered by black shales with interbedded metalimestones layers (Scisti neri Formation) that are Silurian to Early Devonian in age (Corradini, Ferretti, & Serpagli, 1998); and iv) at the top, generally massive metalimestones (Calcari di Villasalto, Carmignani, Conti et al., 2001) that are referable to the Middle Devonian-Early Carboniferous period (Corradini, Barca, & Spalletta, 2003), and marbles (Marmi di Asuni), the age of which is referable to the Devonian based on lithostratigraphic correlation with the Calcari di Villasalto.

*Table 1. Summary of the structural elements recognized in the study area in the different tectonic units andtheir association with relative deformation phases and shortening directions*

| TECTONIC SETTING | Structural elements mapped in the Variscan basement of Laconi-Asuni | Regional features | Deformation phases (and shortening direction when recognised) | Conti, Carmignani & Funedda, 2001, this paper | Conti & Patta, 1998, this paper | Carosi & Pertusati, 1990 | Carmignani et al., 1978 | |
|---|---|---|---|---|---|---|---|---|
| | | | | PHASE NAMES | | | | |
| Crustal thickening | SE trending, isoclinal overturned folds, with axial plane cleavage, SSW-warding thrusts and mylonitic zone (S1, A1, L1) | Early mylonitic deformation in the Barbagia, Meana Sardo and Riu Gruppa unit, folding and main regional foliation in the Gerrei unit | D1: Early SSW-directed thrusting and folding | Gerrei phase | D1 | D1 | D1 | time ↓ |
| | | Final emplacement, late mylonitic deformation, main foliation development in the Meana Sardo and Barbagia units | D1: Main SSW-directed nappe emplacement | Meana phase | | D2 | | |
| | not developed in the study area | Emplacement and main folding in the Sarrabus and Arburese units | D1: W-directed nappe emplacement | Sarrabus phase | D1' | D1 | | |
| | SE dipping, upright folds | Large-scale upirght antiforms and synforms, crenulation cleavage | D1: Late stage N-S shortening | Flumendosa phase | LD1 | D3 | D2 | |
| Tectonic exhumation | SE trending, overturned folds with axial plane cleavage (S2, A2) | Normal faulting, NW-SE folds, crenulation cleavage | D2 | Rio Gruppa phase | D2 | | | |
| ? | SE trending, folds, (S3, A3) | NE-SW folds, crenulation cleavage | D3 | | D3 | D4 | D3 | |

*A, fold axis; S, tectonic foliation; L, stretching lineation; (name of the Variscan tectonic phases after: Carmignani,Cocozza, Minzoni, & Pertusati, 1978; Carosi & Pertusati, 1990; Conti et al., 2001; Conti & Patta, 1998).*

The entire metamorphic succession is intruded by small bodies of Upper Carboniferous to Permian granitoids that widely crop out in the surrounding areas (e.g. southwards of the study area, close to Nureci and Genoni villages). The crystalline basement is unconformably covered by the Mesozoic carbonates (Costamagna & Barca, 2004) and a volcano-sedimentary succession emplaced during the Oligo-Miocene (Funedda, Carmignani, Pertusati, Uras et al., 2011). In neighbouring areas the oldest formations not involved in the Variscan orogenesis are Permian in age (Pittau, Del Rio, & Funedda, 2008).

## 5.4. Tectonic outline

The area is characterized by several km-scale ESE-trending open antiforms and synforms that deform thrusts, folds and cleavages that are related to the early stages of the collisional evolution. These antiforms and synforms, which are related to a NE-SWsub-horizontal shortening, occurred during the late stage of collision and are in turn deformed by NNE-trending upright folds and normal and strike-slip faults that developed during the post-collisional extension. In more detail, it is possible to recognize at least four deformational phases. To distinguish them, and to avoid ambiguities in recognizing and naming the different tectonic phases, we report both the classical nomenclature based on numbers going from the oldest to the youngest (D1, D2, etc.) and the names proposed by Conti, Carmignani, and Funedda (2001) (Table 1):

- D1 shortening phase (Gerrei and Meana phases) that is related to the collisional stage. The main structural features are: km-scale isoclinal recumbent folds with an axial plane cleavage (S1), generally they are synclines with Silurian and Devonian formations at their core and anticlines with Cambrian successions at their core (see geological cross-section in the map). S1 is the main tectonic surface recognizable in the field; generally, it transposed the primary bedding except in some zones of the Rio Gruppa and Meana Sardo units, where the main tectonic foliation refolds and transposes an older relict tectonic foliation probably related to the early stage of the collision phase. The lack of outcrop- and map-scale folds related to the relict foliation (it is only preserved in microlithons at sub-centimetre scale and does not have physical continuity in the field) and the lack of differences in the petrographic features (i.e. there are no differences in metamorphic paragensis or in microstructures) do not support the occurrence of a polyphasal deformation during the D1 phase in this area. Overprinting foliations look likely related to progressive deformation commonly

occurring in areas where high strain deformation developed. Given the observations, and the current state of knowledge, the 'progressive deformation' model must to be preferred rather than a 'polyphasal deformation' model (for a thorough discussion about the Nappe zone in Sardinia see: Carosi & Pertusati, 1990; Conti et al., 2001; Conti, Funedda, & Cerbai, 1998; for a short comment on the general topic see: Fossen, 2010, p. 441). Coeval with, or a short while thereafter, thrusts developed, resulting in the emplacement of the tectonic units to form a stack. They are marked by a hectometre-size ductile shear zone where mylonitic deformation prevails. The thickest mylonite belts developed along the contact between the Rio Gruppa and Gerrei units, as is also common in near-by areas (Funedda, Naitza et al., 2011). Often, the mylonitization is so pervasive that it is impossible to recognize the protolite, just a quartz-feldspatic composition can be inferred, but not the lithostratigraphic unit. The observed microstructures, generally in quartz and subordinately in calcite crystals (e.g. sub-grain rotation, deformation band, twinning, etc.) indicate a lowgrade metamorphism, as described in the other area of the Nappe zone (Casini & Funedda, 2014; Casini, Funedda, & Oggiano, 2010; Conti et al., 1998; Pavanetto et al., 2012). Kinematic indicators along the ductile shear zone and stretching lineations (mostly mineral lineation of muscovite in metarenites and stretched fragments in metaconglomerates and metavolcanites) on the S1 foliation all support a general transport direction of the 'top-towards-S'. A scattering of strike of the stretching lineations that generally affects the Gerrei Unit at the map scale could be related to later deformation phases, but could also be produced by local oblique combination of pure and simple shear or by deformation occurring far from plane strain. The deformation style and the paragenesis along the S1 concur with an increase in deformation and metamorphism from the upper units to the deeper ones (Carosi, Leoni, Paolucci, Pertusati, & Trumpy, 2010; Carosi, Musumeci, & Pertusati, 1990, 1991).

- LD1 shortening phase (Flumendosa phase): all of the structures described in the D1 stage were subsequently deformed by upright, ESE-trending and E-dipping large folds, with a km-scale amplitude and wavelength that developed discontinuous and non-penetrative axial plane crenulation cleavage. The structural style (upright folds, non penetrative cleavage development) suggests a less intense deformation compared to the D1 phase. As mentioned above, these structures are most evident at the map scale and greatly influenced the general architecture of the Variscan basement in

central-south Sardinia. At the regional scale, the enveloping structure of these folds is known as the Flumendosa Antiform (Carmignani, Costagliola et al., 1982).

- D2 extensional phase (Rio Gruppa phase): after the collision, the entire Nappe zone suffered a widespread extension that led to the exhumation of the deepest units of the stack. Accordingly, several tectonic units crop out at the same topographic level. The extension and uplift reactivated the D1 tectonic contacts and foliations with a normal-fault kinematics. This feature is not well expressed in the study area, however, it is very common in neighbouring areas where the D1 thrusts were reactivated as normal faults with an opposite sense of shear on the opposite limbs of the LD1 antiforms (Conti et al., 1999): the 'top-towards- NNE' in the northern limbs and the 'top-towards-SSW' in the southern limbs. During the exhumation in the more highly deformed zones, cm- to dmscale asymmetric overturned folds developed with axes parallel to the LD1 limbs upon which they formed and with the same kinematics as the normal faults. In the most deformed zone, an axial plane cleavage, S2, developed. The result of this reactivation is the major enhancement of the LD1 antiform hinges.

- D3 phase: although poorly developed, it is possible to recognize some NNE-trending upright folds that deformed the D1, LD1 and D2 structural elements. In the eastern-most part of the Flumendosa Antiform, these folds are more intense and possibly related to late Variscan strike-slip corridors (Carmignani, Conti et al., 2001; Funedda, Naitza et al., 2011).

## 5.5. Methods

The map is the result of traditional fieldwork carried out at 1:10,000 scale for a Master's degree thesis project (performed by M.M. under the supervision of A.F. and A.L.) and improved as the preliminary outcome of a PhD project (by M.M.). The starting point of the work was the pioneering structural sketch map at 1:50,000 scale (Figure 2) published by Carmignani, Minzoni et al. (1982). The fieldwork was conducted by applying new knowledge about the structures and the lithostratigraphic succession of the Variscan basement, mostly in the Upper Ordovician succession. The occurrence of a complicated non-cylindrical deformation, which is related to the superimposition of several folds and thrusts with different tectonic transport directions, prevents the balancing and restoration of the geological cross-sections. The trial and error method comparing the

outcrops map and the cross-sections largely improved the definitive map. The geological cross-sections have been drawn by projecting the structural data from the adjacent outcrops generally 10–208 towards N1208 (the mean trend of the LD1 – or Flumendosa phase – antiforms and synforms). This means that, given that the sections are NE-SW oriented, the structures cropping out on the NW side are projected underground and those on the SE side above the topographic level. This assumption is not, however, correct everywhere, given the strong non-cylindricity of the structures and the effect of the D3 folds. As a consequence, we avoid projecting structures that are too far away from the section traces. Nevertheless, this is the most useful way to represent the complex, polyphasal deformation of the study area. The first draft of the map was hand-made, and only the final version of the map, legend, sections and sketches was produced electronically.

## 5.6. Conclusions

The present map completes the detailed mapping of the Flumendosa Antiform. This is one of the most exposed regional structure related to the Variscan collisional nappe stack of Sardinia, and was exhumed during Permian times and deeply eroded during the Pliocene-Pleistocene uplift that involved the Sardinian crust. A polyphasal deformation, which occurred there during the Carboniferous period and is related to the collisional and post-collisional evolution of the Sardinian Variscides, has been confirmed. The existence of such a regional structure, which is composed of several refolded tectonic units with similar lithostratigraphic successions and a slight enhancement of the deformation and metamorphic grade from the shallowest to the deepest and from the foreland to the hinterland, allows the study of the polyphasal evolution of a foreland fold-thrust belt during the continental collision. This is a natural laboratory for testing the evolution of a fold-thrust belt that developed in a ductile regime at the boundary between the upper and lower crust.

### *Software*

The map was compiled by redrawing the geological contacts from a scanned version of the handmade map using Adobe Illustrator CS5.

### *Acknowledgements*

This research has been partially funded by the Regione Autonoma della Sardegna (L.R. n.7, grant to A.L.). A.F. thanks L. Carmignani, P.C. Pertusati and G. Oggiano who 20 years ago introduced him to the mapping of metamorphic basement, often recalling the necessity to return to map the Laconi area. G. Cornamusini, H. Apps and R. Carosi are thanked for their constructive review of the submitted manuscript.

## REFERENCES

Bosellini, A., & Ogniben, G. (1968). Ricoprimenti ercinici nella Sardegna centrale. Annali dell'Universita` di Ferrara, 1, 1–15.

Calvino, F. (1959). Lineamenti strutturali del Sarrabus-Gerrei (Sardegna sud-orientale). Bollettino del Servizio Geologico d'Italia, 81(4–5), 489–556.

Carmignani, L., Carosi, R., Di Pisa, A., Gattiglio, M., Musumeci, G., & Oggiano, G. (1994). The Hercynian chain in Sardinia (Italy). Geodinamica Acta, 7, 31–47.

Carmignani, L., Cocozza, T., Minzoni, N., & Pertusati, P. C. (1978). Falde di ricoprimento erciniche nella Sardegna a Nord-Est del Campidano. Memorie della Societa` Geologica Italiana, 19, 501–510.

Carmignani, L., Conti, P., Barca, S., Cerbai, N., Eltrudis, A., & Funedda, A. (Cartographer). (2001). Foglio 549-Muravera. [Sheet 549-Muravera] [Geological map of Italy on the 1:50,000 scale], ISPRA Servizio Geologico d'Italia, Rome. Retrieved from MURAVERA/Foglio.html http://www.isprambiente.gov.it/Media/carg/549

Carmignani, L., Costagliola, C., Gattiglio, M., Leglise, H., Oggiano, G., & Maxia, M. (1982). Lineamenti geologici della Bassa Valle del Flumendosa (Sardegna Sud-Orientale). In L. Carmignani, T. Cocozza, C. Ghezzo, P. C. Pertusati & C. A. Ricci (Eds.), Guida alla Geologia del Paleozoico Sardo (pp. 95– 107). Guide Geologiche Regionali. Societa` Geologica Italiana.

Carmignani, L., Minzoni, N., Pertusati, P. C., & Gattiglio, M. (1982). Lineamenti geologici principali del Sarcidano-Barbagia di Belvı`. In L. Carmignani, T. Cocozza, C. Ghezzo, P. C. Pertusati & C. A. Ricci (Eds.), Guida alla Geologia del Paleozoico Sardo (pp. 119–125). Guide Geologiche Regionali. Societa` Geologica Italiana.

Carmignani, L., Oggiano, G., Barca, S., Conti, P., Salvadori, I., & Eltrudis, A. (2001). Geologia della Sardegna. Note illustrative della Carta Geologica in scala 1:200.000. Memorie Descrittive della Carta Geologica d'Italia, LX,. Roma: Servizio Geologico d'Italia.

Carosi, R., Leoni, L., Paolucci, F., Pertusati, P. C., & Trumpy, E. (2010). Deformation and illite crystallinity in metapelitic rocks from the Mandas area, in the Nappe Zone of the Variscan belt of Sardinia. Rendiconti online della Societa` gelogica Italiana, 11(2), 395–396.

Carosi, R., Musumeci, G., & Pertusati, P. C. (1990). Le Unita` di Castello Medusa e Monte Grighini (Sardegna centro-meridionale) nell'evoluzione tettonica del basamento ercinico. Bollettino della Societa` Geologica Italiana, 109, 643–654.

Carosi, R., Musumeci, G., & Pertusati, P. C. (1991). Differences in the structural evolution of tectonics units in central-southern Sardinia. Bollettino della Societa` Geologica Italiana, 110, 543–551. Carosi, R., & Pertusati, P. C. (1990). Evoluzione strutturale delle unita` tettoniche erciniche nella Sardegna centro-meridionale. Bollettino della Societa` Geologica Italiana, 109, 325–335.

Casini, L., & Funedda, A. (2014). Potential of pressure solution for strain localization in the Baccu Locci Shear Zone (Sardinia, Italy). Journal of Structural Geology, 66, 188–204. doi:10.1016/j.jsg.2014.05.016

Casini, L., Funedda, A., & Oggiano, G. (2010). A balanced foreland–hinterland deformation model for the Southern Variscan belt of Sardinia, Italy. Geological Journal, 45(5–6), 634–649. doi:10.1002/gj.1208

Cocozza, T., Jacobacci, A., Nardi, R., & Salvadori, I. (1974). Schema stratigrafico-strutturale del Massiccio Sardo-Corso e minerogenesi della Sardegna. Memorie della Societa` Geologica Italiana, 13, 85–186.

Conti, P., Carmignani, L., Cerbai, N., Eltrudis, A., Funedda, A., & Oggiano, G. (1999). From thickening to extension in the Variscan belt - kinematic evidence from Sardinia (Italy). Terra Nova, 11(2/3), 93–99.

Conti, P., Carmignani, L., & Funedda, A. (2001). Change of nappe transport direction during the Variscan collisional evolution of central-southern Sardinia (Italy). Tectonophysics, 332(1–2), 255–273.

Conti, P., Funedda, A., & Cerbai, N. (1998). Mylonite development in the Hercynian basement of Sardinia (Italy). Journal of Structural Geology, 20(2/3), 121–133. doi:10.1016/S0191-8141(97)00091-6

Conti, P., & Patta, E. D. (1998). Large scale Hercynian West-directed tectonics in southeastern Sardinia (Italy). Geodinamica Acta, 11(5), 217–231.

Corradini, C., Barca, S., & Spalletta, C. (2003). Late Devonian-Early Carboniferous conodonts from the "Clymeniae Limestones" of SE Sardinia (Italy). Cour. Forsch.-Inst. Senckemberg, 245, 227–253.

Corradini, C., Ferretti, A., & Serpagli, E. (1998). The Silurian and Devonian sequence in SE Sardinia. Giornale di geologia, 60(ECOS VII - special issue), 71–74.

Costamagna, L., & Barca, S. (2004). Stratigrafia, analisi di facies, paleogeografia e dinquadramento regionale della successione giurassica dell'area dei Tacchi (Sardegna Orientale). Bollettino della Societa` Geologica Italiana, 123(3), 477–496.

Cruciani, G., Franceschelli, M., Musumeci, G., Spano, M., & Tiepolo, M. (2013). U-Pb zircon dating and nature of metavolcanics and metarkoses from the Monte Grighini Unit: New insights on Late Ordovician magmatism in the Variscan belt in Sardinia, Italy. International Journal of Earth Sciences, 102(8), 2077–2096. doi:10.1007/s00531-013-0919-z

Dabard, M. P., Chauvel, J. J., & Loi, A. (1994). Compositional affinities of volcanic fragments in sedimentary rocks using electron microprobe analysis. Sedimentary Geology, 88, 283–299. Fossen, H. (2010). Structural Geology. New York: Cambridge University Press.

Funedda, A., Carmignani, L., Pertusati, P. C., Forci, A., Calzia, P., Serra, M. (Cartographer). (2011). Foglio 548-Senorbı` [Sheet 548-Senorbı`] [Geological map of Italy on the 1:50,000 scale]. Retrieved from http://www.isprambiente.gov.it/Media/carg/548_SENORBI/Foglio.html

Funedda, A., Carmignani, L., Pertusati, P. C., Uras, V., Pisanu, G., & Murtas, M. (2011). Foglio 540-Mandas. Note illustrative [Sheet 540 - Mandas. Explanatory notes]. Note illustrative della Carta Geologica d'Italia in scala 1:50.000, ISPRA-Servizio geologico d'Italia, Rome. Retrieved from http://www. isprambiente.gov.it/Media/carg/note_illustrative/540_Mandas.pdf

Funedda, A., Naitza, S., Conti, P., Dini, A., Buttau, C., Tocco, S. (2011). The geological and metallogenic map of the Baccu Locci mine area (Sardinia, Italy). Journal of Maps, 7(1), 103–114. doi:10.4113/jom.2011.1134.

Funedda, A., Pertusati, P. C., Carmignani, L., Uras, V., Pisano, G., & Murtas, M. (Cartographer). (2011). Foglio 540-Mandas [Sheet 540-Mandas] [Geological map of Italy a the 1:50,000 scale]. Retrieved from http://www.isprambiente.gov.it/Media/carg/540_MANDAS/Foglio.html

Gaggero, L., Oggiano, G., Funedda, A., & Buzzi, L. (2012). Rifting and arc-related early Paleozoic volcanism along the North Gondwana margin: Geochemical and geological evidence from Sardinia (Italy). The Journal of Geology, 120(3), 273–292. doi:10.1086/664776.

Gnoli, M., & Pillola, G. L. (2002). The oldest nautiloid cephalopod of Sardinia: Cameroceras cf. vertebrale (Eichwald, 1860) from the Arenig (Early Ordovician) of Tacconis (South East Sardinia) and remarks on associated biota. Neues Jahrbuch fu¨r Geologie und Pala¨ontologie, Monatshefte, 2002(1), 19–26.

Loi, A., Barca, S., Chauvell, J. J., Dabard, M. P., & Leone, F. (1992). Analyse de la se´dimentation post-phase sarde: le de´pots initiaux a` placers du SE de la Sardaigne. Comptes Rendus de l'Acade´mie des Sciences de Paris, 315, 1357–1364.

Loi, A., & Dabard, M. P. (1997). Zircon typology and geochemistry in the palaeogeographic reconstruction of the Late Ordovician of Sardinia (Italy). Sedimentary Geology, 112, 263–279.

Naud, G. (1979). Les shales de Rio Canoni, formation-repe`re fossilife`re dans l'Ordovicien supe´rieur de Sardaigne orientale. Conse´quences stratigraphiques et structurales. Bulletin de la Socie´te´ ge´ologique de France, 21(2), 155–159.

Naud, G., & Pittau Demelia, P. (1987). Premie`re decouverte d'acritarches du Cambrien moyen a` superieur basal et du Tremadoc-Arenigien dans la basse vallee du Flumendosa: mise en evidence d'un nouveau temoin de la Phase Sarde en Sardaigne orientale. I.G.C.P. No. 5 Newsletter, 7, 85–86.

Oggiano, G., Gaggero, L., Funedda, A., Buzzi, L., & Tiepolo, M. (2010). Multiple early Palaeozoic volcanic events at the northern Gondwana margin: U-Pb age evidence from the Southern Variscan branch (Sardinia, Italy). Gondwana Research, 17(1), 44–58. doi:10.1016/j.gr.2009.06.001

Pavanetto, P., Funedda, A., Northrup, C. J., Schmitz, M., Crowley, J., & Loi, A. (2012). Structure and U–Pb zircon geochronology in the Variscan foreland of SW Sardinia, Italy. Geological Journal, 47(4), 426– 445. doi:10.1002/gj.1350

Pertusati, P. C., Sarria, E., Cherchi, G. P., Carmignani, L., Barca, S., Benedetti, M. (Cartographer). (2002). Foglio 541-Jerzu [Sheet 541-Jerzu] [Geological map of Italy on the 1:50,000 scale]. Retrieved from http://www.isprambiente.gov.it/Media/carg/541_JERZU/Foglio.html

Pillola, G. L., & Leone, F. (1997). Lower Ordovician (Arenig) Trilobites from SE Sardinia (Italy): palaeobiogeographical and structural implications. Second International Trilobite Conference, St. Catharines, Ontario.

Pittau, P., Del Rio, M., & Funedda, A. (2008). Relationships between plant communities characterization and Basin formation in the Carboniferous-Permian of Sardinia. Bollettino della Societa` Geologica Italiana, 127(3), 18–36.

von Raumer, J., Bussy, F., Schaltegger, U., Schulz, B., & Stampfli, G. (2012). Pre-mesozoic alpine basements— Their place in the European Paleozoic framework. Geological Society of America Bulletin, 125(1–2), 89–108. doi:10.1130/B30654.1

Rossi, P., Oggiano, G., & Cocherie, A. (2009). A restored section of the "southern Variscan realm" across the Corsica-Sardinia microcontinent. Comptes Rendus Geoscience, 341(2-3), 224–238. doi:10.1016/j.crte. 2008.12.005

## GEOLOGICAL MAP OF THE LACONI-ASUNI AREA (Original format A0)

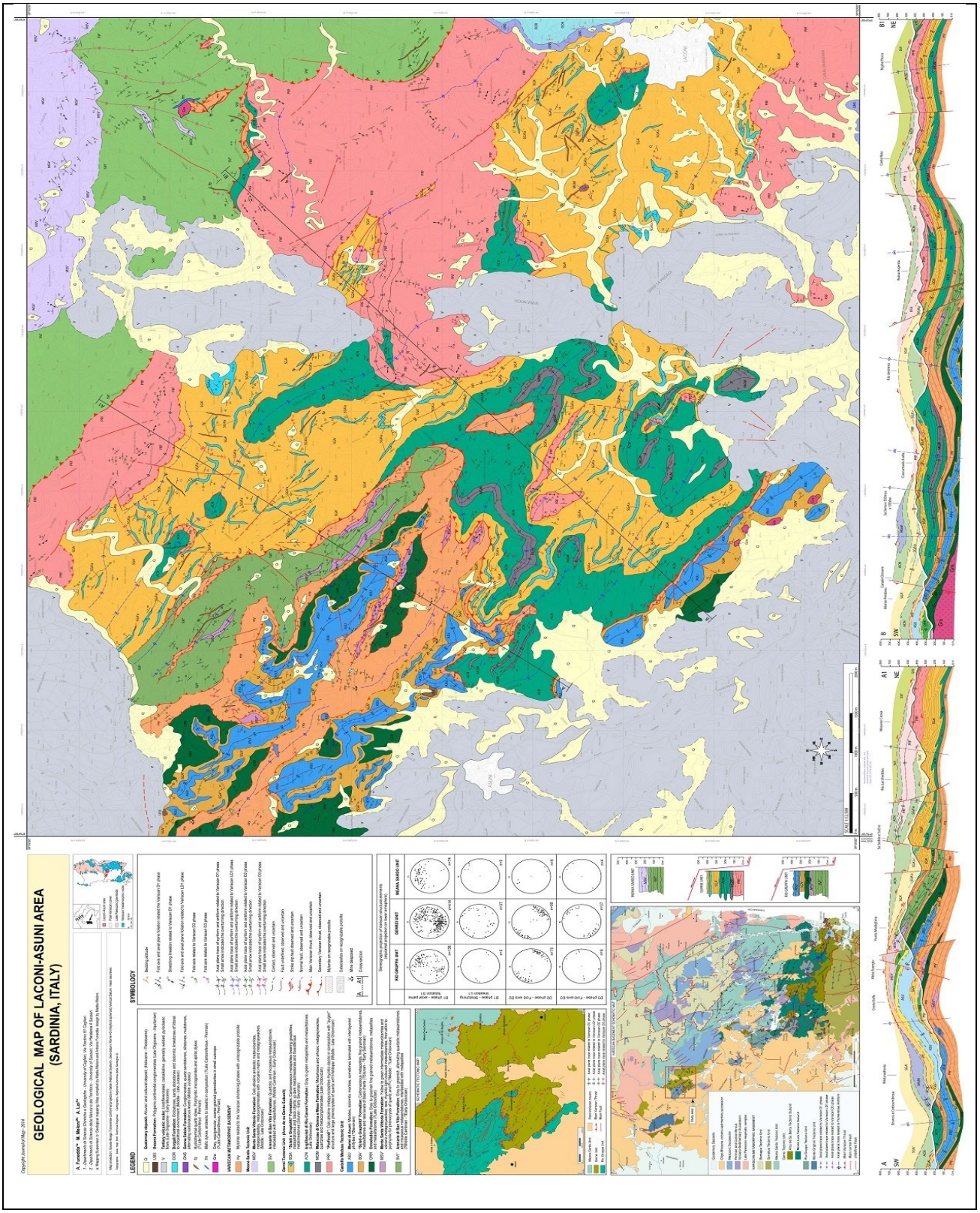

# 6. THE GADONI AREA)

The region of Gadoni at first sight shows straight differences with respect the external nappe zone of south eastern Sardinia. These consisting in a more complex late to post collisional deformation and occurrence of a wide tectonic unit (i.e, the Postgotlandiano auct). The mapped area extends between 39°56'20"/9°04'59" (NW corner) and 39°51'47"/9°13'16" and covers an area of about 100 square kilometers in the southern slope of the Gennargentu massif and has the mining village of Gadoni as main geographic reference around the most important mining district of central Sardinia (Funtana Raminosa and Giaccuru mines), active since Roman Age.

## 6.1 INTRODUCTION

The first studies in this area date back to the early 1900, when a thriving mining developed, in particular in the Funtana Raminosa area several studies dealt with ore bodies (Dessau G., 1937; Zuffardi 1967 & 1969). Other contributions to the study of the geological frame were given between 1960 and 1980 (Bosellini A. & Ogniben G. 1968) and later by Dessau et al., 1982; and Carmignani et al. 1982). The lack of recent geological studies made difficult to insert the region within the modern geological view of the nappe zone ( Oggiano et al. 2010; Gaggero et al 2012) hence the upgrade of the still poorly defined geological-structural and stratigraphic model starting from a detailed geological mapping was necessary.

The study area is located in the Variscan Nappe Zone of the central Sardinia along the so called Barbagia Synform, which is one of the main regional features related to the only post nappe, late collisional, phase as far recognized in this area (LD1 Phase: Conti et al., 1998), which develops large, NNW trending, folds with tens kilometric wavelength. The main tectonic unit of this part of the nappe building is formed by a huge terrigenous sequence metamorphosed under green schist facies condition which at first sight lacks of metavolcanics and metalimestones that, conversely, characterize the tectonic units of the external nappe zone, which outcrops in some tectonic windows. An important contact aureole, associated with late Variscan intrusives, affects a vast portion of the region. Particularly, skarn with mixed base metal sulfides and calc-silicates form where the intrusives came in contact with the carbonate rocks of the Meana Sardo unit.

## 6.2 STRATIGRAPHIC OUTLINE

Generally the tectonic units of the nappe zone share similar lithostratigraphic successions, Middle Cambrian to the Early Carboniferous in age. This is not the case of the Gadoni district, in fact the lower unit (Meana sardo unit, Carmignani et al., 1982) differs from the upper unit (Barbagia unit Carmignani et al., 1982) ) , which in this sector of the nappe building is a monotonous metapelitic-metarenacceous sucession namely the “Gennargentu Phyllites” Pertusati et al. 2002 (**Fig.62**). The age of this unit was ascribed to lower Carboniferous (Vai & Coccozza, 1974) on the base of the geometrical position above the Devonian limestone; Dessau et al. 1982 recognized its allochthonous

origin and tentatively attributed a Cambrian-Lower Ordovician age on the base of lithostratigraphic correlations.

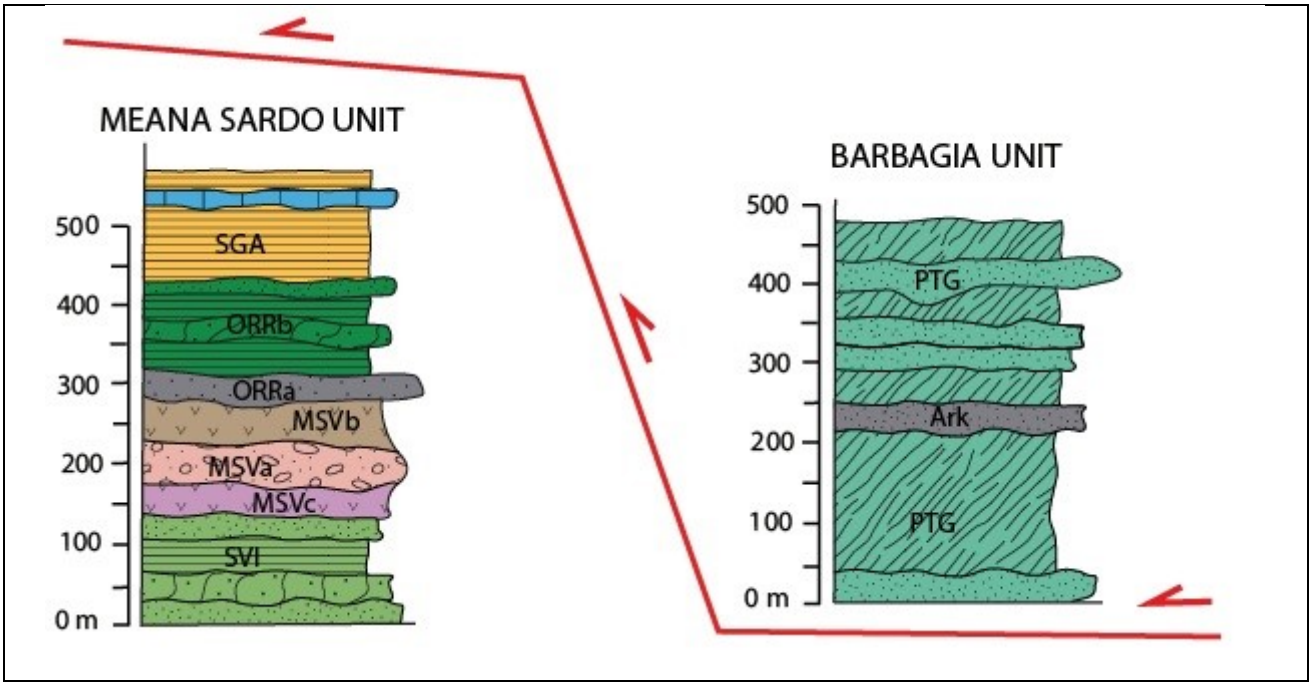


*Figure 62) Schematic lithostratigraphic columns of the Variscan tectonic units in the Gadoni area.*

## 6.2.1 MEANA SARDO UNIT

This unit near Gadoni exhibits the most complete exposition including the sardic uncomformity which probably in this unit is reduced to a mere disconformity. From the bottom are distinguishable the following formations:

**San Vito Fm (Arenarie di San Vito Auct.).** The metasandstones of San Vito Formation (Arenarie di San Vito, Calvino, 1959) are located at the base of the tectonic Meana Sardo Unit. They consist of alternating layers of variable thickness (from centimetric to metric) of fine sandstones, sandstones, gray-green mudstones and siltstones (**Fig.63**). The sedimentary structures are almost transposed, even if in the limbs of isoclinal folds the primary layering coincides with the main cleavage is possible to observe sedimentary structures such as cross laminations and ripples. The composition of the sandy fraction is made by meta-arkose or quartzite. On the base of acritarchs

associations a Middle Cambrian -Early Ordovician age was obtained for this formation (Tongiorgi et al, 1982; Di Milia et al. 1993).

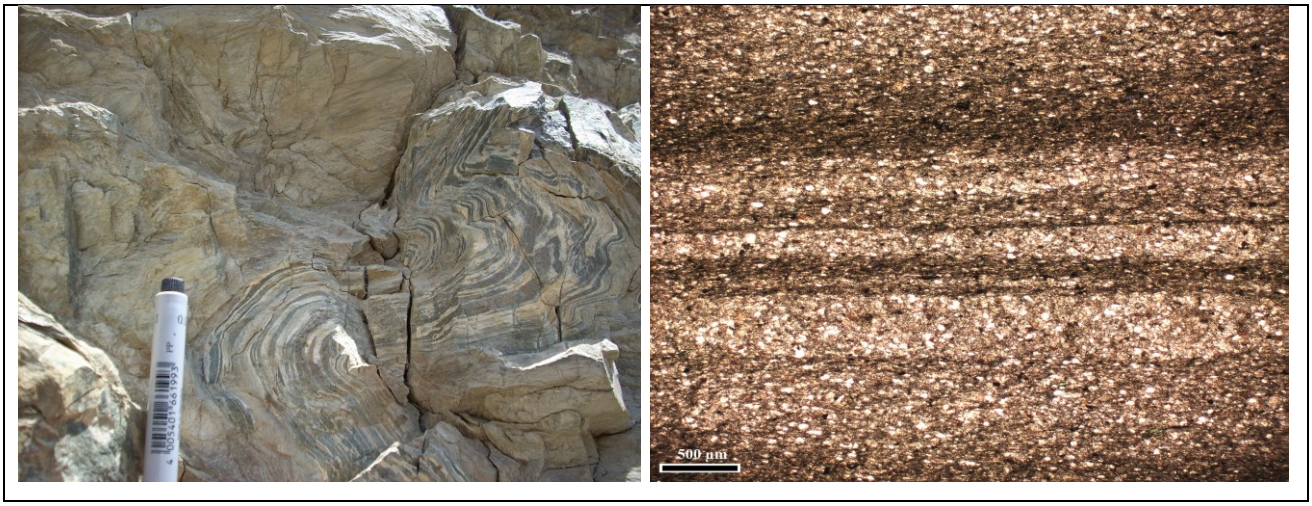


*Figure 63) Arenarie di San Vito formation.*

**Monte Santa Vittoria Formations.** The Monte Santa Vittoria Formation was previously divided into three informal lithostratigraphic units: Manixeddu, Monte Corte Cerbos, and Serra and Tonnai (Minzoni et al., 1975). Recently these informal lithostratigraphic units have been redefined as lithofacies within the unique metavolcanic and metaepiclastic Monte Santa Vittoria Formation. In the study area all the three lithofacies are well represented. The very base of the formation is conglomeratic (Manixeddu Fm. auct.) with clats of rhyolite and, at less extent of quartzite and older metamorphic rocks), this epiclastic lithofacies is capped by meta-rhyolite (Monte Corte Cerbos Fm. uct.) consisting of light gray-green, commonly schistose, rock containing quartz and feldspar augen.

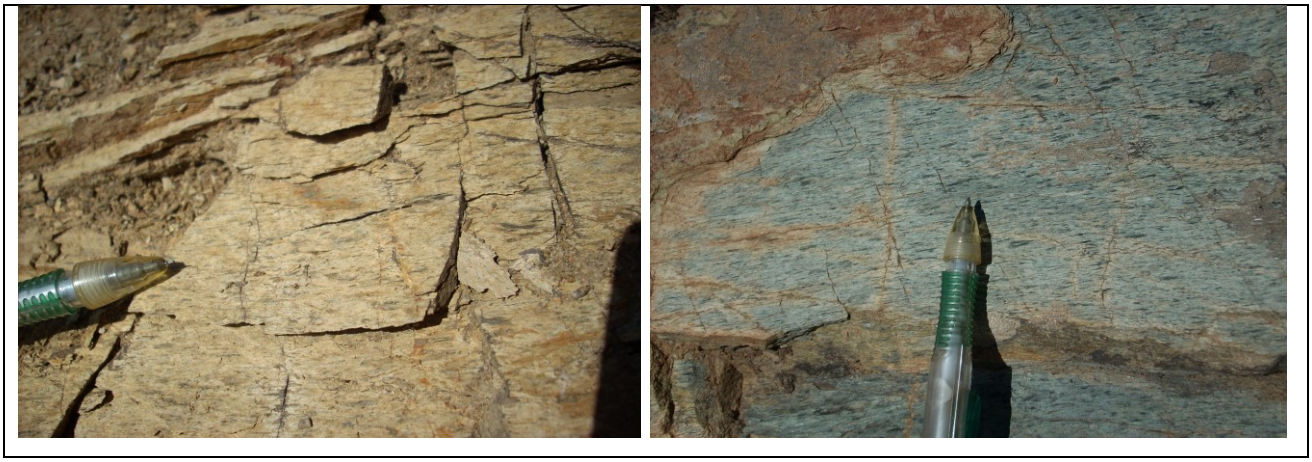

*Figure 64) Monte Santa Vittoria Formation.*

The top of the formation is represented by meta-basalts and meta-andesites, deep green in colors with chlorite in lepidoblastic levels and albite porphyroclasts and calcite and/or epidote in the groundmass (Serra Tonnai Fm. auct,) (**Fig.64 & 65**). The age is Middle-Late Ordovician based on both biostratigraphic and radiometric datations (Oggiano et al. 2010).

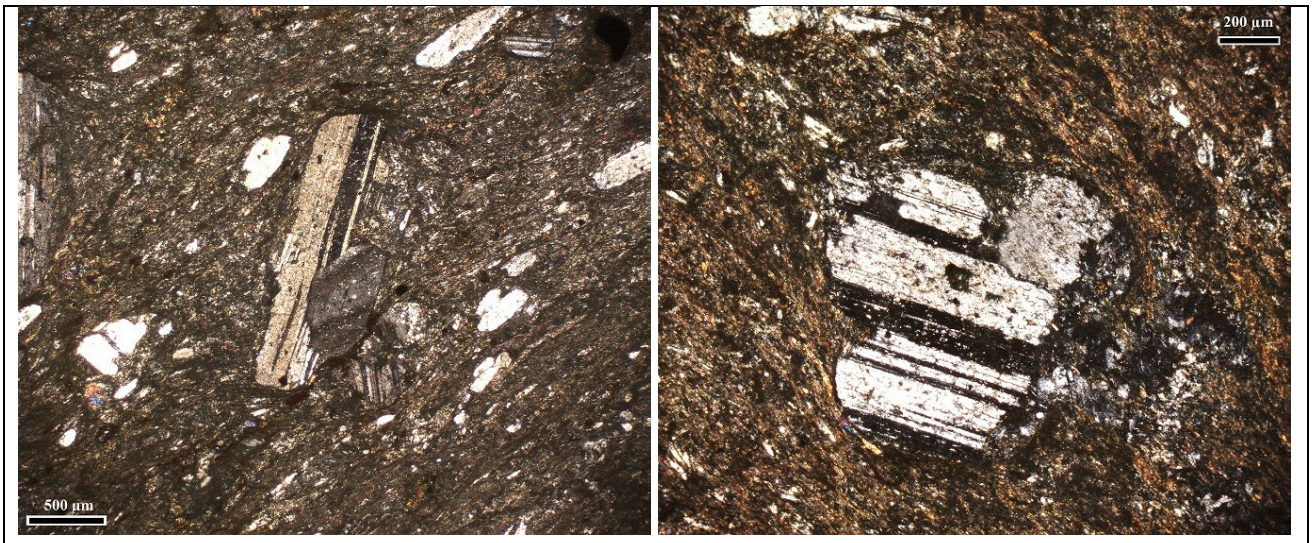


*Figure 65) Monte Santa Vittoria Formation.*

**Orroeledu Formations** (Bosellini & Ogniben, 1968) **.** The Orroeledu Formation represents an important crossing point of the upper Ordovician transgression; it consists of alternations meta-arkose, meta-greywackes, phyllites with quartz-sericitic-chloritic matrix (**Fig.66**). The fine-to coarse-grained lithic wackes are often enriched in heavy minerals. These enrichments corresponds to possible shoreface deposits. In the coarse-grained facies titaniferous minerals (rutile, pseudo-rutile, anatase) prevail whereas in the fine-grained ones, zircon and monazite are dominant, making these deposits worthy of prospection for REE. This formation is comparable for age and environment to the Punta Serpeddì Fm (Loi et al., 1992), which in the Sarrabus unit in Southern Sardinia, where a the age of this formation is attributable to Late Ordovician (Loi & Dabard, 1997).

**Black Shales Formation (Scisti Neri Fm;** Corradini, Ferretti, & Serpagli, 1998); The Black Shales Formation is an excellent marker inside the Meana Sardo Unit; it consists of very Black shales (originally carbonaceous) alternating with layers of gray siltstones. In the upper part of the sequence there are a limestones and the carbonate mudstones (**Fig.67**), known in the literature as "Schisti a Tentaculiti" ). In this sequence they have not been found microfossils, the cause could be

attributed to the high degree of deformation and with recrystallization. The age of this sequence refers to Silurian to Early Devonian (Corradini, Ferretti, & Serpagli, 1998); and iv) at the top, generally massive metalimestones (Calcari di Villasalto, Carmignani, Conti et al., 2001) that are referable to the Middle Devonian-Early Carboniferous period (Corradini, Barca, & Spalletta, 2003), and marbles (Marmi di Asuni), the age of which is referable to the Devonian based on lithostratigraphic correlation with the Calcari di Villasalto.


*Figure 66) Orroeledu Formations*


*Figure 67) Meta-limestone in the) Black Shales Formation.*

### 6.2.2 BARBAGIA UNIT

The Barbagia unit in the Gadoni District is represented almost exclusively by the grey phyllites of the, which farther north - according to Dessau et al., 1982 is represented by a more complete succession that includes Siluro Devonian deposits.

**Gray Phyllites of Gennargentu Formation** (Pertusati, P. 2002) "Postgotlandiano" Auct. The Gray phyllite of Gennargentu Fm ("Postgotlandiano"; Vai & Coccozza, 1974), consists of a thick succession (apparent thickness of 1500 m) of irregular levels of micaceous sandstone, quartzite, phyllite affected by a green schist metamorphism (**Fig.68**). The phyllites have a typical silver, light gray color, with intercalation of dark, greenish levels; locally quartzites and meta-arkose occur in metric horizons. This formation is also characteristic for the pervasive occurrence of quartz in deformed veins and mullions. The basal contact with the underlying Meana Sardo Unit is marked by mylonitic belts with decametric thickness.


*Figure 68) Gray Phyillites of Gennargentu Fm*

Mylonitic and cataclastic zones (**Fig.69**) also occur within this unit in correspondence of local thrust and/or low angle normal shears. In thin section the phyllite are dominated by lepidoblastic levels of muscovite and, at less extent, by other coloured phyllosilicates such stilpnomelane and possibly vermiculite.


*Figure 69) Mylonitic belts in the Gray Phyillites of Gennargentu Fm.*

Small porphyroblasts of albite and several prismatic accessories like tourmaline, monazite and rutile are common. The quartzites and arkoses horizons (**Fig.70**) are less deformed and show a bimodal distribution of quarts grain size some of which, are well rounded despite the deformation. The supposed similarity with the San Vito formation (Dessau et al.1982) is now partially confirmed by the U-Pb age obtained by detrital zircons (559±15 Ma, 576 ±15 Ma), which even if suggest an older maximum age of this deposits compared with the maximum age of 539 ±23 Ma of the San Vito Formation, in any case show a similar provenance as suggested by the zircon ages spectrum.

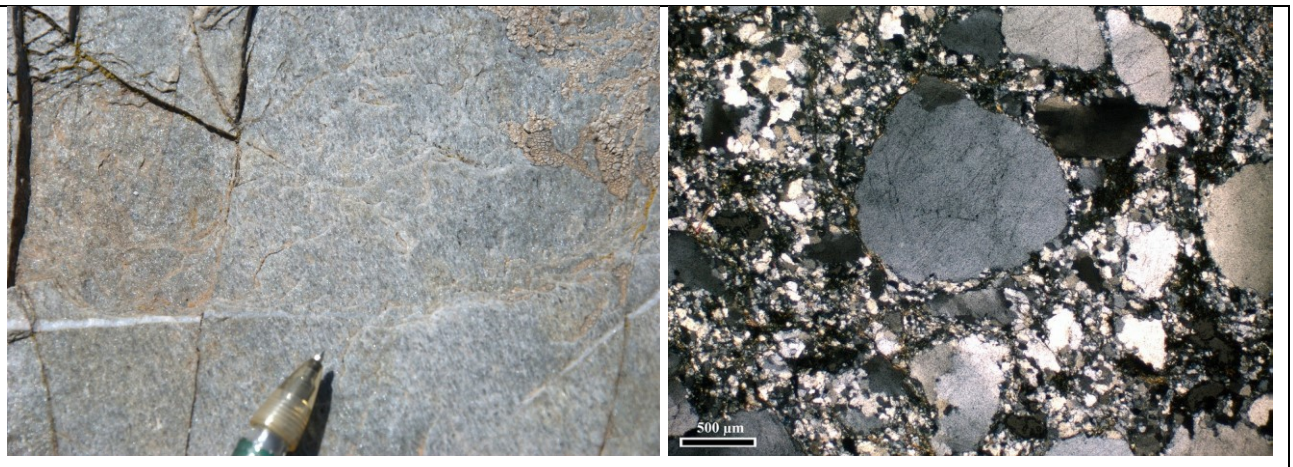


*Figure 70) Quartzites and arkoses horizons*

### 6.2.3 LATE PALEOZOIC MAGMATISM

In the study area there are many intrusive bodies, hypabissal dykes and stocks and also lava flows. Andesite and quartz porphyry are the most represented volcanic and sub-volcanic rocks whereas granodiorites are the most diffuse the intrusives. The latter occur in some granodiorite are the only plutonic rocks. They crop in hectometric bodies, which possibly are the wide intrusive counterpart of the wide Seui volcanic sub-volcanic complex (Cassinis et al., 2003). The granodiorite is fine to medium grained rock with weak oriented texture marked by biotite crystals in the range of 15% in modal proportion, plagioclase of andesine composition is more abundant than quartz, K-feldspar has interstitial growth, prismatic amphibole are rare, allanite, apatite and zircon are the main accessory phases (**Fig.71**). This intrusion form wide contact aureole that led to suppose they are surficial apophysis of a wider deep intrusion.


*Figure 71) Granodirite*

### 6.2.4 THE POST-VARISCAM COVERS.

**Genna Selole Formation**. The first unit of the local Jurassic cover is represented by continental to transitional siliciclastic deposits of the Genna Selole Formation represented by quatz conglomerate, grayish silty deposits baring lignite seams and clay (**Fig.72**). On the base of palynomorphs the age was referrd to Bajocian-Bathonian age (Dieni et al., 1983; Del Rio, 1985; Costamagna et al., 2004).

**Dorgali Formation**. The Dorgali formations (Amadesi et al. 1961; Calvino et al. 1972; Dieni & Massari 1985; 1987; Costamagna et al., 2004) is made of a dolostone brownish and pinkish dolostones (**Fig.72**). Locally, in some marly-limestone beds are abundant Brachiopods, Echinoids, Ammonites, Belemnites and Foraminifers of Middle Jurassic (Bathonian-Callovian; Dieni & Massari 1985).

*Figure 72) Genna Selole (left) and Dorgali Formation (right).*

**Quaternary Deposit.** Are represented by alluvial and colluvial deposit the Holocene-Pleistocene age. Only in the Flumendosa valley are preserved some old fluvial terraces possibly referable to the MIS-5 stage.

## 6.5. Tectonic outline

The Variscan tectonics in central Sardinia was subdivided into two main events (Dessau et al 1982). The first event is related to the collisional dynamic and was splitted into different synmetamorphic phases, which were named in different ways. The first two phases were responsible of the nappe emplacement, recumbent isoclinal folds with associated axial planar, pervasive, synmetamorphic foliation namely D1 and D2 (Carmignani et al. 1982, Carosi e Perusati 1990; Oggiano, 1994) and D1-LD1 (Conti e Patta 1998). The late, post nappe and post metamorphic shortening gave rise to wide regional antiforms of varied axial direction, the most important of which is NNW oriented.

The second event is linked to the collapse of the chain. It led to exhumation of HT/LP metamorphic units through low angle normal shears (Casini and Oggiano; 2008), inversion of collision related

thrusts, vertical shortening that generated isoclinal and drag folds with sub-horizontal axial plane and recycling of older foliation.

As in the southern part of the area (Laconi–Asuni area) there is a wide outcrop of Gerrei and Riu Gruppa units we also refer to the labeling of (Conti et al. 2001).

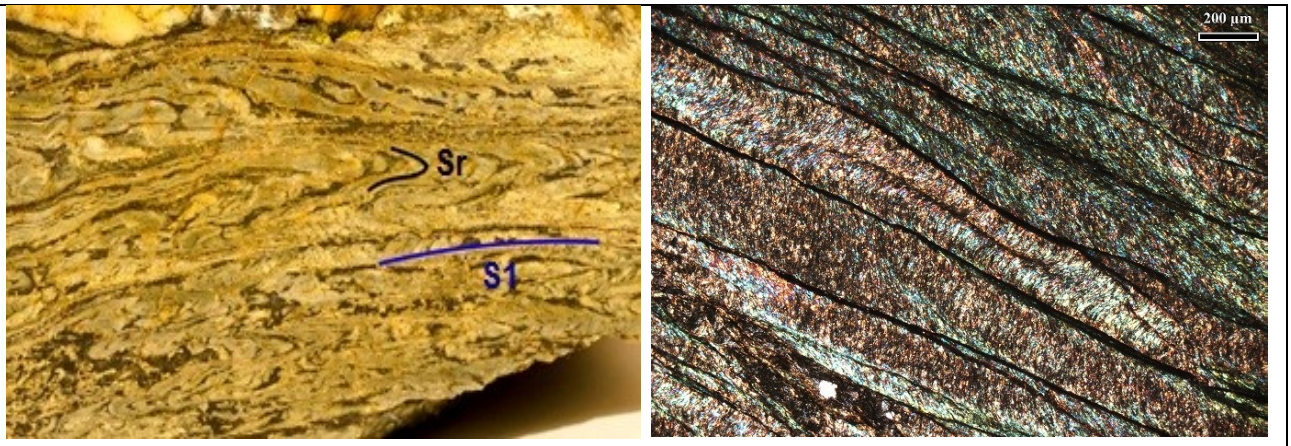


*Figure 73) Sr/S1 in the Gennargentu Gray Phyllite (Postgotlandiano auct.)*

- **Shortening phase (Meana phases)**: This phase within the tectonic Meana unit generated isoclinal non-cylindrical folds, to which the dominant foliation in the field (S1) is associated. This foliation is not the unique that affects these rocks, actually and old relic foliation (Sr) is detectable in thin section, and rarely at the outcrop scale, within microlithons defined by the S1 (**Fig.73**). The stretching lineations L1, associated to the D1 phase is well expressed, especially by porphyroclasts in metavolcanites (**Fig.75**). The direction of tectonic transport according to kinematic indicator (σ, δ and shear band) is top to the SW in the Meana Sardo unit (**Fig.74 & 75**). In the in the Gennargentu Gray Phyllite (Postgotlandiano) the stretching direction less univocal and dispersed by a more complex post-nappe tectonics. The kinematic indicator iside the shear zones point to an usual tectonic transport toward the northern quadrants. This transport evidently must be referred to the post collisional phase.

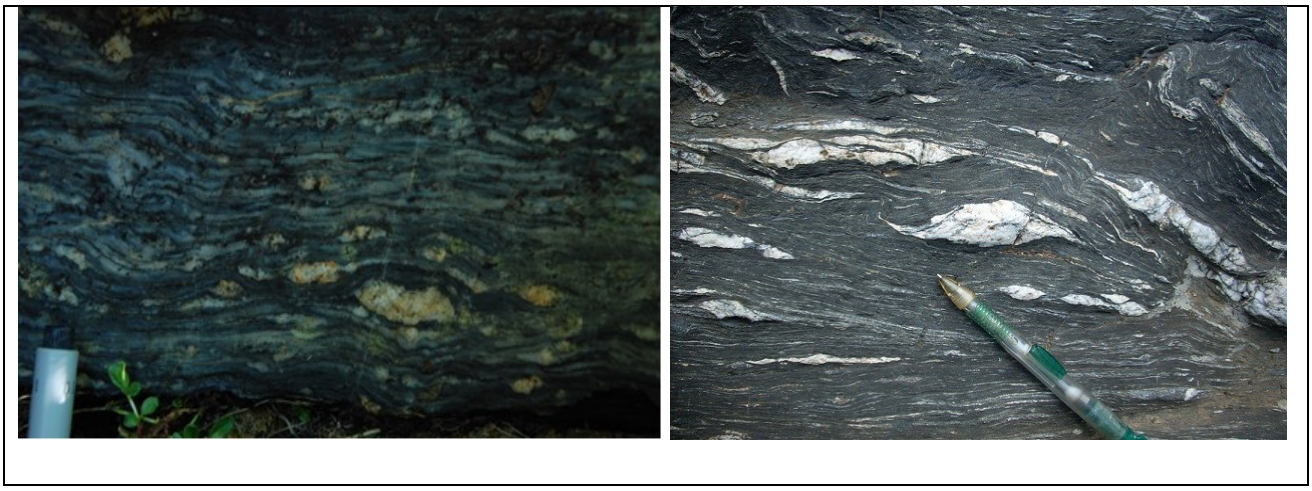

*Figure 74) Left: Milonyte shear zone; Right: Quartz boudin defining a σ structure (dx shear zone in Silurian phyllite).*

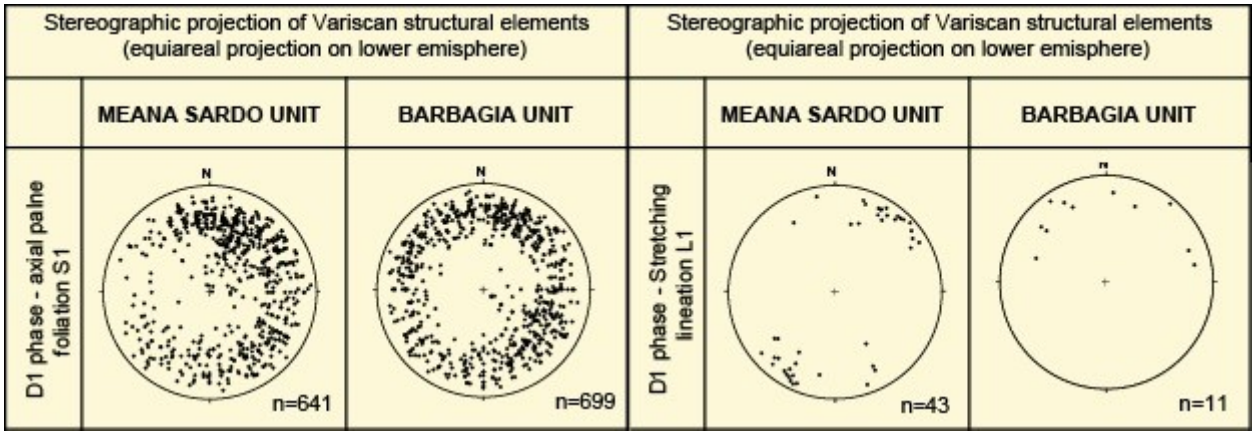


*Figure 75) Stereographic projection of axial plane S1 phase and Stretching lineation L1 in the Meana Sardo Unit and in the Barbagia Unit.*

- **Post Nappe shortening structures (Flumendosa phase):** The occurrence of a late shortening phase postdating the regional metamorphism and the nappe emplacement is ubiquitous in the nappe zone. It generated upright antiforms and synforms, with plurikilometric wavelength. This phase has been labelled in different ways in different zones. Traditionally, as it follows two schistogenous, synmetamorphic deformations was named D3. Conti et al. 2001 who considered the shortening dynamic as a unique long lasting tectonic phase assigned to this deformation the name or also Flumendosa phase as the Flumendosa antiform is the most important structure. In the study area the post-nappe

tectonic exhibits two shortening, almost orthogonal, directions the interference of which generate dome and basin with radius in the range of 5-6 km. The Giaccuru dome is one of the most evident. As in its core are hosted huge mineralized skarns. The dome of Giaccuru is generated by the interference of two upright antiform trending respectively N130 and N50. The reciprocal timing of the different shortening directions between the two sets of upright is is not easy. Their contemporaneity, as product of uniaxial symmetric shortening, cannot be completely ruled out.

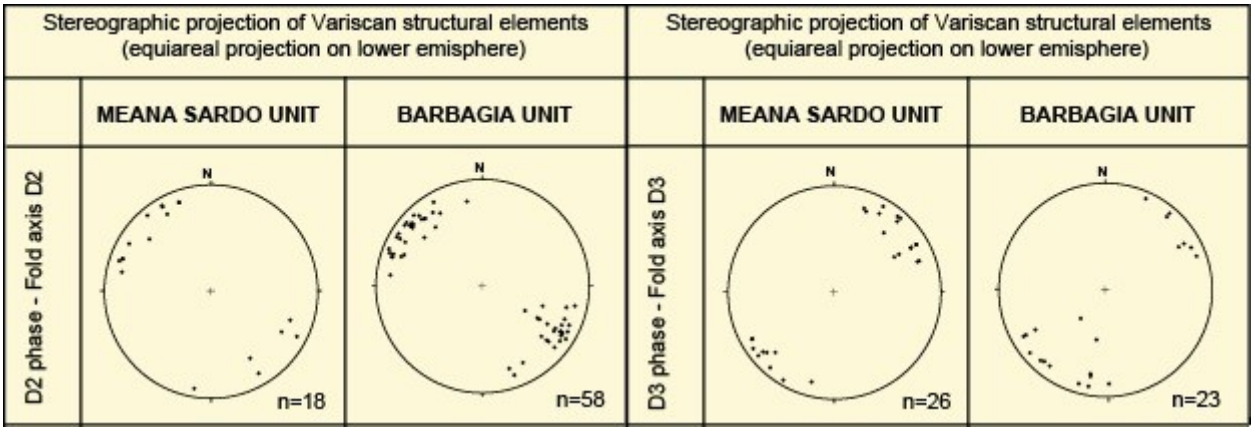


*Figure 76) Stereographic projection of fold axis of the extensional post collisional phase in the Meana Sardo Unit and in the Barbagia Unit.*

- **The extensional post collisional phase (Riu Gruppa):** After the shortening and thickening phase the postcollisional evolution took place all over the chain with different extensional structures according to the different structural levels. In the nappe zone the extensional tectonic occurred within the ductile regime at middle–upper crustal level whereas at more surficial level step normal faults in brittle regime grew generating several Permian-Carboniferous basins. This phase in the nappe zone is widely controlled by the post-nappe collisional structure (Conti et al. 1999; Casini and Oggiano 2008). Along the limbs the main antiforms the vertical shortening generated: **i**) drag folds with centrifugal vergence with respect to the hinge line; **ii**) reactivation of collisional thrusts into low angle normal shear zone; **iii**) exhumation of deep units with LP/HT metamorphic overprint; **iv**) recycling of previous foliations (**Fig.77**). In the study area, particularly around the late collisional dome structures, the extensional phase generated low angle shear zones, which clearly reactivated

the "Postgotlandiano" overthrust into normal shear zones with motion away from the culmination. In this way strong directional variation of the tectonic transport can be observed along with strong variability of the axial direction of folds produced by vertical shortening (**Fig. 76**). The structure, which at the best shows the above listed extensional features is the Giaccuru dome. In this antiformal structure the "Postgotlandiano" Thrust was reactivated as low angle shear zone with down dip motion, according to the original attitude acquired after the late collisional folding deformation.

Figure 77) Kink bands related to the late shortening phase.

## 6.3 GEOLOGY AND ORES

The Gadoni district is characterized by several ore deposits; the main mineralization are metal sulfides such as blende, galena, chalcopyrite, pyrite, and trace of bismutinite only in the Giaccuru dome is the dominant ore is magnetite associated to huge skarns with garnet, pyroxene and amphibole and epidote gangue. Skarns can form during regional or contact metamorphism, apart the products due to isochemical processes that can derive from mixed carbonate and silica protoliths - for which the term calc-silicate fels is more appropriate, a true skarn is to be connected to a variety of metasomatic processes involving fluids of magmatic, metamorphic, meteoric, and/or marine origin (**Fig.78**) (Meinert L. D., 1992). As a fact skarn occur within metamorphic aureole, along faults and major shear zones. Anyway what defines a skarn, is the mineralogy which includes a

wide variety of calc-silicates in any case dominated by garnet, anphyboles, of the tremolite-actinolite series and vesuvianite.

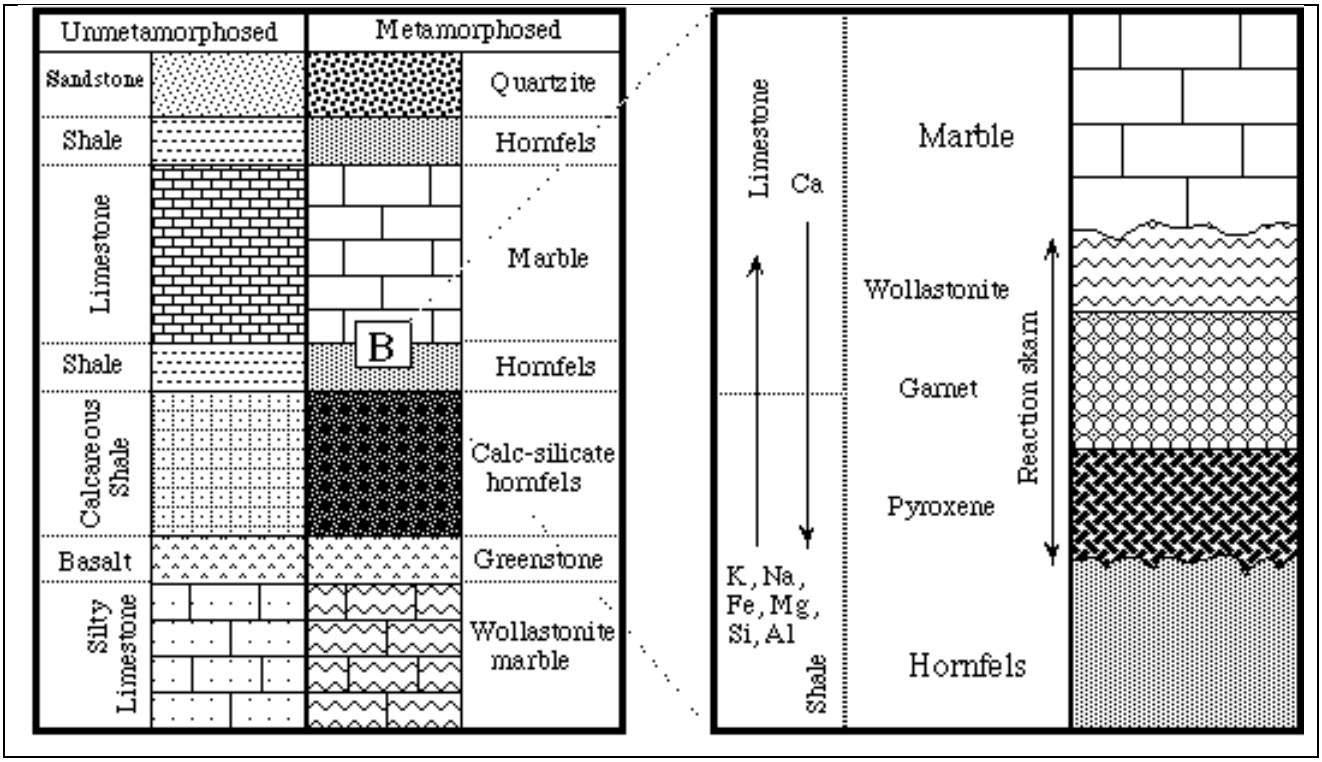


*Figure 78) Skarn reactions (Meinert L. D., 1992)*

Several hypothesis were advanced on the origin of the mineralizations in the Gadoni district; apart some works of the first half of 19$^{th}$ century (Dessau, 1937) who considered the ore as exoskarn linked to a granodioritic magma, no recent genetic studies were performed on this important ore bodies. Only some papers and short notes of the eighties were performed by Minzoni et al. 1975 and Garbarino et al., 1981. All these studies attributed a syngenetic, extrusive-sedimentary, origin to these deposits possibly linked to the Upper Ordovician volcanism. Such faint hypothesis, rather than by geological and petrological evidences, was supported by the need of apply also to the Sardinia ores the massive sulphydes, Kuroko-type model, which was popular in that time (Ishihara, 1974).

### 6.3.1 The Giacurru Fe-Skarn lode

The lode of Giacurru is the largest Fe-skarn in Sardinia; some mining explorations in the eighties allowed quantifing in 8 x $10^3$ tons of magnetite the reserves of the deposit. In places zinc dominates over iron in the form of sphalerite; in this case also traces of galena are present. The skarn is favored by the interaction between supercritical fluids and the mixed carbonate-shale succession of Devonian age.

The mineral association is made of dominant garnet of andradite-grossularite composition, with very low component in both spessartine and pirope (1-2 %) (**Fig.80**). Andradite dominate close to Zn- skarns whereas grossular is ubiquitous and is invariably associated to magnetite; in places some pyrope rich-garnets were observed. Anphyboles are invariably of actinolite composition. Piroxene is hedembergite-diopside with minor component of johansenite. Epidote is generally localized in veins tat crosscut the massive magnetite and associated with pyrite, zoisite, scapolite is common even if allanite is not rare (**Fig.79**). The minerals of epidote group are evidently retrograde, and probably associated with late circulation of epithermal fluids. Even if the EDX analyses did not allow quantitative thermometry through Garnet-Pyroxene thermometer (Wells, 1977) , it can be estimate that the andradite and the pyrope rich garnet formed at temperature > 500 °C, whereas epidote and pirite, pirrotite associations formed at temperature below 300 °C.

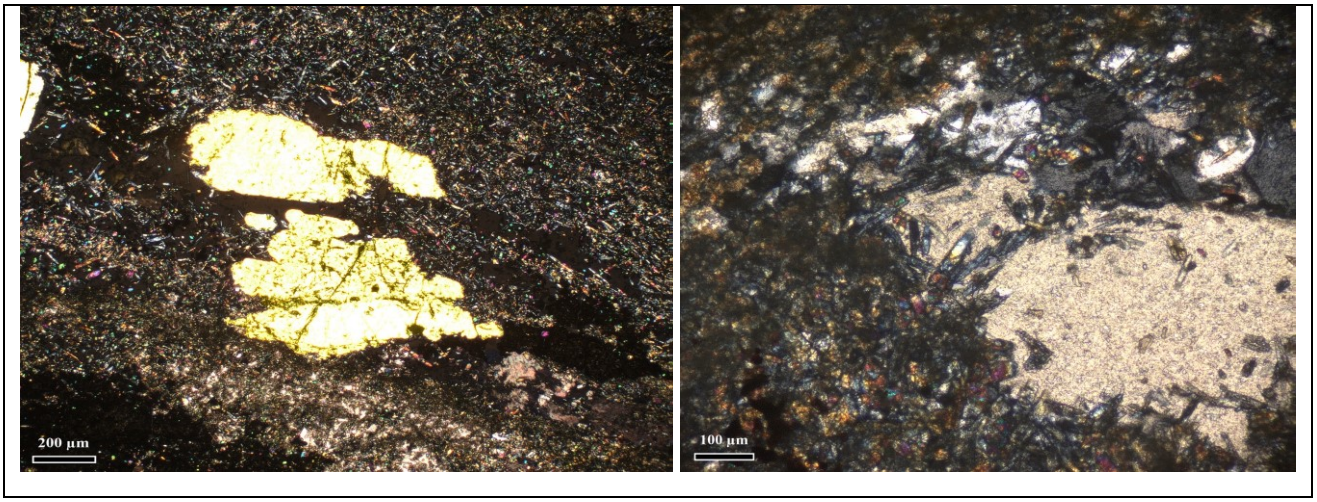


*Figure 79) Left: Scapolite; Right: zoisite from Giaccuru area.*

The skarn of Giaccuru is localized in the core of a dome antiform which generated due to the interference of late folding phases trending N130 (Flumendosa Phase Conti et al. 2001) with

another late compressional phase oriented N50, never detected before. Worthy of note is the absence of any contact effect on the overlaying Gray Phyllites of the Barbagia units. These are in sharp contact with the skarn along a mylonitic zone with kinematic indicators pointing to a northwestern tectonic transport. Such evidence suggests that the overthrust of the *Gray Phyllites of Gennargentu* on the Meana Sardo Unit was reactivated as low angle normal shear and have escaped the thermal front that conversely invested the Devonian core of the lower unit. This tectonic inversion is linked to the post-collisional evolution and possibly enhanced the emplacement of a plutonic body of which the granodiorite GR110 could be an apophysys.

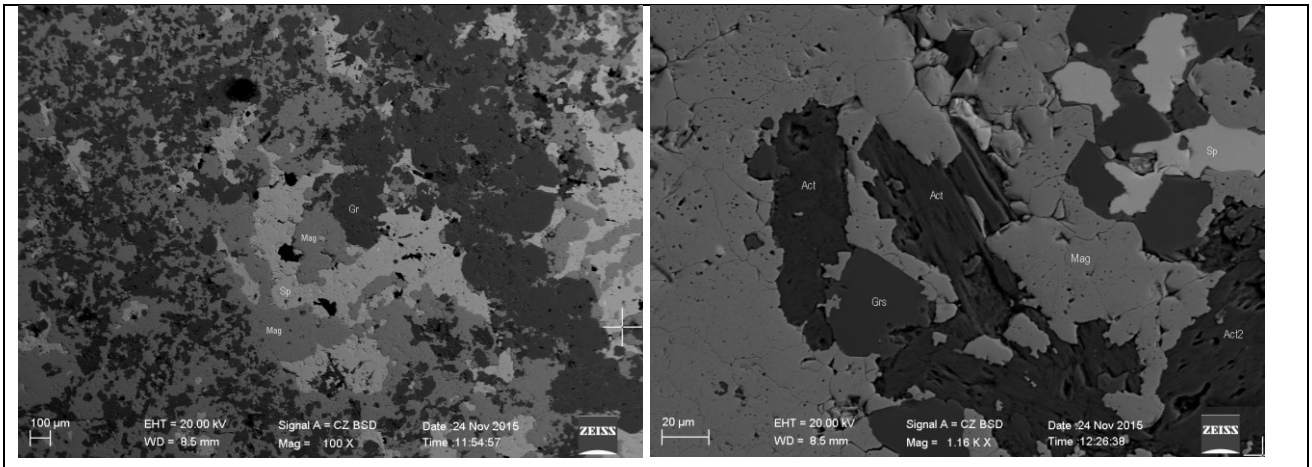


*Figure 80)* SEM images, *Giacurru Fe-Skarn: andradite, grossular, actinolite, sphalerite, magnetic.*

## 6.3.2 Funtana Raminosa Mine Area

Funtana Raminosa was one of the most important mine of Sardinia, which was operating since roman age for the extraction of copper. The main mineralizations, as Skarns deposits linked to the occurrence of Siluro-Devonian carbonate rocks. The ore is mostly made of mixed Zn-Pb-Cu-Fe sulfides with minor bismutinite and magnetite (**Fig.81**). Silver, rarely native or in the form of own mineral phases is in the range of 500 ppm. Apart this minerals of economic interest a long list of other primary sulfides were reported in the mine internal reports, including the cadmium phase hawleyite (Stara et al., 1999) . The sample we could analyse were picked from the dump of the old mine and from some outcrops in the S. Gabriele area. Among the gangue silicate is worthy the occurrence of ilvaite in addiction to grossular-andradite garnets and diopside that suggest temperature higher than 500°C (**Fig.82**). High temperature (T> 450 °C) sulfides are represented by

remnant of a solid solution between Calcopyrite and sphalerite (Sugaki et al.1987), within sphalerite chrisytals (**Fig.83**). Retrograde associations are represented by epidote and galena which crystallizes in fractures.

The mapping of the area highlighted that the deposits of Funtana Raminosa are linked to the GR110 granodiorite, which crops a few hundred meters from the main mineralized area it is rather improbable that the mineralization is to be linked to a N-S trending rhyolitic dike (Gran Dicco auct.) intruded within a major sub-vertical faults. The mineralization are mainly of disseminated to massive, when the metasomatism affects carbonate boudins. Anyway metasomatism is enhanced by the occurrence of cleavage and microshear that acted as preferential pathways for the metal rich fluids.

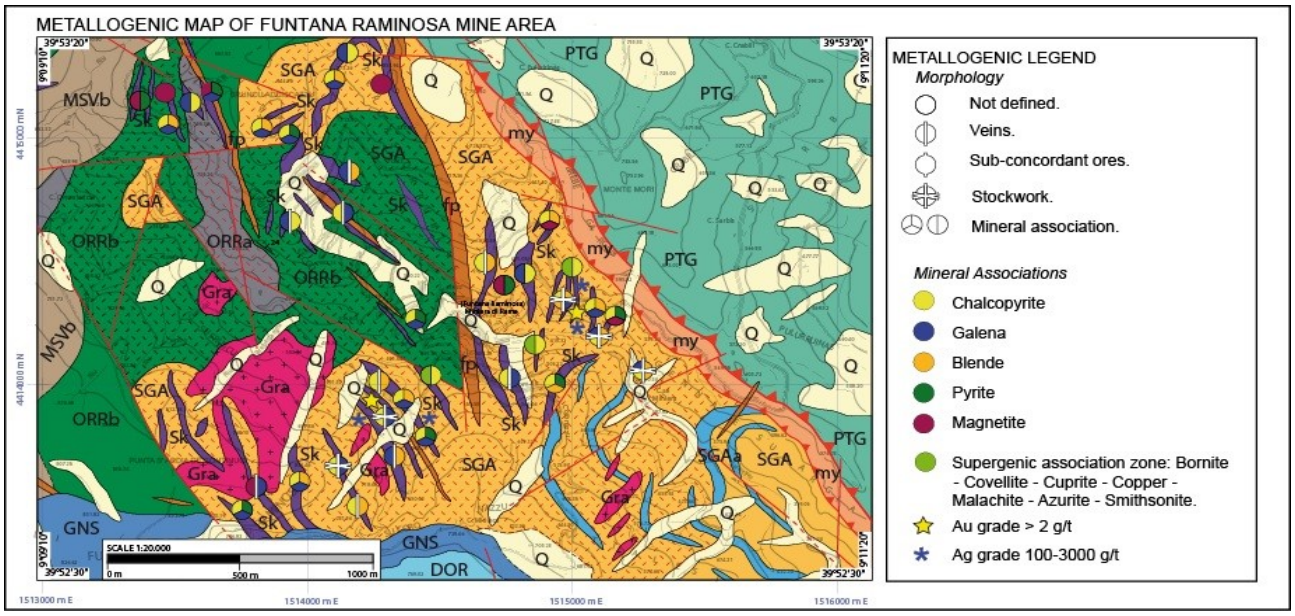


*Figure 81) Metallogenic map of the Funtana Raminosa area.*

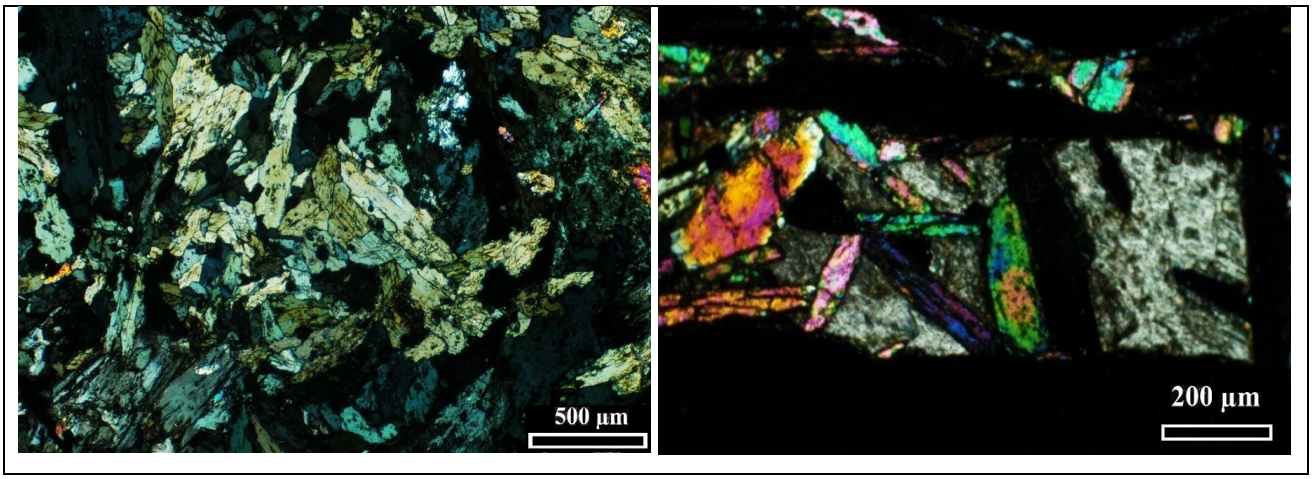


*Figure 82) Anphyboles and Pyroxenes and epidotes from Funtana Raminosa mining.*

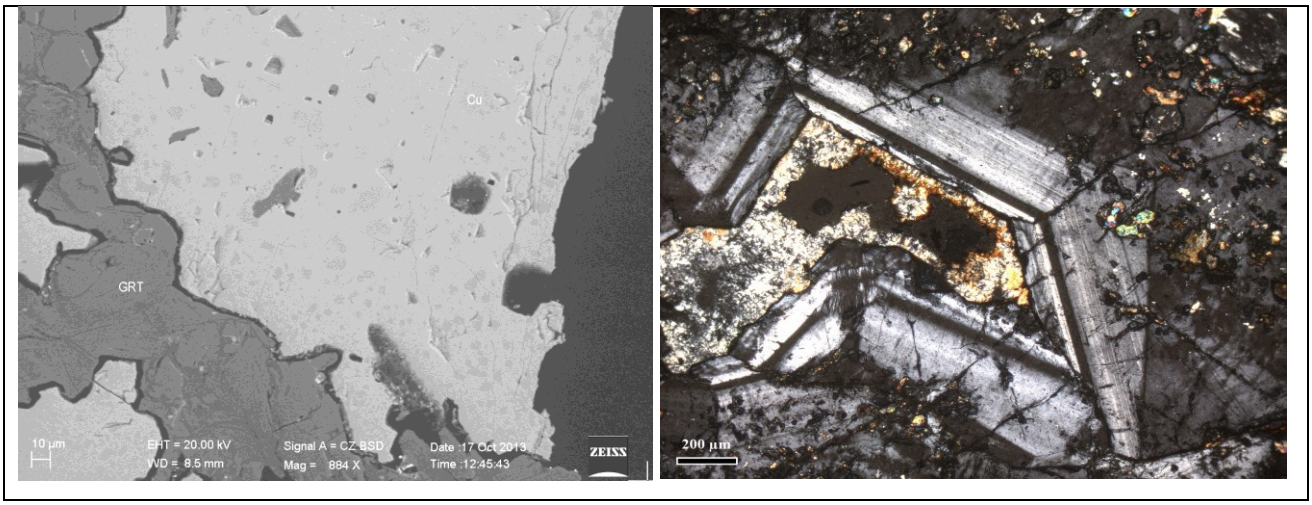


*Figure 83) Left:* SEM images, solid solution between Calcopyrite and sphalerite; *Right:Vesuvianite.*

## 6.4.2 REE

Apart the classic skarn ores, the radiometric survey evidenced interesting concentrations of REE in the Upper Ordovician trangressive meta-sediments. This concentration has to be referred to placer type accumulation heavy minerals such as ilmenite, zircon and monazite. The havy minerals occur as dark millimeter to centimeter layers within the Orroeleddu Fm. Some samples of this meta-sandstone were analysed by ICP-MS amd INAA (**Tab. 1-2 & 3**) and revealed a ∑REE of 4000-6000 ppm (**Fig.84**). Such a high value is rather interesting anis worthy of detailed prospection within this formation.

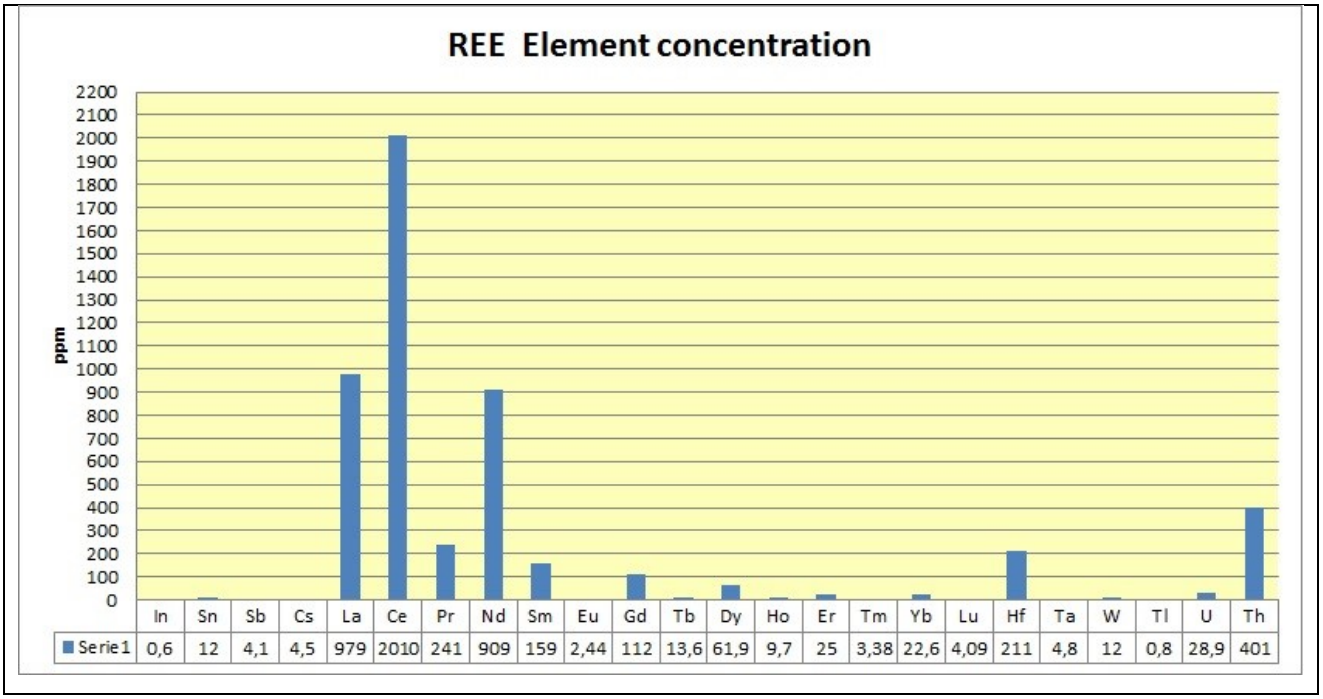


*Figure 84) REE element concentration (ICP-MS) in the Upper Ordovician trangressive meta-sediments.*

# REFERENCE


Amadesi E., Cantelli C., Carloni G.C. & Rabbie. (1961) -Ricerche geologiche sui terreni sedimentari del foglio 208 Dorgali. Giorn. di Geol.: 28, 59-87, Bologna.

Bosellini A. & Ogniben G. (1968) - Ricoprimenti ercinici nella Sardegna centrale. Ann. Univ. Ferrara: 1, 1-15, Ferrara.

Calvino, F. (1959). Lineamenti strutturali del Sarrabus-Gerrei (Sardegna sud-orientale). Bollettino del Servizio Geologico d'Italia, 81(4–5), 489–556.

Calvino F. (1972) - Note Illustrative della Carta Geologica d'Italia, Foglio 227-Muravera, pp. 60, Servizio Geologico d'Italia, Roma.

Carmignani, L., Minzoni, N., Pertusati, P. C., & Gattiglio, M. (1982). Lineamenti geologici principali del Sarcidano-Barbagia di Belvı`. In L. Carmignani, T. Cocozza, C. Ghezzo, P. C. Pertusati & C. A. Ricci (Eds.), Guida alla Geologia del Paleozoico Sardo (pp. 119–125). Guide Geologiche Regionali. Societa` Geologica Italiana.

Carmignani, L., Oggiano, G., Barca, S., Conti, P., Salvadori, I., Eltrudis, A., Funedda, A. & Pasci, S., 2001. Geologia della Sardegna. Note illustrative della Carta Geologica in scala 1:200.000. Servizio Geologico d'Italia: Roma.

Carosi, R., & Pertusati, P. C. (1990). Evoluzione strutturale delle unità tettoniche erciniche nella Sardegna centro-meridionale. Bollettino della Società Geologica Italiana, 109(2), 325-335.

Casini, L., Cuccuru, S., Maino, M., Oggiano, G., Puccini, A., & Rossi, P. (2015). Structural map of Variscan northern Sardinia (Italy). Journal of Maps,11(1), 75-84.

Casini, L., & Oggiano, G. (2008). Late orogenic collapse and thermal doming in the northern Gondwana margin incorporated in the Variscan Chain: a case study from the Ozieri Metamorphic Complex, northern Sardinia, Italy. Gondwana Research, 13(3), 396-406.

Cassinis, G., Cortesogno, L., Gaggero, L., Ronchi, A., Sarria, E., Serri, R., & Calzia, P. (2003). Reconstruction of igneous, tectonic and sedimentary events in the latest Carboniferous–Early Permian Seui Basin (Sardinia, Italy), and evolutionary model. Boll Soc Geol It, 2, 99-117.

Conti, P., & Patta, E. D. (1998). Large scale Hercynian West-directed tectonics in southeastern Sardinia(Italy). Geodinamica Acta, 11(5), 217–231.

Conti, P., Carmignani, L., Cerbai, N., Eltrudis, A., Funedda, A., & Oggiano, G. (1999). From thickening to extension in the Variscan belt - kinematic evidence from Sardinia (Italy). Terra Nova, 11(2/3), 93–99.

Conti, P., Carmignani, L., & Funedda, A. (2001). Change of nappe transport direction during the Variscan collisional evolution of central-southern Sardinia (Italy). Tectonophysics, 332(1–2), 255–273.

Corradini, C., Ferretti, A., & Serpagli, E. (1998). The Silurian and Devonian sequence in SE Sardinia. Giornale di geologia, 60(ECOS VII - special issue), 71–74.

Corradini, C., Barca, S., & Spalletta, C. (2003). Late Devonian-Early Carboniferous conodonts from the "Clymeniae Limestones" of SE Sardinia (Italy). Cour. Forsch.-Inst. Senckemberg, 245, 227–253.

Costamagna, L., & Barca, S. (2004). Stratigrafia, analisi di facies, paleogeografia e dinquadramento regionale della successione giurassica dell'area dei Tacchi (Sardegna Orientale). Bollettino della Societa` Geologica Italiana, 123(3), 477–496.

Del Rio M. (1985) - Palynology of Middle Jurassic black organic shales of "Tacco di Laconi", Central Sardinia, Italy. Boll. Soc. Paleont. It.: 23, 325-342, Modena.

Dessau, G. (1937): Studi sulla miniera di Fontana Raminosa (Sardegna). Per. Miner., 8, 177-215.

Dessau G., Duchi G., Moretti A. & Oggiano G. (1982) – Geologia della zona del Valico di Correboi (Sardegna centro-orientale). Rilevamento, tettonica e giacimenti minerari. Boll. Soc. Geol. It.: 101, 497-522, Roma.

Dieni I., Fischer J.C., Massari F., Salard-Cheboldaeff M. & vozenin-Serra C. (1983) - La succession de Genna Selole (Baunei) dans le cadre de la paléogéographie mésojurassique de la Sardaigne orientale. Mem. Soc. Geol. It.: 36, 117-148, Roma.

Dieni I. & Massari F. (1985b) - Mesozoic of Eastern Sardinia. "19th European Micropaleontological Colloquium-Guide Book", AGIP, Sardinia, October 1-10, 1985, 66-78.

Dieni I. & Massari F. (1985c) - Mesozoic of Lanaitto Valley. "19th European Micropaleontological Colloquium-Guide Book", AGIP, Sardinia, October 1-10, 1985, 221-232.

Dieni, I., & Massari, F. (1987, May). Le Mésozoique de la Sardaigne orientale: Groupe Français du Crétacé. Sardinia.

Di Milia A., Tongiorgi M. & Albani R. (1993) - Acritarch findings in early paleozoic low-grade metasediments of Sardinia (Italy): A review. Revista Espanola de Paleontologia: 8, 170- 176, Madrid.

Gaggero, L., Oggiano, G., Funedda, A. & Buzzi, L., 2012. Rifting and arc-related early Paleozoic volcanism along the North Gondwana margin: geochemical and geological evidence from Sardinia (Italy). The Journal of Geology.

Garbarino C., Maccioni L., Padalino G., Tocco S. & Violo M. (1981) - Le mineralizzazioni stratiformi di solfuri misti della Sardegna centrale quale prodotto di un vulcanismo di margine continentale di età ordoviciana: proposta di un modello geodinamico e genetico. Mem. Soc. Geol. It.: 22, 145- 150, Roma.

Ishihara, S. (1974). Magmatism of the Green Tuff tectonic belt, northeast Japan. Mining Geol. Spec. Issue, 6, 235-250.

Loi, A., Barca, S., Chauvell, J. J., Dabard, M. P., & Leone, F. (1992). Analyse de la se´dimentation post-phase sarde: le de´pots initiaux a` placers du SE de la Sardaigne. Comptes Rendus de l'Acade´mie des Sciences de Paris, 315, 1357–1364.

Loi, A., & Dabard, M. P. (1997). Zircon typology and geochemistry in the palaeogeographic reconstruction of the Late Ordovician of Sardinia (Italy). Sedimentary Geology, 112(3), 263-279.

Meinert, L. D. (1992). Skarns and skarn deposits. Geoscience Canada, 19(4).

Minzoni N. (1975) - La serie delle formazioni paleozoiche a Sud del Gennargentu. Boll. Soc. Geol. It.: 94, 347-365, Roma.

Oggiano, G. (1994). Lineamenti stratigrafico-strutturali del basamento del Goceano (Sardegna centro-settentrionale). Bollettino della Società Geologica Italiana, 113(1), 105-115.

Oggiano G., Gaggero L., Funedda A., Buzzi L. & Tiepolo M. 2010. Multiple early Paleozoic volcanic events at the northern Gondwana margin: U–Pb age evidence from the Southern Variscan branch (Sardinia, Italy). Gondwana Research 17, 44–58.

Pertusati, P. C., Sarria, E., Cherchi, G. P., Carmignani, L., Barca, S., Benedetti, M., ... & Pintus, C. (2002). Note Illustrative della Carta Geologica d 'Italia alla scala 1: 50.000, Foglio 541 Jerzu.

Stara, P., Rizzo, R., Sabelli, C., & Ibba, A. (1999). I minerali di Funtana Raminosa (Gadoni, Sardegna centrale). Riv Mineral Ital, 1, 10-27.

Sugaki, A.; Kitakaze, A.; Kojima, S. 1987. Bulk compositions of intimate intergrowths of chalcopyrite and sphalerite and their genetic implications. Mineralium Deposita, Vol. 22, p. 26-32.

Tongiorgi M., Bellagotti E., Di Milia A. & Trasciatti M. (1982) - Prima datazione su basi paleontologiche (Acritarchi) della Formazione di Solanas (Tremadociano-Arenigiano) (Meana Sardo, Sardegna Centrale). In: Carmignani L., Cocozza T., Ghezzo C., Pertusati P.C. & Ricci C.A. (Eds.), Guida alla Geologia del Paleozoico Sardo. Società Geologica Italiana. Guide Geologiche Regionali: 127-128, Cagliari.

Vai G.B. & Cocozza T. (1974) - Il "Postgotlandiano" sardo, unità sinorogenica ercinica. Boll. Soc. Geol. It.: 93, 61-72, Roma.

Wells, P. R. (1977). Pyroxene thermometry in simple and complex systems. Contributions to mineralogy and Petrology, 62(2), 129-139.

Zuffardi, P. (1967). The genesis of stratiform deposits of lead-zinc and barite in Sardinia.

Zuffardi, P. (1969). Remobilization of ores and minerals. Convegno sulla rimobilizzazione dei minerali metallici e non metallici, 322p.: Cagliari.

## GEOLOGICAL MAP OF THE GADONI AREA (Original format A0)

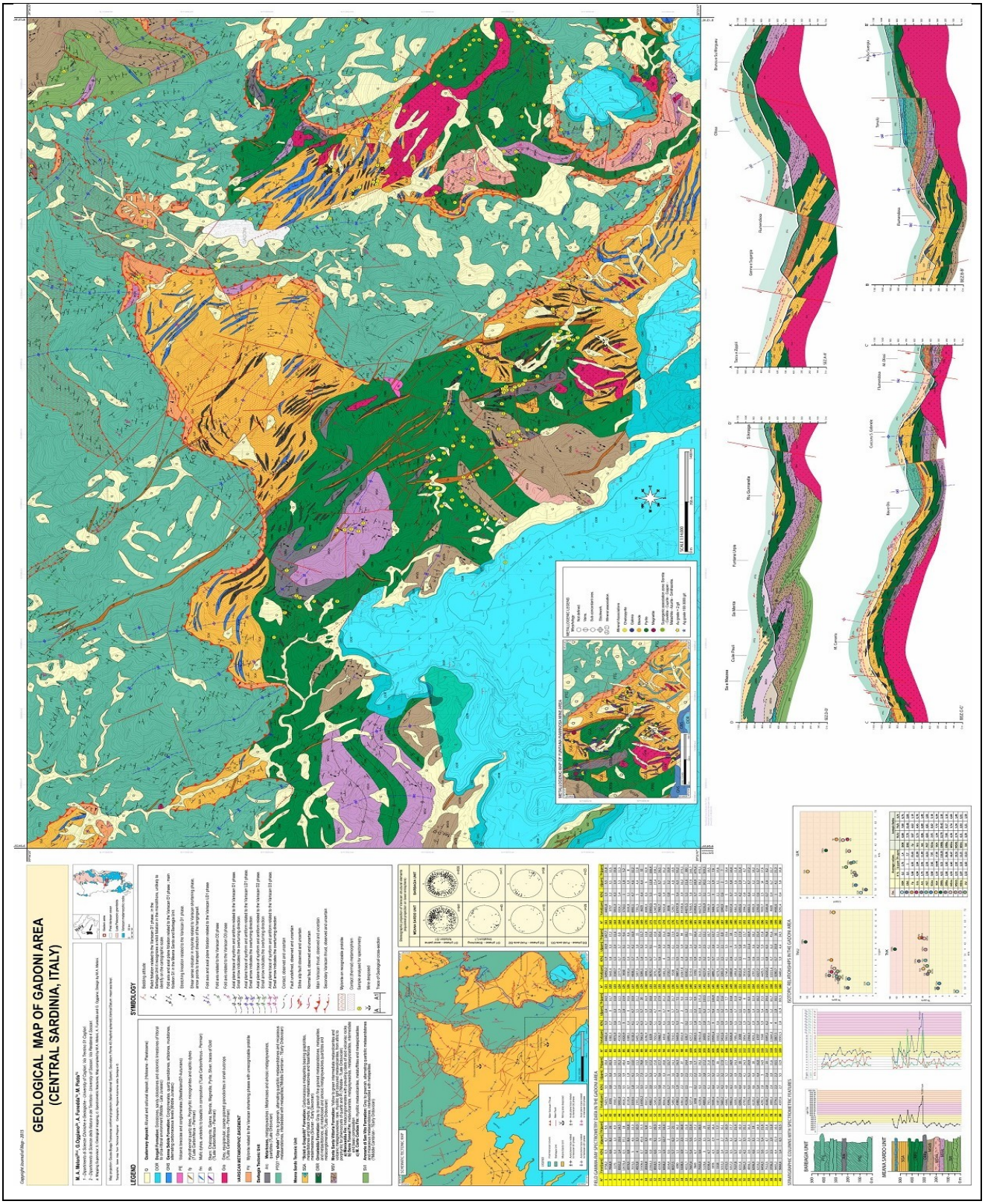

# 7. Conclusions

The geological mapping of the two areas ads a robust contributes to the knowledge of the nappe zone of the Sardinia Variscides. Beside the reconnaissance work in a still poorly known area, the field mapping allow to definitely clean out the stratigraphy and the structure of the Laconi-Asuni area from several uncertainties, which stretch's over the northern limb of the Flumendosa antiform. The tectonic contact of the Meana unit with the Gerrei unit, defined by Carmignani et al., 1985 near Laconi, is now well defined along the whole length of the antiform and the deepest unit (Riu Gruppa unit) has been subdivided in a discrete number of tectonic slices sone of wich is made by Cambro-Ordovician metasandstone previously attributed to the Gerrei unit.

The Gadoni Area was the most challenging due to the widespread occurrence of the unknown Barbagia Units, represented by the Gray Phyllites of Gennargentu (" Postgotalndiano auct."). In the lack of biostratigraphic, and even lithostratigraphic, markers, within terrigenous similar units in order to face the problems related to the reconstruction of the tectonic frame we tested some tool like gamma ray, which in Sardinia were successfully employed to discriminate between similar high grade metamorphic units and between coalescent intrusions and of the C-S batholith (Casini et al 2015; Pistis et al. 2015).

Moreover in order to better define and compare the unknown metamorphic terrains, the zircon study, including U/Pb geochronology, was performed.

The tectonic frame of the area was sketched in satisfactory way, wich also allowed defining the relatioships between the stratigraphical and structural frame with the ore bodies, so shedding light on the ore genesis.

Considering the data obtained here, the following conclusive considerations can be proposed:

- The Gamma ray survey allowed to distinguish the Upper Odovican metasandstone from other similar other ways indistinguishable metasediments pertaining to both the Gray Phyllites of Gennargentu ("Postgotalndiano auct.") and to the S.Vito Formation due to the accumulation of radiogenic heavy minerals;

- The zircon typology allowed to ascertain that the Upper Ordovician metasandstones, in the Gadoni area, are almost totally fed by the dismantling of the Mid-Ordovician volcanic arc in a region where no older rocks were exposed along structural hights. This datum is quite different from that of an Upper Ordovician quartzite sampled in the Corr'e Boi unit (Dessau et al 1982), which conversely shows a dominant Cryogenian –Stenian frequency and only 10% referable to the Ordovician arc. This difference suggests a different palaeogeographic provenance for the Corr'e Boi unit compared to the Meana Sardo Unit;

- The frequency Histograms in the "Postgotlandiano" and in the S.Vito Formation. show similar distributions of U/Pb ages. These are quite similar from the Archaeozoic to the late Ediacarian. The S.Vito Fm. in any case differs for having a good concordant zircon of 539+/-23 Ma, infact similar ages are not present in the "Postgotlandiano that shows only Precambrian zircons the youger of which yielded 559+/-15 Ma. This datum has it definitely stated an old age for the "Postgotlandiano" nappe, the sedimentation of which started at least in the Ediacarian and suggests that a common, old craton was the source area of both the internal and external nappes involved in the orogenic wedge of the Sardinian Variscides. The detrital source shows a same similarity to that of other Variscan sector that were located in Galatian Superterrane (von Raumer and Stampfli 2008) facing the Arabian and or the eastern Tuareg sheld (Meinhold et al. 2012);

- The important ore bodies of the Gadoni district are strictly related to more or less boudinaged Siluro-Devonian carbonate that favoured the formation of skarn deposits during the emplacement of the GR110 granodiorite during the post collisional extension (299+/- 3 Ma) that led to the formation of the Giacurru dome.

- The Upper Ordovician trangressive meta-sediments show interesting concentrations of REE (from 4000 to 6000 ppm), worthy of detailed prospection future, in within this formation.

# REFERENCE


Carmignani L., Gattiglio M., Minzoni N., Oggiano G. & Pertusati P.C. - 1985- L'Unità tettonica di Meana Sardo indipendenza tettonica dei porfiroidi di base. Gruppi di lavoro CNR: "Paleozoico" e " Evoluzione Magmatica e Metamorfica della crosta fanerozoica". Riunione scientifica. Siena13-14 dic. 1985. Note brevi, 89-90.

Casini, L., Cuccuru, S., Maino, M., Oggiano, G., Puccini, A., & Rossi, P. (2015). Structural map of Variscan northern Sardinia (Italy). Journal of Maps, 11(1), 75-84.

Dessau G., Duchi G., Moretti A. & Oggiano G. (1982) – Geologia della zona del Valico di Correboi (Sardegna centro-orientale). Rilevamento, tettonica e giacimenti minerari. Boll. Soc. Geol. It.: 101, 497-522, Roma.

Meinhold, G., Morton, A. C., & Avigad, D. (2013). New insights into peri-Gondwana paleogeography and the Gondwana super-fan system from detrital zircon U–Pb ages. Gondwana Research, 23(2), 661-665.

Pistis, M., Loi A., & Dabard M.P. (2015). Influence of sea-level variations on the genesis of palaeoplacers, the examples of Sarrabus (Sardinia, Italy) and the Armorican Massif (Western France). Comptes Rendus Geoscience (in press).

von Raumer, J. F., & Stampfli, G. M. (2008). The birth of the Rheic Ocean—Early Palaeozoic subsidence patterns and subsequent tectonic plate scenarios. Tectonophysics, 461(1), 9-20.

# APPENDIX 1 (CHEMICAL DATA)

# TABLE 1 (FUS-Na2O2) (INAA) (FUS-ICP)

| Elements | Unit | D. Limit | A. Method | F. Raminosa | S. Gabriele | G. Romana | Giaccuru | B.Add.125 | B.Add.126 |
|---|---|---|---|---|---|---|---|---|---|
| Pb | % | 0.01 | FUS-Na2O2 | | 13.8 | | | | |
| Zn | % | 0.01 | FUS-Na2O2 | | 8.82 | 34 | 11.7 | | |
| Mass | g | | INAA | 2.04 | 2.85 | 2.37 | 2.38 | 1.55 | 1.84 |
| Au | ppb | 2 | INAA | 86 | < 2 | < 2 | < 2 | < 2 | < 2 |
| As | ppm | 0.5 | INAA | 422 | < 0.5 | 4.6 | 97.8 | 7.2 | < 0.5 |
| Br | ppm | 0.5 | INAA | < 0.5 | < 0.5 | < 0.5 | < 0.5 | < 0.5 | < 0.5 |
| Cr | ppm | 5 | INAA | 57 | 8 | 11 | 44 | 110 | 176 |
| Ir | ppb | 5 | INAA | < 5 | < 5 | < 5 | < 5 | < 5 | < 5 |
| Sb | ppm | 0.2 | INAA | 2.4 | 8 | 1.6 | 10.2 | 0.9 | 1.2 |
| Sc | ppm | 0.1 | INAA | 7.5 | 3.3 | 5 | 5.8 | 17.9 | 23.8 |
| Se | ppm | 3 | INAA | 58 | 147 | < 3 | 7 | < 3 | < 3 |
| SiO2 | % | 0.01 | FUS-ICP | 17.63 | 7.57 | 19 | 18.48 | 73.17 | 61.04 |
| Al2O3 | % | 0.01 | FUS-ICP | 8.68 | 2.55 | 5.01 | 4.71 | 13.59 | 12.1 |
| Fe2O3(T) | % | 0.01 | FUS-ICP | 38.05 | 43.43 | 6.24 | 31.92 | 0.86 | 10.05 |
| MnO | % | 0.001 | FUS-ICP | 0.628 | 0.254 | 0.404 | 0.337 | 0.008 | 0.105 |
| MgO | % | 0.01 | FUS-ICP | 2.04 | 0.95 | 1.35 | 2.12 | 0.39 | 1.66 |
| CaO | % | 0.01 | FUS-ICP | 2.47 | 0.95 | 3.21 | 11.93 | 0.24 | 0.73 |
| Na2O | % | 0.01 | FUS-ICP | 0.06 | 0.01 | 0.03 | 0.05 | 0.1 | 0.09 |
| K2O | % | 0.01 | FUS-ICP | 0.17 | < 0.01 | 0.09 | 0.02 | 4.12 | 2.45 |
| TiO2 | % | 0.001 | FUS-ICP | 0.348 | 0.095 | 0.178 | 0.263 | 3.275 | 6.284 |
| P2O5 | % | 0.01 | FUS-ICP | 0.14 | 0.11 | 0.03 | 0.1 | 0.28 | 0.4 |
| LOI | % | | FUS-ICP | 9.21 | 7.21 | 11.4 | 3.07 | 1.91 | 3 |
| Total | % | 0.01 | FUS-ICP | 79.42 | 63.13 | 46.94 | 72.99 | 97.94 | 97.9 |
| Sc | ppm | 1 | FUS-ICP | 8 | 3 | 5 | 5 | 21 | 28 |
| Be | ppm | 1 | FUS-ICP | 1 | 4 | < 1 | 2 | 1 | 2 |
| V | ppm | 5 | FUS-ICP | 85 | 88 | 37 | 47 | 152 | 242 |
| Ba | ppm | 3 | FUS-ICP | 22 | < 3 | 9 | 22 | 410 | 503 |
| Sr | ppm | 2 | FUS-ICP | 89 | 51 | 112 | 34 | 24 | 74 |
| Y | ppm | 2 | FUS-ICP | 7 | < 2 | 14 | < 2 | 290 | 273 |
| Zr | ppm | 4 | FUS-ICP | 62 | 19 | 50 | 64 | 4694 | 8801 |

*Table 1) FUS-Na2O2, INAA, FUS-ICP Analysis in the Gadoni mine district.*

# TABLE 2 (FUS-MS)

| Elements | Unit | D. Limit | A. Method | F. Raminosa | S. Gabriele | G. Romana | Giaccuru | B.Add.125 | B.Add.126 |
|---|---|---|---|---|---|---|---|---|---|
| Cr | ppm | 20 | FUS-MS | 60 | < 20 | 20 | 30 | 80 | 110 |
| Co | ppm | 1 | FUS-MS | 310 | 67 | 312 | 44 | 2 | 15 |
| Ga | ppm | 1 | FUS-MS | 8 | 8 | 8 | 11 | 22 | 25 |
| Ge | ppm | 1 | FUS-MS | 3 | 4 | 2 | 3 | 3 | 5 |
| As | ppm | 5 | FUS-MS | 149 | < 5 | < 5 | 70 | 10 | 12 |
| Rb | ppm | 2 | FUS-MS | 19 | < 2 | 5 | < 2 | 145 | 86 |
| Nb | ppm | 1 | FUS-MS | 7 | 2 | 4 | 5 | 38 | 69 |
| Mo | ppm | 2 | FUS-MS | < 2 | 9 | < 2 | < 2 | 2 | 3 |
| In | ppm | 0.2 | FUS-MS | 89.5 | 3 | 82.9 | 9.8 | 0.2 | 0.6 |
| Sn | ppm | 1 | FUS-MS | 157 | 1 | 42 | 136 | 12 | 12 |
| Sb | ppm | 0.5 | FUS-MS | 2.8 | 7.6 | 2 | 12.2 | 4.2 | 4.1 |
| Cs | ppm | 0.5 | FUS-MS | 5.5 | < 0.5 | 0.8 | < 0.5 | 3.6 | 4.5 |
| La | ppm | 0.1 | FUS-MS | 23.6 | 14 | 24.8 | 17.6 | 568 | 979 |
| Ce | ppm | 0.1 | FUS-MS | 43 | 20.6 | 42.2 | 32.6 | 1200 | 2010 |
| Pr | ppm | 0.05 | FUS-MS | 5.35 | 3 | 4.82 | 4.18 | 152 | 241 |
| Nd | ppm | 0.1 | FUS-MS | 21.3 | 11.5 | 18.3 | 16.6 | 609 | 909 |
| Sm | ppm | 0.1 | FUS-MS | 4.7 | 2.5 | 3.6 | 3.4 | 119 | 159 |
| Eu | ppm | 0.05 | FUS-MS | 2.11 | 0.54 | 1.05 | 1.16 | 2.49 | 2.44 |
| Gd | ppm | 0.1 | FUS-MS | 3.9 | 2.5 | 3.3 | 3.5 | 104 | 112 |
| Tb | ppm | 0.1 | FUS-MS | 0.7 | 0.4 | 0.4 | 0.6 | 13.6 | 13.6 |
| Dy | ppm | 0.1 | FUS-MS | 3.9 | 2.1 | 2.2 | 3.3 | 63 | 61.9 |
| Ho | ppm | 0.1 | FUS-MS | 0.8 | 0.4 | 0.4 | 0.6 | 9.4 | 9.7 |
| Er | ppm | 0.1 | FUS-MS | 2.1 | 1 | 1.1 | 1.7 | 21.6 | 25 |
| Tm | ppm | 0.05 | FUS-MS | 0.31 | 0.13 | 0.14 | 0.23 | 2.51 | 3.38 |
| Yb | ppm | 0.1 | FUS-MS | 1.9 | 0.9 | 1 | 1.4 | 15.9 | 22.6 |
| Lu | ppm | 0.04 | FUS-MS | 0.29 | 0.15 | 0.15 | 0.22 | 2.56 | 4.09 |
| Hf | ppm | 0.2 | FUS-MS | 1.5 | 0.5 | 1.5 | 1.8 | 111 | 211 |
| Ta | ppm | 0.1 | FUS-MS | 0.3 | 0.1 | 0.3 | 0.4 | 2.8 | 4.8 |
| W | ppm | 1 | FUS-MS | 38 | < 1 | < 1 | 7 | 7 | 12 |
| Tl | ppm | 0.1 | FUS-MS | < 0.1 | 0.5 | 0.3 | < 0.1 | 1.1 | 0.8 |
| Bi | ppm | 0.4 | FUS-MS | 566 | 2.3 | 13.2 | 4.8 | 5.1 | 5.9 |
| Th | ppm | 0.1 | FUS-MS | 6.2 | 2 | 5.2 | 6.4 | 243 | 401 |
| U | ppm | 0.1 | FUS-MS | 1.6 | 0.5 | 1.9 | 1.3 | 15.9 | 28.9 |

*Table 2) FUS-MS Analysis in the Gadoni mine district.*

# TABLE 3 (TD-ICP) (ICP-OES)

| Elements | Unit | D. Limit | A. Method | F. Raminosa | S. Gabriele | G. Romana | Giaccuru | B.Add.125 | B.Add.126 |
|---|---|---|---|---|---|---|---|---|---|
| **Ni** | ppm | 1 | TD-ICP | 73 | 20 | 47 | 87 | 9 | 16 |
| **Zn** | ppm | 1 | TD-ICP | 2570 | > 10000 | > 10000 | > 10000 | 178 | 373 |
| **Cd** | ppm | 0.5 | TD-ICP | 50.1 | 1290 | 3730 | 1140 | 2.1 | 4.1 |
| **S** | % | 0.001 | TD-ICP | 11.6 | 6.62 | 16 | 4.23 | 0.006 | 0.023 |
| **Cu** | ppm | 1 | TD-ICP | > 10000 | 6670 | 744 | 843 | 20 | 130 |
| **Ag** | ppm | 0.3 | TD-ICP | > 100 | 34 | 29.1 | 6.3 | 0.7 | 0.5 |
| **Pb** | ppm | 5 | TD-ICP | 2430 | > 5000 | 3970 | 908 | 26 | 66 |
| **Ag** | ppm | 3 | ICP-OES | 502 | | | | | |

*Table 3) TD-ICP, ICP-OES, Analysis in the Gadoni mine district.*

# EDS Analysis

| *Element* | *App* | *Intensity* | *Weight%* | *Weight%* | *Atomic%* | *Compd%* | *Formula* | *Number* |
|---|---|---|---|---|---|---|---|---|
| | *Conc.* | *Corrn.* | | *Sigma* | | | | *of ions* |
| *Al K* | *0.54* | *0.5932* | *0.69* | *0.12* | *0.85* | *1.30* | *Al2O3* | *0.13* |
| *Si K* | *1.74* | *0.7853* | *1.68* | *0.11* | *1.99* | *3.59* | *SiO2* | *0.30* |
| *S K* | *2.56* | *0.8526* | *2.28* | *0.15* | *2.36* | *5.68* | *SO3* | *0.35* |
| *Ca K* | *0.61* | *1.0984* | *0.42* | *0.10* | *0.35* | *0.59* | *CaO* | *0.05* |
| *Fe K* | *82.00* | *0.9365* | *66.26* | *0.49* | *39.43* | *85.24* | *FeO* | *5.89* |
| *Zn K* | *3.23* | *0.8458* | *2.89* | *0.35* | *1.47* | *3.59* | *ZnO* | *0.22* |
| *O* | | | *25.79* | *0.42* | *53.56* | | | *8.00* |
| *Totals* | | | *100.00* | | | | | |
| | | | | | | | *Cation sum* | *6.94* |

*Table 4) Elements EDX analysis, Magnetite composition.*

| Element | App | Intensity | Weight% | Weight% | Atomic% | Compd% | Formula | Number |
|---|---|---|---|---|---|---|---|---|
| | Conc. | Corrn. | | Sigma | | | | of ions |
| Mg K | 0.80 | 0.6304 | 0.94 | 0.14 | 0.93 | 1.57 | MgO | 0.13 |
| Al K | 11.60 | 0.8285 | 10.40 | 0.22 | 9.25 | 19.65 | Al2O3 | 1.24 |
| Si K | 18.23 | 0.8927 | 15.17 | 0.24 | 12.96 | 32.46 | SiO2 | 1.74 |
| Ca K | 20.36 | 1.0011 | 15.12 | 0.25 | 9.05 | 21.15 | CaO | 1.22 |
| Fe K | 18.51 | 0.8475 | 16.23 | 0.35 | 6.97 | 20.88 | FeO | 0.94 |
| O | | | 39.73 | 0.40 | 59.57 | | | 8.00 |
| Totals | | | 100.00 | | | 95.71 | | |
| | | | | | | | Cation sum | 5.43 |

*Table 5) Elements EDX analysis, Garnet composition.*

| Element | App | Intensity | Weight% | Weight% | Atomic% | Compd% | Formula | Number |
|---|---|---|---|---|---|---|---|---|
| | Conc. | Corrn. | | Sigma | | | | of ions |
| Al K | 0.43 | 0.6946 | 0.24 | 0.04 | 0.19 | 0.46 | Al2O3 | 0.02 |
| Si K | 0.78 | 0.8844 | 0.35 | 0.04 | 0.26 | 0.74 | SiO2 | 0.03 |
| S K | 31.25 | 0.8913 | 13.69 | 0.22 | 9.11 | 34.18 | SO3 | 1.10 |
| Ca K | 0.36 | 0.9867 | 0.14 | 0.04 | 0.08 | 0.20 | CaO | 0.01 |
| Fe K | 24.85 | 0.8897 | 10.90 | 0.23 | 4.17 | 14.03 | FeO | 0.50 |
| Cu K | 23.37 | 0.8126 | 11.23 | 0.29 | 3.77 | 14.06 | CuO | 0.45 |
| Zn K | 11.88 | 0.8128 | 5.71 | 0.26 | 1.86 | 7.10 | ZnO | 0.22 |
| O | | | 49.76 | 0.66 | 66.38 | | | 8.00 |
| Totals | | | 100.00 | | | | | |
| | | | | | | | Cation sum | 4.05 |
| | | | | | | | | |

*Table 6) Elements EDX analysis, Calcopyrite composition.*

| *Element* | *App* | *Intensity* | *Weight%* | *Weight%* | *Atomic%* | *Compd%* | *Formula* | *Number* |
|---|---|---|---|---|---|---|---|---|
| | *Conc.* | *Corrn.* | | *Sigma* | | | | *of ions* |
| *Mg K* | *2.66* | *0.6515* | *7.78* | *0.10* | *7.22* | *11.97* | *MgO* | *0.13* |
| *Al K* | *0.38* | *0.7705* | *0.94* | *0.05* | *0.79* | *1.49* | *Al2O3* | *1.24* |
| *Si K* | *10.83* | *0.9442* | *21.84* | *0.16* | *17.53* | *35.56* | *SiO2* | *1.74* |
| *Ca K* | *4.42* | *0.9867* | *8.52* | *0.09* | *4.79* | *6.70* | *CaO* | *1.22* |
| *Fe K* | *6.25* | *0.8423* | *14.13* | *0.16* | *5.71* | *8.16* | *FeO* | *0.94* |
| *O* | | | *46.79* | *0.40* | *59.57* | *36.12* | | *8.00* |
| *Totals* | | | *100.00* | | | | | |
| | | | | | | | *Cation sum* | *5.43* |

*Table 7) Elements EDX analysis, Amphibole composition.*